Project Number: KLB1101

Device to Dynamically Stretch Cells during Microscopic Visualization

A Major Qualifying Project

Submitted to the Faculty of the

WORCESTER POLYTECHNIC INSTITUTE

In partial fulfillment of the requirements for the

Degree of Bachelor of Science

Submitted by:

_____

Brent Duoba

_____

Joseph Lombardo

_____

Kyaw Thu Minn

_____

Juan Rodriguez

Date: 04/26/2012

Approved:

_____

Professor Kristen L. Billiar, Advisor

_____

Professor Domhnull Granquist-Fraser, Co-advisor

Table of Contents

List of tables

List of figures

Authorship page

Key: All – Brent Duoba, Joseph Lombardo, Kyaw Thu Minn, Juan Rodriguez; BD – Brent Duoba, JL – Joseph Lombardo, KTM –Kyaw Thu Minn, JR –Juan Rodriguez

Sections	**Author**
Abstract	KTM
Introduction	KTM
Background	All
Project Strategy	All
Design Alternatives	All
Final Design	All
Final Device Validation	All
Discussion	All
Conclusions and Recommendations	All
References	All
Appendices	All
Review and edit	All

Acknowledgements

We would like to thank Professor Kristen Billiar, Professor Domhnull Granquist-Fraser, Lisa Wall, Mehmet Kural, John Favreau, Joseph St. Germain, Dr. Taskin Padir, Victoria Huntress, Dr. Adriana Hera, and Peter Duoba for their insights and help in finishing this project. Special thanks go to Haydon Kerk Motion Solutions, Inc. for donating four linear actuator motors for completion of this project.

Abstract

Cells in physiological systems are constantly subjected to various mechanical forces. Different types and profiles of mechanical forces have varying effects on cellular functions, activities, and pathologies. Therefore, it is important to understand how different mechanical forces dictate cellular functions of different cell types. Several commercial devices have been developed to study cellular responses to substrate strain in vitro. However, drawbacks of these devices include the inability to provide "real-time" analysis of cellular responses, non-uniform uniaxial and equibiaxial strains as well as limited operation time. In order to overcome such shortcomings, a novel stretch device using four linear motors to apply cyclic mechanical stretch to cells was developed. Using finite element analysis, a unique Polydimethysiloxane (PDMS) substrate was designed and fabricated to translate mechanical forces from the motors and apply uniform strain to the cells seeded on the substrate. This new system will facilitate mechanobiology studies by enabling cyclic stretching of cells biaxially at variable strains (0 – 30%), directions (pure uniaxial to equibiaxial) and frequencies (0.01 – 1Hz) for a minimum of 6 hours as well as allowing "real time" analysis of cells under a standard inverted microscope while stretch is applied. Validation studies confirmed that the device can operate for a minimum of 6 hours without exceeding the room temperature. High Density Mapping (HDM) analysis showed better uniform strain patterns and increased in area of uniform strain fields in the newly designed well compared to commercially available well.

Introduction

Cells and tissues in human body are constantly under dynamic conditions, meaning they are continuously changing in response to various chemical, electrical as well as mechanical signals exerted on them. Among these signals, mechanical signals play a particularly important role by dictating the functions and activities in various cells in the human body. Mechanical forces have been shown to regulate cell orientation, morphology, remodeling, differentiation, proliferation, gene expression, production of cytokines and growth factors as well as extracellular matrix (ECM) protein synthesis [1-8]. Some common examples include constant bone development and remodeling due to cyclic mechanical forces exerted on them [9], heart valve repair stimulated by constant mechanical forces exerted by blood flow [7] and muscle growth elicited by mechanical stimulation during exercises [10].

Mechanical forces have a significant effect on tissue homeostasis and pathophysiology. For example, endothelial and interstitial cells on heart valve leaflets are constantly under varying mechanical forces caused by continuing pulsatile blood flow. These mechanical forces are thought to be responsible for continual damage of these cells as well as leaflet tissue repair [7]. Additionally, it has been shown that in the presence of mechanical forces, endothelial cells lining on blood vessels reorient themselves in a way to reduce the constant mechanical force they suffer. However, failure to respond properly to these mechanical forces, may lead to diseases such as atherosclerosis [18]. Another common example of mechano-sensitive cells are muscle cells which grow under intermittent stress caused by daily activities and exercises but atrophy in the absence of muscle activities [10]. Due to the significant impact of mechanical loads on various

cellular activities and functions, it is essential to understand how these physical forces influence the cells and tissues.

In order to better understand the mechanical forces and their effects on the cells and tissues *in vivo*, laboratory settings are used to replicate the mechanical stimulations on cells *in vitro*. Devices have been built in an effort to study mechanotransduction and mechanobiology of cells under compressive, tensile or shear stresses. There are commercial devices such as Flexcell® Tension System from Flexcell International Corporation and Strex Cell Stretching System from B-Bridge International, Inc. Also, several groups have built their own devices in order to fit their custom needs to carry out specific experiments. These devices can be designed to apply stress using motors, vacuum or hydraulic pressures. Additionally, they can provide stresses in various directions at a variety of strain rates and frequencies. For example, tensile testing devices can be designed to provide strain ranging from uniaxial (tensile stress in one direction) to equibiaxial (equal tensile stresses in two perpendicular axes simultaneously). By combining various directions, frequencies and strains, these devices can be fabricated to provide mechanical stimulations that closely mimic those found *in vivo*. These devices allow for testing of different mechanical forces on a variety of cells and their effects on functions and activities of the cells. In addition to providing mechanical forces, some devices integrate viewing platforms that allow for viewing of cells while they are loaded. This unique functionality permits observation of cell orientation and other pathways real-time as the cells are being stretched. Traditionally cells need to be fixed to be viewed under a microscope after desired amount of mechanical forces at specific times have been applied. Therefore, if one needs to observe the effects of certain mechanical stimulation on cells, for example, at 2, 4 and 6 hour, three cell cultures will have to be stretched, and fixed. However, with devices which allow real-time

viewing, only one cell culture needs to be stretched and observed at 2, 4 and 6 hour or at any interval desired. Therefore, cell stretching device with microscope viewing ability is very desirable since it not only allows traditional mechanobiology experiments, but also increases efficiency.

The goal of this project is to design, build and test a cell stretching device that can stretch cells biaxially at variable strains, axial ratios, and frequencies as well as allow for viewing of cells under a standard inverted microscope while stretch is being applied. The device will apply mechanical stretch along two axes and assure an area with uniform strain within which cells will be seeded. The cells will be seeded on an elastic cell culture well made of polydimethylsiloxane (PDMS). The device must allow observation of cell orientation over a period of stretching. This project will be accomplished with a $1,000 budget by April 2012.

Background

Mechanobiology *in vivo*

Upon investigation and experimentation, it is now consensus among scientists that the stimulus of mechanical stresses affects numerous activities and functions of the cells. Cells may experience mechanical forces in three forms, such as tension, compression and shear (Fig. 1). Depending upon the type of mechanical force and the rates at which the force is applied, various cells in body will respond differently [13].

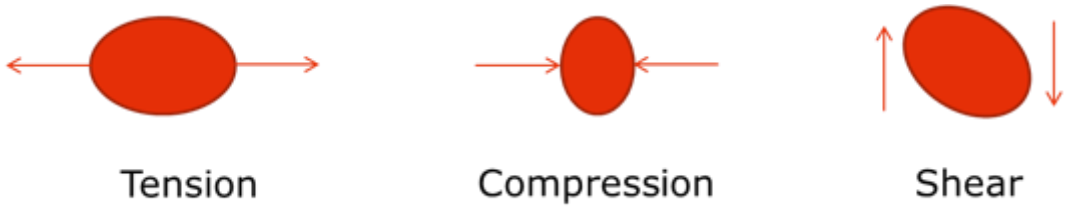

Figure 1. Schematic of different mechanical forces

The mechanical stress is very important in the body. It is an essential trigger for countless messages between cells and appropriate cellular responses to their environment, such as changes in adhesion, proliferation, locomotion, morphology, and synthetic profile [12]. Not only does it exist in many different areas of the body and on a variety of different cells but it also acts on these cells in diverse ways, and due to multiple distinct causes. Most often, the stress experienced is cyclic, as a load is removed and applied alternatingly, or as the magnitude or direction of the load changes. A pertinent review of mechanobiology reveals the varying effects of stretch on a multitude of cells, some of which include cells found in muscles, the heart and cardiovascular system, the lungs, connective tissue, skin and bones [13].

Arteries and cardiovascular muscle cells have prompted tremendous interest in mechanobiology regarding mechanical stress, and are commonly utilized in the study of the

field. They are a natural choice, as the pulsatile nature of blood pressure constantly causes them to be cyclically strained [14]. After investigation of these vascular cells and their profile of deformation, it has been validated that proliferation, apoptosis, and migration of vascular cells, as well as the synthesis, degradation, and reorganization of ECM are all moderated by cyclic mechanical stretch [14]. With this, the presence and importance of stretched cells *in vivo* is increasingly confirmed.

Other prominent tissues that regularly sustain and react to mechanical stress are muscles, notably skeletal muscle cells. This muscular tissue is not only stretched routinely through daily events, but also during exercise, through which the muscles undergo extreme stress. Mass and strength of muscle are dependent on many stimuli, including mechanical stress, and can change rapidly [10]. Without this stress, the muscles atrophy, resulting in loss of strength and mass. When this stress is immense and frequently induced, it enhances the muscle's strength and mass. This happens in two ways: when muscles endure stress, the fibers undergo trauma, specifically referred to as "muscle damage." This activates muscle satellite cells, which proliferate to the damaged area, fusing to the muscle fibers. The fused muscle fibers repair the damage, increasing muscle size, and forming new muscle protein strands [15]. Biochemical activities are affected as well by such mechanical stimulations. In response to mechanical forces, myriad cell signaling factors and proteins, such as mTORC1, eIF3f, eIF2B, FoxO, AMPK, and PGC1α, are transmitted to regulate growth and protein synthesis. For example, Goodman et al. have proven that signaling by mTORC1 is controlled via numerous stimuli, prominently in response to hypertrophic stimuli, including mechanical loading. They also stated that decrease in mechanical loading leads to atrophy of the muscles, as these and other signals cease to be transmitted without an applied mechanical load [10], thereby demonstrating the crucial importance of exercise

and mechanical stress on muscle cells. Likewise, mechanical forces have significant influence on other mechano-sensitive cells such as chondrocytes in articular cartilage, endothelial cells in blood vessels, fibroblasts in ligaments, osteocytes in bones, tenocytes in tendons and skins and so on, regulating their functions and maintaining the biochemical homeostasis [13]. Therefore, studying these physical forces and their effects on cells is crucial in understanding cell functions, homeostasis and equilibrium. Furthermore, these understandings will have implications on biomedical applications such as tissue engineering, cancer treatment, gene therapy and wound healing.

Mechanobiology *in vitro*

The realization of the importance of mechanical forces on cellular responses has prompted several *in vitro* studies of mechanobiology. Among the various mechanical responses observed in cells, reorientation or realignment of cells is the most prominent reaction. Cells alter their orientation when they are mechanically stretched. For example, when endothelial cells and actin filaments were mechanically stretched, they were observed to orient their longer axis perpendicular to the direction of stretch applied while static cells remained in random orientation[2]. In addition, cells may change functions and activities including morphology, proliferation, differentiation, as well as protein and gene expressions due to an external load or stretch [13]. Leung et al. found that cyclic loading of rat aortic medial cells up-regulated certain protein expression [16]. In addition, cyclic stretch stimulated structural alignment of MSCs leading to differentiation of smooth muscle cells without any added growth factors [3]. These findings strongly emphasize the effects of mechanical stimuli on the behavior of cells.

Cell Orientation and Alignment Due to Mechanical Stretch

The reorientation of cells when mechanical stretch is applied has been studied. MSCs were mechanically strained with Flexercell system at 1Hz with 10% elongation for 2 days. The mechanically stressed MSCs were observed to change in morphology and orientation. Unlike unstrained MSCs, which were randomly oriented, mechanically stretched MSCs show perpendicular orientation to the axis of the strain. In addition, these strained MSCs were observed to change their morphology to spindle shape [17]. In addition, 15% strain at 1Hz was applied to MSCs for 2hr to investigate orientation of F-actin filaments. It has been found that stress fibers aligned perpendicular to the axis of the applied mechanical strain [3]. Hsu et al. also reported similar reorientation of cells when exposed to mechanical stretch. Bovine aortic endothelial cells were stretched at 10% cyclic uniaxial stretch for 4 hours in a range of 0.1 Hz to 1 Hz frequencies. It has been found that stress fibers realign themselves perpendicular to the axis of the strain. The extent of such perpendicular reorientation increases as the frequency of the stretch increases [18]. The reorientation of actin stress fibers perpendicular to strain axis may be due to adaptation process in order to minimize the amount of stress the cell suffers [3]. Furthermore, it has been suggested that improper cells alignment may lead to complications. For example, Hsu et al. has indicated that failure of endothelial cells to align at atrial branches may result in atherosclerosis [18]. Additionally, the ability of the cells to reorient themselves highlights the fact that cells sense and dynamically respond to the mechanical stimuli applied to them [18].

Significance of Mechanical Stretch on Skin and Wound Healing

The effects of mechanical stretch on skin have been particularly interesting due to the findings that indicate enhanced dermal healing contributed by stretch [19, 20]. Langrana et al. found that mechanical stimulation applied on healing incision of procine models promoted healing and remodeling of dermal tissue [21]. Several other studies have demonstrated that cyclic stretch on

animal models of skin contributed to increased cellular proliferation in the epidermis and vascularity in dermis as well as increased expressions of neuropeptides and growth factors [19, 20]. During dermal healing, scar formation occurs when fibroblasts remodel the fibrin-rich provisional matrix remodeling. The resulting scar is hugely affected by the mechanical environment that the scar is exposed to. It has been found that cyclic stretch in animal skin models resulted in more complaint and stronger scar but the scar has been found to have decreased contracture and thickness [21, 22]. The increase in strength of the scar may be explained by the behaviors of fibril such as the fibril alignment, enhanced entanglement of the fibrils, bundling of the fibrils and so on [22]. In contrast, undesirable outcomes such as hypertrophic scarring, edema, and scar lengthening as well as widening may be observed due to stretching [23, 24]. Therefore, in order to provide the stretch that allows optimum recovery of wound healing, thorough understanding of mechanisms underlying the effects of stretching on cells is required. Such understanding may be obtained from *in vitro* skin cells or tissue stretching experiments that will allow for an optimum treatment regimen for dermal wound healing.

Effects of Mechanical Forces on Musculoskeletal Cells

Mechanical forces also play a huge role in human musculoskeletal system. Cells in musculoskeletal forces experience various mechanical forces on a daily basis. Such mechanical forces, such as tension, compression and shear stresses, regulate cellular functions including but not limited to cell proliferation, differentiation and gene expression [1]. Every cell and tissue in the musculoskeletal system, including bone, tendon, ligament and cartilaginous tissues, has remarkable ability convert mechanical stimuli into biochemical signals [25]. Musculoskeletal cells respond to tensile strain by realigning actin stress fibers and nucleoli, orienting themselves relative to the direction of tensile stress applied[25]. In addition, progenitor bone cells cultured and

stretched in linear collagen gel construct have been shown to increase expression of bone morphogenetic protein-2 mRNA expression, realign the actin fibers and increase proinflammatory cytokines synthesis [4]. Wang et al. reported that cyclic 10% uniaxial stretching at 1Hz applied to rat bone marrow mesenchymal stem cells lengthened and realigned the cells. Moreover, compared to control groups, cyclically stretched cells expressed collagen types I and III mRNAs as well as tenascin-C mRNA significantly higher after 12 hours and 24 hours respectively [5]. In addition to tensile forces, compressive stresses also play an important role in musculoskeletal system. Compressive forces not only contribute to cartilage formation but also impact osteogenesis [25]. Rath et al. reported 10% saw-tooth profile cyclic compressive strain applied at 0.5 Hz to osteoblasts in 3-D scaffold upregulated expression of bone morphogenic protein-2, runt-related transcription factor 2 and MAD homolog 5 all of which enhanced expression of genes and proteins required for extracellular matrix. These findings indicate that compressive strain on osteoblasts can promote osteogenesis. However, exposure to 20% compressive strain was found not to be osteogenic [6]. According to these findings, different regimes of mechanical stimuli have varying effects on musculoskeletal cells and their functions. Therefore, understanding of various mechanical responses may lead to useful therapeutic application such as bone, cartilage or tendon regeneration.

Mechanical Forces on Heart Valve Cells

Heart valve cells, including endothelial and interstitial cells, are under constant mechanical forces caused by constant pulsatile blood flow in the heart. This dynamic mechanical environment has influences on the remodeling and repair of the cells. Due to the continuing mechanical loads, these cells are continually damaged. At the same time, such varying loads act as mechanical signals that are converted into molecular signals for leaflet tissue repair.

Remodeling of extracellular matrix in heart valves has been shown to be induced by the application of mechanical strains [28]. Ku et al. reported significantly increased expression of mRNA for type III collagen when aortic valve interstitial cells in 2D culture are stretched cyclically for 14% at 0.6Hz [29]. In addition, GAGs and proteoglycans, integral ECM components of valve tissues which have significant influence on the material and structural behavior of the valves, are also regulated by cyclic stretching conditions [28]. The understanding of GAG and proteoglycans regulation is important since their synthesis play a role in pathological conditions such as myxomatous mitral valve disease. In the study conducted by Gupta et al., cells from mitral valve leaflets and chordate were seeded in 3D collagen gels and cyclically stretched at 2%, 5% or 10% strain at 1.16Hz for 48hr. It has been found that total GAG released was lowest in 10% and highest in 2%, while total GAG released in cyclically strained group was significantly lower than in control unstrained groups. Likewise, the amount of proteoglycan released was lowest in 10% and highest in 2% [28]. These findings correlate with the myxomatous mitral valve leaflets and chordae in which low loading magnitudes and increased concentration of GAGs are observed in diseased conditions [30]. These findings highlight the need to understand the various mechanical forces acting on the cells found in heart valves and their effects. Understanding the mechanobiology in heart valve cells will enable better treatment of heart valve pathologies as well as better designing of engineered tissue for heart valves.

Effects of Mechanical Stimulation on Differentiation and Proliferation of Mesenchymal Stem Cells

Mesenchymal stem cells are important cells in therapeutic applications due to their ability to proliferate as well as differentiate into various cell lineages. Recent studies have indicated that mechanical stimulation can enhance the proliferation capacities of MSCs [3, 8, 31]. Choi et al. reported increased proliferation of MSCs when exposed to cyclic mechanical stretch. They

reported enhanced proliferation when MSCs were strained at 5% compared to 0% strain. The findings has been supported by a separate study in which it has been found that cyclically loaded MSCs at 5%-10% strain rates significantly increases proliferation rates within a few hours of stretching [3]. Similarly, Koike et al. showed that compared to unstrained MSCs, increased proliferation was observed in MSCs subjected to 5%, 10% and 15% strain using Flexercell Strain system [31]. According to these findings, it is evident that mechanical stimulation plays a significant role in proliferation capacities of MSCs.

Transdifferentiation of MSCs can be induced by chemicals, growth factors and/or co-culture of cells *in vitro* [32]. Recent studies have explored the effects of mechanical stimuli on MSCs and the effects of stretch differentiation patterns of these cells. Different mechanical regimen contributes to different differentiation of MSCs. Rangappa et al. investigated the role of cyclic stretch on human MSCs by stretching at 1Hz using the Flexercell system with 4% and 8% elongation of cells alternating every 12 hours for 7 days under 5% CO_2 and 37^{o}C. They found that such cyclic stretch induces gene expression of neurogenic lineage such as synaptobrevin, macrotubule associated protein (MAP-2), and Galactocerebroside, as well as those of cardiogenic lineage including Connexin-43 and BMP-2 [32]. Such understanding will enable preconditioning of MSCs to transplant into myocardial infarct patients enabling enhanced effectiveness of MSCs by promoting cardiac differentiation [33]. Ghazanfari et al. applied uniaxial strain of 5% and 10% for 1,2 and 4 hr. Application of such cyclic stretch promoted better proliferation of MSCs in 10% than both 5% and control. Interestingly, the MSCs exposed to cyclic stretch of 10% strain at 1Hz significantly promoted gene expression of α-smooth muscle actin at 2hr [3]. In addition, mechanical stimuli on MSCs have also been shown to promote osteogenic differentiation. A short period of cyclic strain of 0.2% strain for 40 min on rat MSCs

upregulated mRNA expression of Cbfa1 and Ets-1, which are important transcription factor in the differentiation of MSCs into osteoblast, as well as ALP, a specific osteoblast marker. This finding indicates that mechanical strain may play a vital role in bone formation in distraction osteogenesis by inducing differentiation of MSCs into osteoblast [34]. Additionally, specific mechanical stress on MSCs may promote expression of anterior cruciate ligament (ACL) cells. Lee et al. stretched human MSCs at 1Hz and 10% elongation for 2 days and compared the expression of important ligament cell markers including collagen type I and III as well as tenascin-C between four experimental groups – control, MSCs co-cultured with ACL cells, mechanically strained MSCs and mechanically strained MSCs after ACL co-culture. It has been found that the latter two groups showed increased mRNA expression of collagen type I, III and tenascin-C compared to the first two groups. Such findings may be important for programming MSCs into better differentiation of ACL cells in ACL treatment [17]. These findings indicate the significance of mechanical stimuli on the differentiation patterns of MSCs. Corresponding to various mechanical strains, MSCs may be programmed to enhanced differentiation and proliferation of specific cell types needed for desired therapeutic applications. Therefore, understanding on how different profiles of mechanical strains will affect on MSCs may be crucial for clinical application of such cells.

Methods to Achieve Mechanical Stimulation of Cells *in vitro*

Several different systems have been developed to achieve mechanical stimulation of cells *in vitro*. Some of the most popular functional attributes of these systems are devices utilizing electric motors, hydrostatic pressurization, and regulated vacuum pressure [35]. Each of these three major methods employs a different technique to achieve the same common goal, mechanical

stimulation of cells in vitro. This section outlines each of these three methods and reviews devices that utilize such methods.

Electric Motorized Devices

Commercial Devices

One of the most common functional attributes of a cell stretch system is the utilization of electric motors. In general, these systems are built around a well, or elastic membrane, where cells are seeded onto a substrate that has been adhered to the membrane. Popular commercial wells include the B-Bridge International, Inc. biaxial silicon stretch chamber and the B-Bridge International, Inc. uniaxial silicon stretch chamber (Fig. 1.) [36]. Biaxial stretch can be obtained by physically pulling the substrate (via the well) outward along two perpendicular axes, X, and Y. Uniaxial stretch, on the other hand, can be achieved by pulling the substrate (via the well) outward along a single axis, X [35].

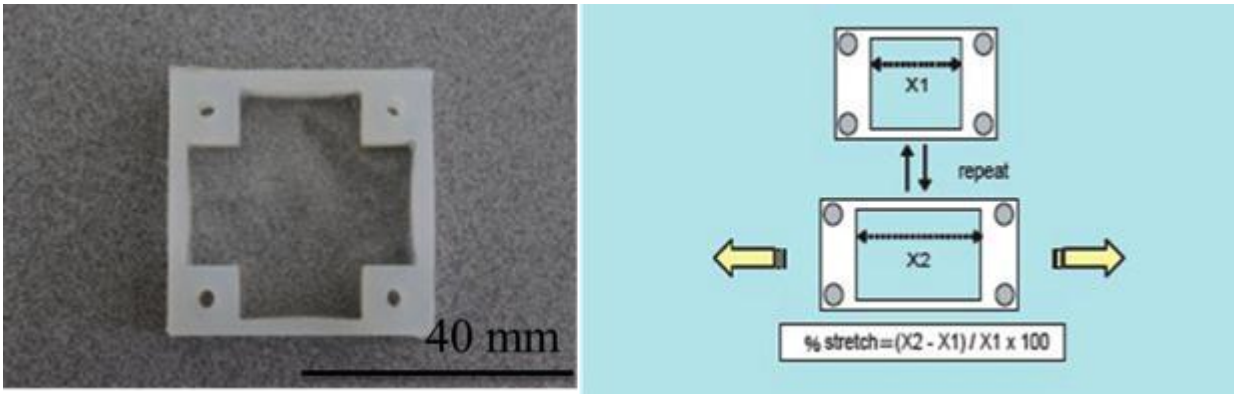

Figure 2. B-Bridge International, Inc. biaxial well (left) and uniaxial well being stretched along X axis (right) (Reprinted with permission)

B-Bridge International, Inc. has commercially developed microscope mountable devices for both uniaxial and biaxial stretch. Facilitating their "Strex Cell Stretching System", B-Bridge International, Inc. has created their devices to cyclically stretch membranes from 1-20% stretch at frequencies between 1-60 cycles/minute utilizing two distinct wave patterns, square wave

pattern or sinusoidal wave pattern (Fig. 2.). Computer controlled selection of strain programs is highly dependent on cell line and experimental procedure. For example, a smaller stretch and lower frequency may be better suited when studying bone cell regeneration or capturing calcium influx images. However, a 20% stretch at 60 cycles/minute sinusoidal stretch would be more appropriate for morphological analysis of cardiomyocytes or signal transduction in endothelial cells lining blood vessels [36].

Figure 3. Examples of square wave and sinusoidal wave strain patterns (Reprinted with permission)

Designed for short term studies (~20 minutes of continuous stretch), the B-Bridge International, Inc. ST-190-XY is capable of both biaxial and uniaxial stretch at frequency ranges from .01 Hz to 1 Hz for a maximum of 20% Strex well stretch. Using specially designed software unique to B-Bridge International, Inc., the ST-190-XY's dual stepper motors are programmed to drive two metal frames closer or further apart (Fig. 4.). Attached to the metal frames is the biaxial silicon chamber (or membrane) and is stretched or compressed depending on the movement of the frames. As shown in schematic (Fig. 5.), motor A moves frame A along the threaded rod A upward or downward while motor B moves frame B along threaded rod B left or right. These, in turn, moves frame C and D along threaded rod C and D, respectively. Thus, compression or tension of the silicone substrate, which has a fixed end at one corner and attached

to frame A, B and C at other corners, is achieved depending of the motor movement. For example, alternating upward and downward movement of frame A by motor A together with alternating leftward and rightward movement of frame B by motor B will stretch the silicone substrate equibiaxially. In addition, the ST-190-XY fits on most microscope stages allowing for real-time observations and fits in most laboratory incubators to maintain proper cell conditions [36].

Figure 4. B-Bridge International, Inc. ST-190-XY (Reprinted with permission)

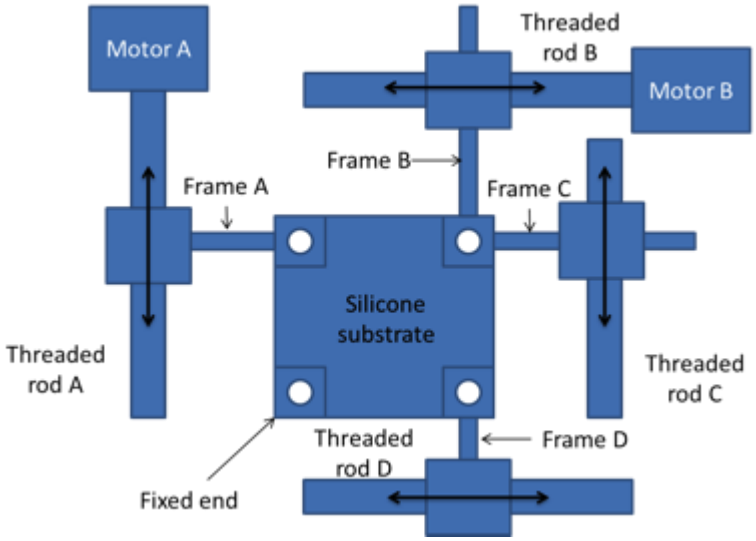

Figure 5. Schematic of ST-190-XY

Custom Devices

In several studies, researchers have designed and built their own electric motor devices to mechanically stretch cells. In a study by Hsu et al., bovine aortic endothelial cells were subjected to cyclic uniaxial stretch via a custom-built device belonging to Department of Biomedical Engineering Professor, Ronald Kaunas, of Texas A&M University. The device, as pictured in Figure 4, facilitates four computer operated linear actuators capable of applying sinusodially-varying stretch of different magnitudes (0-20%), patterns (pure uniaxial, equibiaxial, etc.) and frequencies (0.01-1 Hz). The device sits on an inverted microscope stage and utilizes the B-Bridge International, Inc. biaxial and uniaxial silicon stretch chambers (Fig. 6) [37].

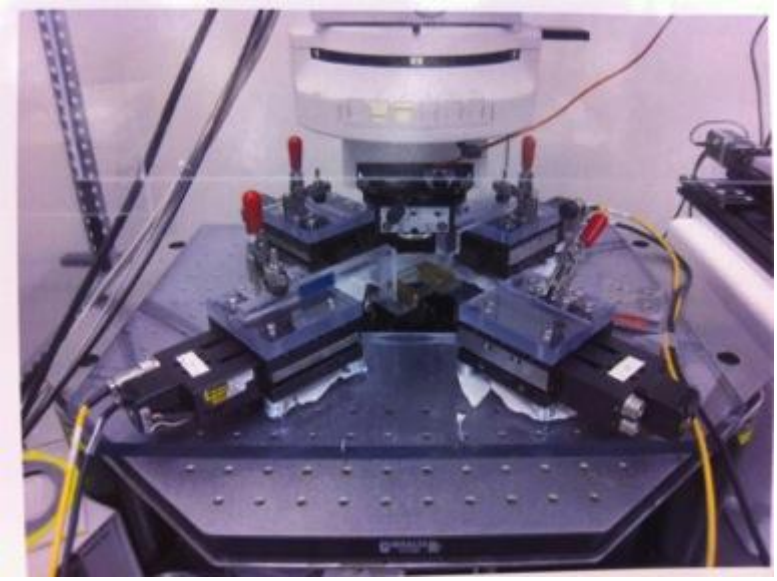

Figure 6. Texas A&M University custom-built stretch device with four linear actuators (Reprinted with permission)

Another custom-built device was designed and built by a group of 3rd year mechanical engineering students at Imperial College of London, England. Supervised by Dr. E.M. Drakakis of the Department of Bioengineering, the eight motor design was developed with the means of studying the effects of mechanical "training" on differentiated cardiac myocytes. The group

hopes that by stretching the cells and utilizing different stretch patterns and strain rates, the cells will develop the necessary strength and morphology to withstand heartbeat after implantation (Fig. 7.). The device was designed to operate with a frequency range of 0.01-10 Hz, 0-80% percentage of stretch and with several different stretch patterns (pure uniaxial to equibiaxial) operating under microscope real-time viewing. The device facilitates a user friendly touch screen with heat dissipation components (fans and heat sinks) and printed circuit boards (PCB) for controller and driver components. In order to compensate for the innovative 8-directional stretching system, the group developed their own membrane [38].

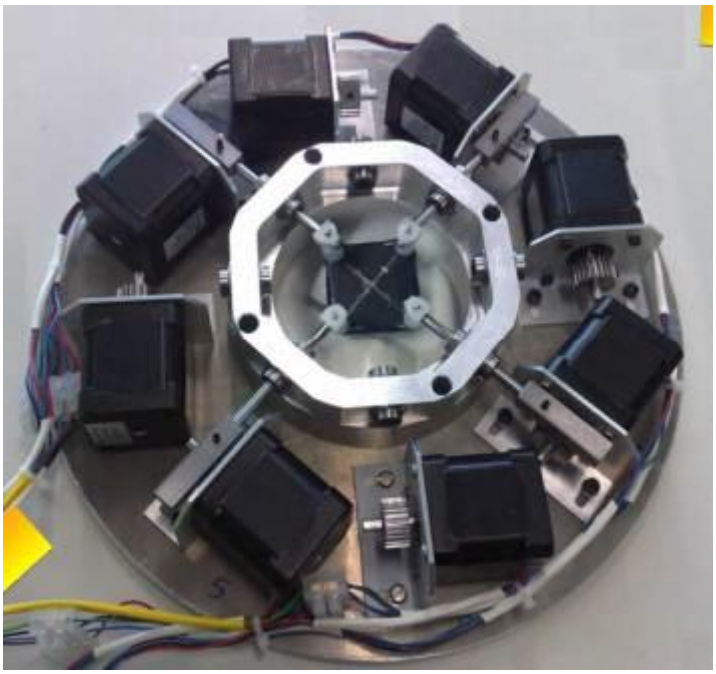

Figure 7. Imperial College of London custom-built stretch device with eight motors (Reprinted with permission)

In order to study the effects of uniaxial strain on mesenchymal stem cells (MSCs), a custom-built device was developed by Park et al at The Center for Tissue Bioengineering at the University of California-Berkeley. The device consists of six parallel chambers for the stretching of six custom-made silicone membranes, clamped stationary at one end and attached to a

cam/rotator system on the other (Fig. 8). The cam is driven by a motor and belt system, stretching the membranes with cultured cells in a sinusoidal motion. Strain rates are selected by inserting strain-designated "keys" into the cam arm and frequencies of 0.01-1 Hz are precisely selected through the motor's controller. This device is not meant to fit on a microscope stage for real-time observations but can fit in most commercial incubators [38].

Figure 8. University of California-Berkley custom-built uniaxial stretch device (Reprinted with permission)

Regulated Vacuum Pressure Devices

Devices utilizing regulated vacuum pressure to stretch a substrate are available commercially. A successful example is the Flexcell family of devices developed by the Flexcell International Corporation. They manufacture a number of devices, the ones most relevant to this project being the Flexcell tension systems. The Flexcell StageFlexer is especially pertinent, as it is meant to be used while mounted on a microscope in real time. Paired with the Flexcell vacuum pump unit, the StageFlexer contains a valving mechanism to adjust and maintain

pressure to obtain the strain needed. Both gradient biaxial strain and equibiaxial strain are obtainable with this device depending on the usage procedure of the device stage. They use membranes manufactured by Flexcell International [40]. Schematic of how Flexcell achieves stretch can be seen in Figure 11. Briefly, cells are seeded onto a soft substrate. The substrate is placed on top of the loading post. When the vacuum is applied, the regions of the substrate not on top of the loading post will move downward, stretching the regions of the substrate on the loading post. This mechanism essentially provides stretch on the cells. When the vacuum is removed, the substrate will return to its initial position. The repetitive applying and removing of vacuum is done to achieve cyclic biaxial or uniaxial stretch on the cells.

Cells have commonly been seeded and stretched using Flexcell products in laboratory settings. Authors Park et al. discuss their procedure for applying equibiaxial strain to a cell-loaded substrate. In this experiment, however, a different Flexcell model is used (Flexcell TensionPlus system) which does not permit real time microscopic viewing [38]. An example of a Flexcell® stretching device and the schematic of how it achieves stretch can be seen in Figure 10 and 11 below.

Figure 9. An example of vacuum pressure Flexcell stretching device (Reprinted with permission)

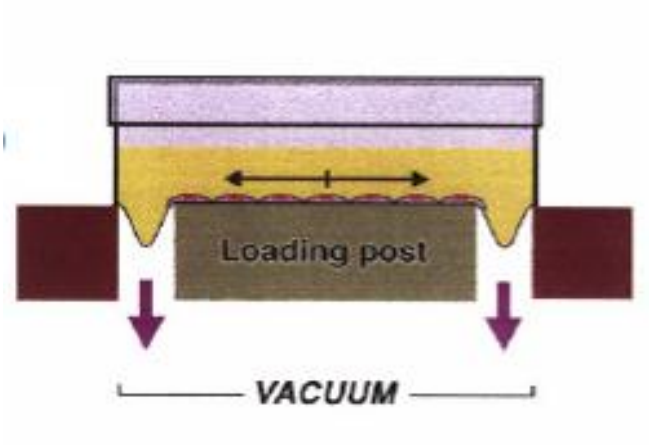

Figure 10. Schematic of how Flexcell works (Reprinted with permission)

Devices using Hydrostatic Pressurization:

Currently, Cell Lines Service (Germany) provides cell-stretching devices that use pressure as stretching force. This device consists of three main parts, namely the pressure chamber, the power supply and the stretching unit. The desired cells can be seeded onto six-well-

plate with elastic membranes. Power supply unit applies power to the pressure chamber. The pressure chamber generates cyclic pressure changes above and below atmospheric pressure. According to the change in pressure, the flexible membranes on which cells are seeded are deformed up or down causing stretch on the cells. The pressure chamber is connected to the stretch units with small tubings to relay pressure changes into elastic membrane deformations [39]. The mechanism through which the device achieves stretch is similar to Flexcell. Instead of applying vacuum as in Flexcell, the device applies pressure lower or higher than atmospheric pressure to stretch and release the substrate. This device, named the S1 Cell Stretcher, is commercially available from Cell Lines Service and is shown as below (Fig. 11).

Figure 11. S1 Cell Stretcher from Cell Lines Service

In addition to the commercial devices and custom devices, there are cell stretching devices patented at the United States Patent and Trademark Office. A few selected devices are discussed in Appendix A.

Despite these available devices to study mechanobiology, there are certain limitations associated with each device. For example, Flexcell stretching devices and hydraulics devices are limited in studying cells under uniaxial strain due to non-uniform uniaxial strain fields.

Additionally, such systems need a vacuum chamber or pressure chamber, which can be cumbersome to use. One other limitation is the ability to observe cells under a microscope while being stretched. The “real time” viewing is an important function since it will allow experimenters to observe effects of mechanical stretch on cells as they are stretched. For example, when reorientation of cells under stretch is studied, “real time” viewing will allow understanding of the relation between stretching time and orientation of cells at each specific time point. While such function is available for devices such as ST-190-XY, their operation time is extremely limited to approximately 20 min, possibly restricting a variety of experimental designs. Flexcell International Corporation also offers devices such as Flexcell® StageFlexer® and Flexcell® StageFlexer® Jr. that can fit under the microscope. However, the major limitation with Flexcell® devices is the inability to provide uniform strain patterns when uniaxial stretch is performed on cells. Moreover, high cost is associated with the commercially available devices.

Considering the limitations of the current devices, the project intends to facilitate better mechanobiology study by significantly improving upon the functions and addressing the existing shortcomings of current devices. Therefore, this design project will aim at developing a device that will stretch cells accurately at variable strain and axial rates as well as frequencies while allowing “real time” viewing of stretching cells.

Project strategy

Initial Client Statement

Our primary goal in this MQP is to design a device that would cyclically stretch cells on a microscope stage at a range of strain rates. This device would mainly be used in research concerning the structure and alignment of cells under stress. The device had to be built with precision, and among other functions, stretch cells with a high degree of versatility. This meant stretching cells in a strip biaxial (1:0) configuration to an equibiaxial configuration (1:1), and any ratio in between. The device would also have to be compact enough in order to be mounted on a standard inverted microscope, and it has to provide proper cell culture conditions to keep the cells alive. After an introductory meeting with the client, an initial client statement was created, shown below.

"Design, build, and test a cost efficient device that will accurately stretch cells from uniaxially to equibiaxially at a range of strain rates cyclically. The device will be used on a standard inverted microscope during operation in order to view the effects of loading on cell structure and alignment. The device must operate for a minimum of six hours, as well as provide proper cell culture conditions. Lastly, the device should be safe to use and user friendly."

Once written, the initial client statement would be revised through an iterative process including client meetings and interviews, and further clarification of what the device was intended to do.

Objectives

In order to fully understand the project assigned to the team, the features of the device were described through objectives and constraints. The objectives, or goals, were features of the

design that the team would focus on in order to develop as close to a device as the client envisioned. Through iterative feedback with the client, an objectives tree was created underlining the primary features of the desired design (Fig. 12).

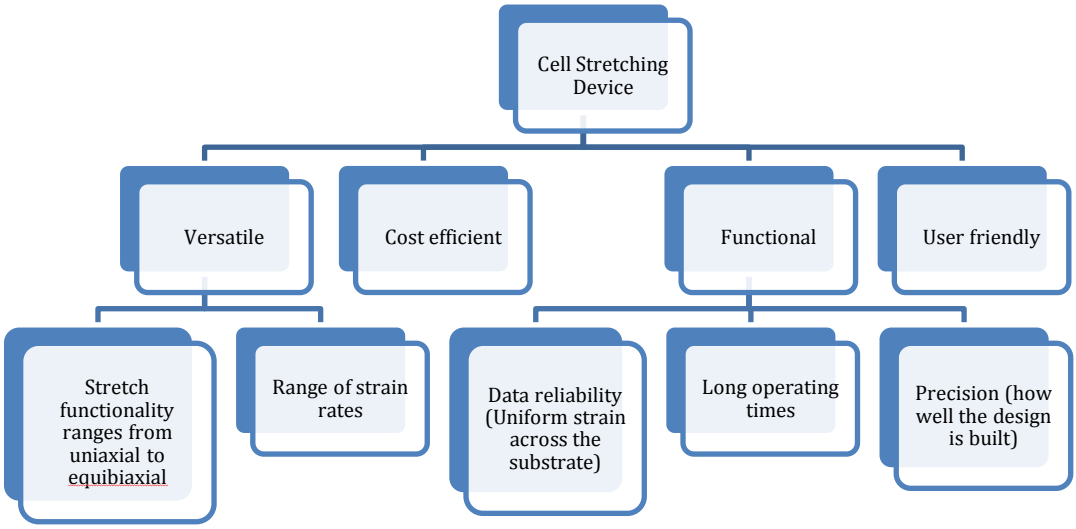

Figure 12. Objective tree of the design

The tree (Fig. 12) shows all of the objectives intended for the design grouped under four main objectives: versatility, functionality, cost efficient, and user friendly. Comprised of these main objectives, a pairwise comparison chart (PCC) was created to determine the importance of each objective (Table 1). Completed by the client, the PCC would serve as a tool for evaluating all alternative designs created for the project.

Table 1. Pairwise comparison chart comparing 1st level objectives

GOALS	Versatile	Cost efficient	Functional	User friendly	SCORE
Versatile	X	1	0	1	2
Cost efficient	0	X	0	0	0
Functional	1	1	X	1	3
User friendly	0	1	0	X	1

As shown by Table 1, the client wanted the design to be functional above all else. The term functional was defined by the client as "how well the design works". This objective includes precision (how well the design is built), long operating times, and data reliability (uniform strain percentage across the substrate). The second objective with regards to importance is versatility. This objective incorporates all of the stretching profiles possible on the device, specifically different forms of stretching (uniaxial/equibiaxial), multiple strain rates, total substrate strain, and duty cycles. Lastly, user friendly and cost efficient placed 3rd and last in terms of importance, respectively. Overall, the PCC reflects the client's interest in obtaining a well-built device that incorporates as many functions as possible, with a focus on accuracy.

Constraints

Constraints are design specifications that the final design had to meet. The device had to be compact enough to fit on top of a microscope stage. To complete this requirement, a suitable microscope had to be chosen. A Zeiss microscope modified with a motorized stage was chosen by the client for this project. The microscope, located at Gateway Park, was measured for dimensions to better understand the space constraints for the final device, shown below in Fig. 13. The final device needs to be compact enough to fit on to the microscope stage shown. Specifically, the entire device needs to fit on the microscope stage of 160x110 mm shown by

double headed blue arrows in Fig. 13. However, since the client expressed desire to use XY motorized stage on the scope, the device needs to sit atop the motorized stage (152x103 mm, shown by double headed green arrows, Fig. 13). Additionally, protrusions on the microscope stage shown by black arrows in Fig. 13 also constraint the overall shape of the final device. While on the motorized stage, the device could not cause damage to the tray or to the microscope. The cells stretched must be incubated and kept under homeostatic conditions. If the device were to utilize electronics to control the motors, some type of protection against heat and humidity should be present. The overall design of the device had to be safe to use, causing harm to neither the user nor the cells being stretched. Lastly, the device should cost no more than $1,000.

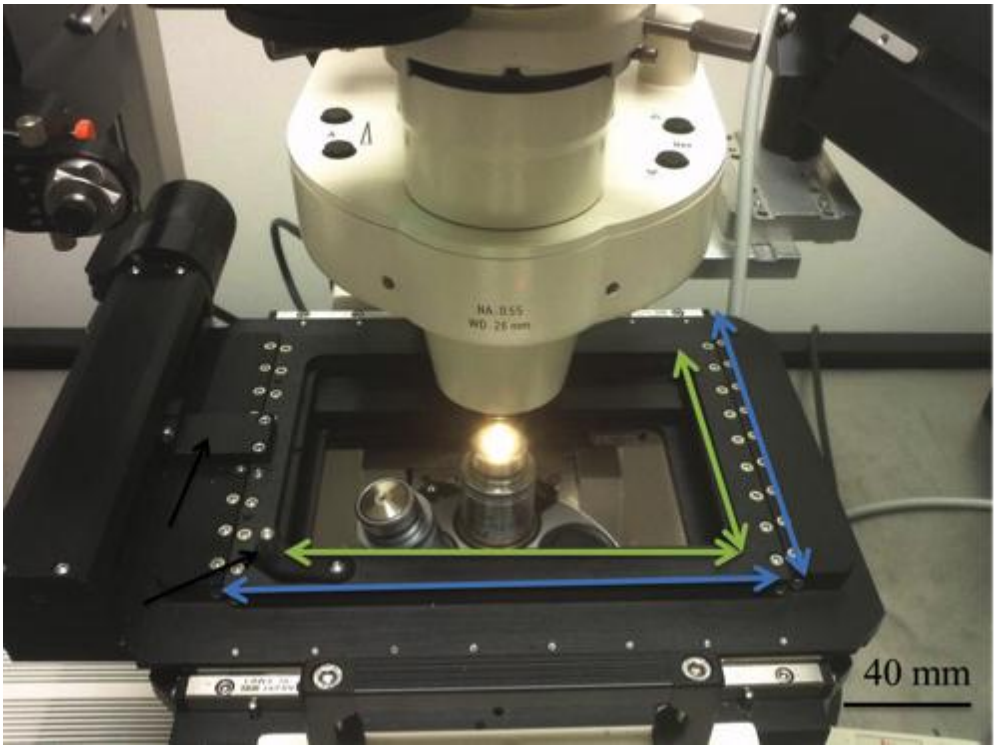

Figure 13. Base Plate of the Zeiss Microscope on which the final device needs to fit

Functions and Specifications

The primary goal of this project was to design a device that can cyclically stretch cells at a range of strain rates. The final design would include different stretching configurations ranging from strip biaxial (i.e. pure uniaxial) to equibiaxial, including every ratio between the two configurations. The motors in the design would apply a force to stretch the well to a minimum of 5% and a maximum of 30%, while also remaining within 10% accuracy. The strain field generated on the well can vary from area to area, but it must be uniform in the center of the well. The strain rate applied by the motors would range from 0.01Hz to 1Hz, or one cycle every 100 seconds to 1 second, respectively. In addition, the motors would be programmed in a fashion to allow the strain rate to increase or decrease mid-cycle. A 40x microscope magnification lens will be used to view the cells while on the device.

Revised Client Statement

Initial client statement was revised after extensive research on existing cell stretch devices was accomplished. Afterwards client interview was performed to better understand specific needs of the client as well as to establish better defined functions and specifications. Revised final client statement is shown below:

> *"Design, build, and test a cost efficient device that will cyclically stretch cells biaxially at a range of strain rates. The device will be used on a standard inverted microscope during operation in order to view the effects of loading on cell structure and alignment. The device must operate for a minimum of six hours, as well as provide proper cell culture conditions. Lastly, the device should be safe to use and user friendly."*

Design Alternatives

Functions and means

In order to determine alternative designs to achieve desired functions, function-mean chart was created. The functions desired in the final design were listed on the first column. Afterwards all the possible means to achieve each particular function were put together. Doing so expanded the design area. For the function-mean chart shown below, there will be 54 ways to achieve the functions. Exploring different means to achieve functions helped developing different alternative designs.

Table 2. Function-Mean Chart

Functions	**Means**					
	1	2	3			
Stretch Cells (Device Material)	Aluminium	Steel	Plastic			
Stretch Cells (Drive Force)	DC Motor	Stepper Motor	Servo Motor	Linear Actuator	Vacuum (suction)	Hydraulic Pressure
Controllable Interface	Manual Switches	Controller Board and Software	Mechanical			

Alternative Designs

After our client statement was successfully developed, the team started developing concepts how the design could be accomplished. Considering the various objectives the device is

intended to achieve and functions that it is aimed to perform, four different approaches were developed. Each of these four alternative designs incorporates the use of different possible means created in function mean chart so that each design carries out the desired functions. Each alternative design will be discussed in the following sections.

Four Motor Design

The first four-motor design is one that incorporates linear actuators (Fig. 14, B) placed 90° from each other in order to provide the linear force needed to stretch the wells. By using these linear motors, the design will be compact and relatively lightweight. The motors would be secured to the base plate motor mounts (Fig. 14, C) to restrict motion in all directions, only being connected to the well via function-specific detachable hooks. By incorporating detachable hooks (Fig. 14, D and E), the design would be able to achieve two types of stretch depending on the configuration of the device. In one configuration, all four motors are connected to the well at the corners to provide equibiaxial strain (Fig. 14). In order for the device to perform pure uniaxial stretching, a different configuration is required. In this second configuration (Fig. 14), the well is rotated 45° and the hooks used for equibiaxial stretching would be replaced by two different types of hooks. The first connects the linear actuator to two corners on the well; this motor and the one across from it would stretch the cells uniaxially. In order to prevent the Poisson's effect from preventing pure uniaxial stretch, another hook that serves as a lid would cover the remaining two sides of the well, preventing the walls from deflecting inward while allowing strain in the uniaxial direction.

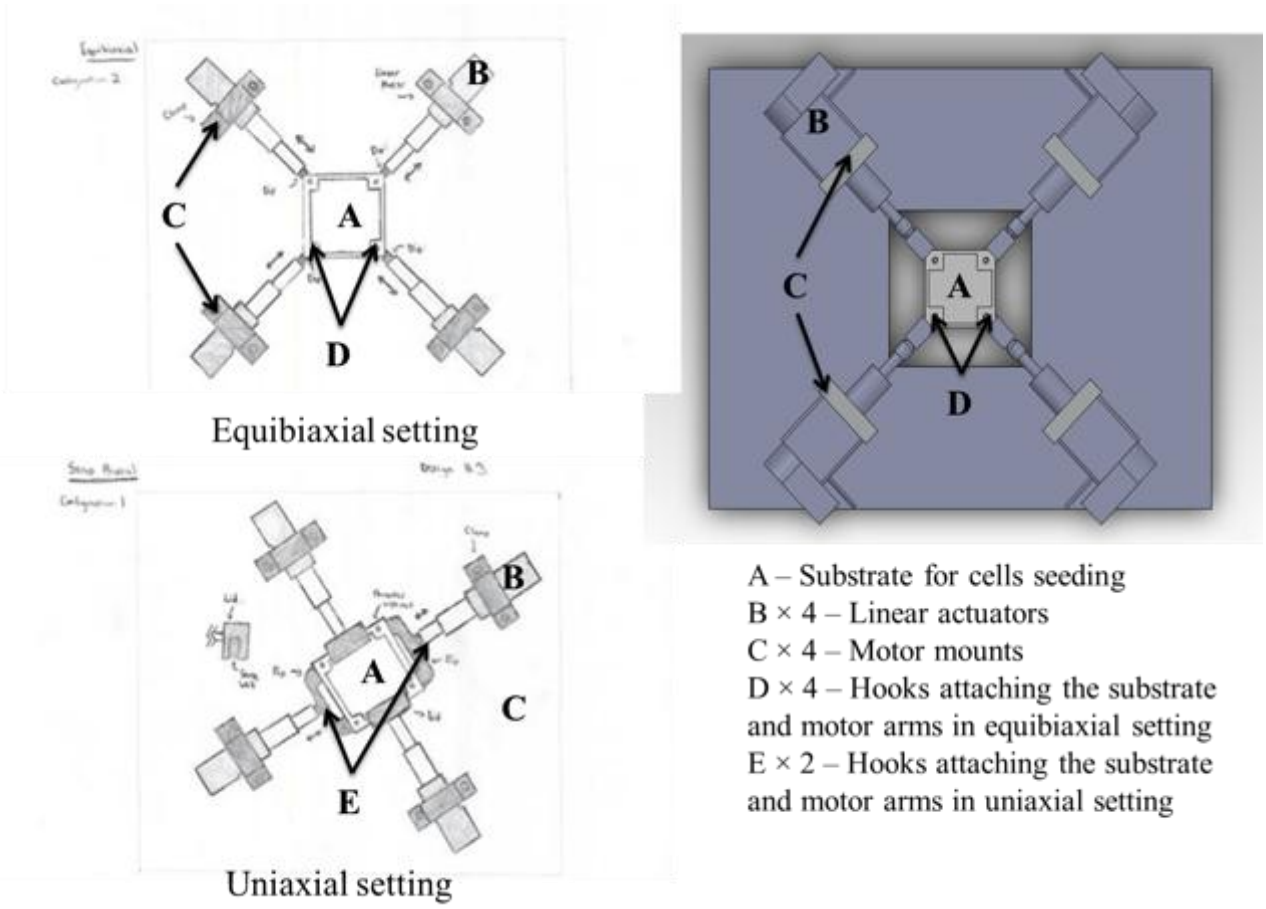

Figure 14. Four motor design

Two Motor ST-190-XY Reverse-Engineered Design

The two-motor design is a replica of the STREX motor device. This device utilizes two stepper motors (Fig. 15, A) connected to threaded rods (Fig. 15, B). On each threaded rod there is a bearing (Fig. 15, C) that is driven axially once the rod rotates. This provides the force necessary to stretch the well in the x and y direction on two corners. The third corner (Fig. 15, D) is stretched in both directions, achieved through the linear rods (Fig. 15, E) connected to a third block, while the fourth corner (Fig. 15, F) is held fixed. This device was designed to be rigid, with multiple linear slides and bearings to keep the threaded and non-threaded rods linear. Due to

the amount of parts required for the design and the limited space available on the microscope tray, the device would have to be as compact as possible to conserve space.

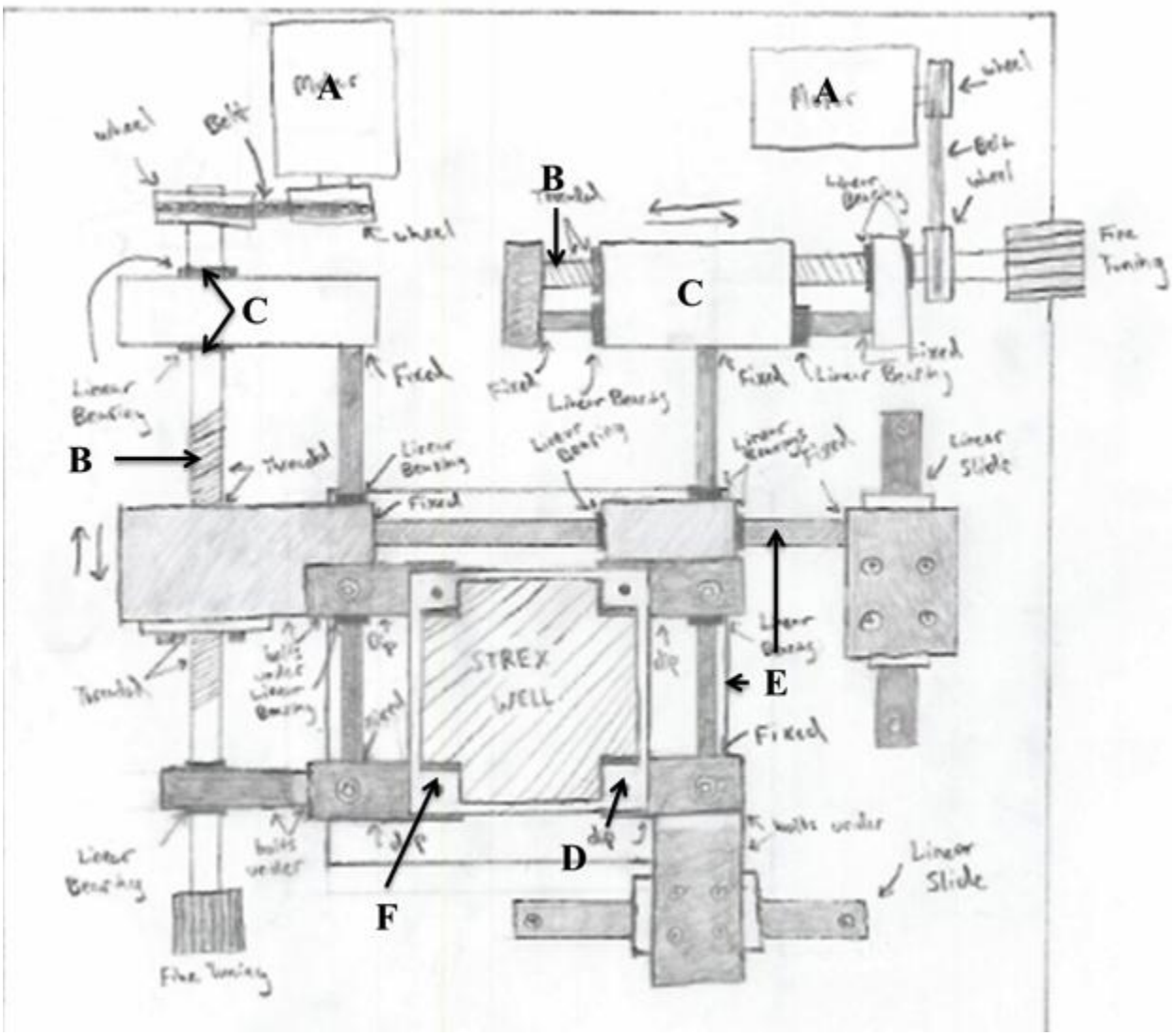

Figure 15. Two motor design with stepper motors and belt drive

Four Motor Design with Attached Corner

The second four-motor design is a compact and simple design that uses linear actuators to achieve stretch profiles ranging from pure uniaxial to equibiaxial. This design is similar to the STREX in concept, but it is different in how it achieves stretch across the well. While the

STREX uses two motors, threaded rods, and linear bearing to achieve stretch in three corners, this design uses four motors, with two set up in a stacked motor configuration. The four motors are named A_1, A_2, B_1, and B_2 for clarification. Motors of the same letter will stretch the well to the same strain and at the same strain rate. One corner of the well would remain fixed, while the remaining three would be attached to motors to achieve stretch. Two motors are placed on the corners adjacent to the fixed one. These two motors, A_1 and B_2, will stretch the well biaxially. In order to achieve an even strain field in the well, the remaining two motors (A_2 and B_1) are placed in a stacked configuration. Motor B_1 is connected to a raised platform whose motion is restricted to that of the motor via a linear slide. On the raised platform, motor A_2 is connected to the well via a dipped hook. In conjunction with the other motors, this configuration will allow uniform strain across the well.

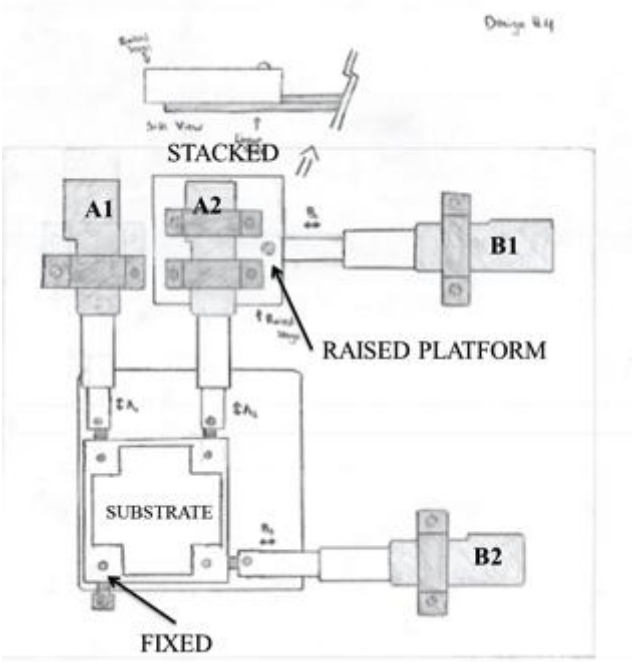

Figure 16. Four motor design with double stacked motors

Two Motor Design with Linear Actuators

The second two-motor design is similar to the first STREX in all but motor choice. This design would be driven by linear actuators instead of stepper motors. This choice was made in the attempt to minimize the size of the design, as the threaded rod and belt mechanism require a large amount of space. Since linear actuators already convert rotational force to linear force, these components would no longer be required. This design would retain the majority of the linear bearings and slides in order to keep the design as rigid as possible.

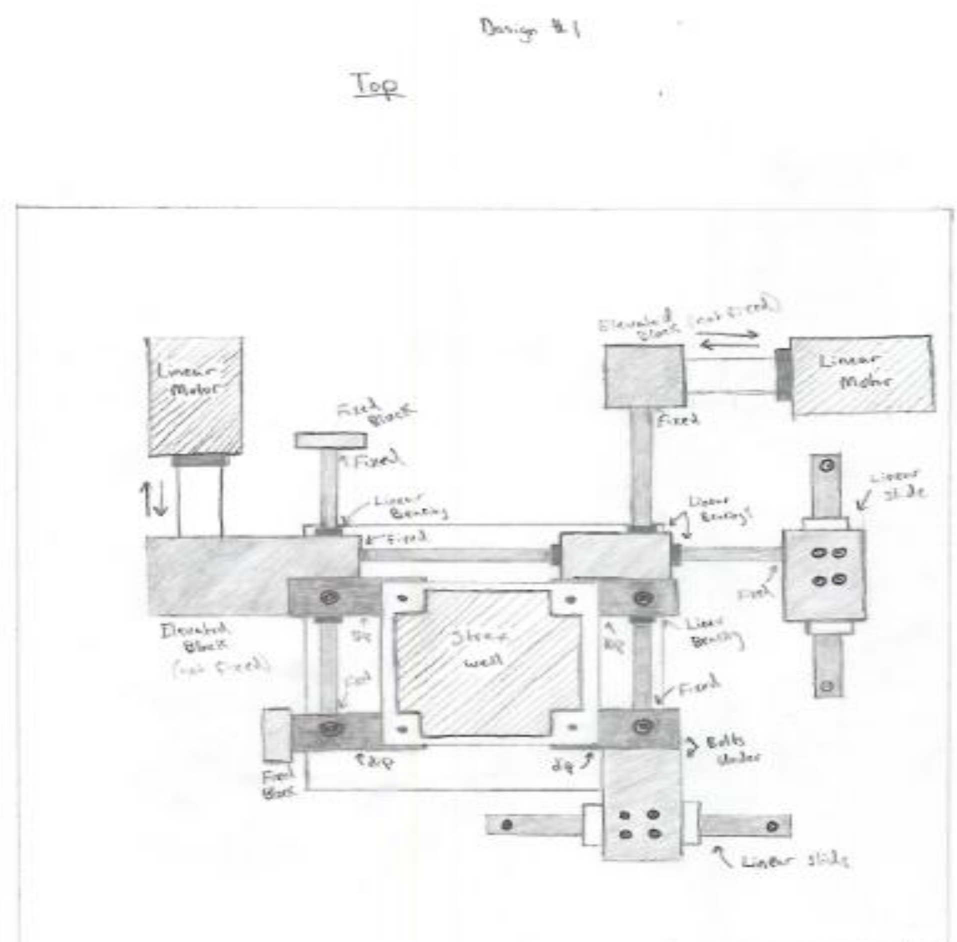

Figure 17. Two motor design with linear actuators

Design Decision

Evaluation Matrix

In order to choose the final design, an evaluation matrix was created. The evaluation matrix compared the constraints and the objectives to the four alternative designs. The team assigned weighting factors to determine the importance of each objective. The weighting factors were derived from PCC. The objective that scored highest (functionality) in PCC was assigned weighting factor of 4 and the objective that scored lowest (cost efficient) was assigned 1. The metrics for scoring the objectives was also assigned and are shown as below:

0 – 25: Design will not meet objective

25 – 50: Design will meet objective with restrictions

50 – 75: Design satisfies the objective, but does not optimize it

75 – 100: Design fully meets the objective

After the scores were summed up, the four motor system with double stacked motors achieved the highest score. Consequently, this design was chosen as the final design. The evaluation matrix can be seen in Table 3.

Table 3. Evaluation matrix for deciding the final design

Constraints (C) & Objectives (O)	Four motor system	Four motor system with double stacked motors	Two motor Strex reserve-engineered design	Two motor system with linear actuators
C: Must fit on the microscope stage	✓	✓	✓	✓
C: Must not damage microscope stage	✓	✓	✓	✓
C: Cells must be viable at all time while being stretched	✓	✓	✓	✓
C: Must be safe for user	✓	✓	✓	✓
O: Versatile (x3)	50x3 = 150	100x3=300	100x3=300	100x3=300
O: Cost efficient (x1)	90x1=90	95x1=95	50x1=50	65x1=65
O: Functional (x4)	80x4=320	90x4=360	60x4=240	70x4=280
O: User friendly (x2)	60x2=120	100x3=300	100x3=300	100x3=300
TOTAL	**680**	**1,055**	**890**	**945**

Modeling of Chosen Design

In order to completely conceptualize the chosen design, a CAD SolidWorks model was made of the four motor designs with double stacked motors.

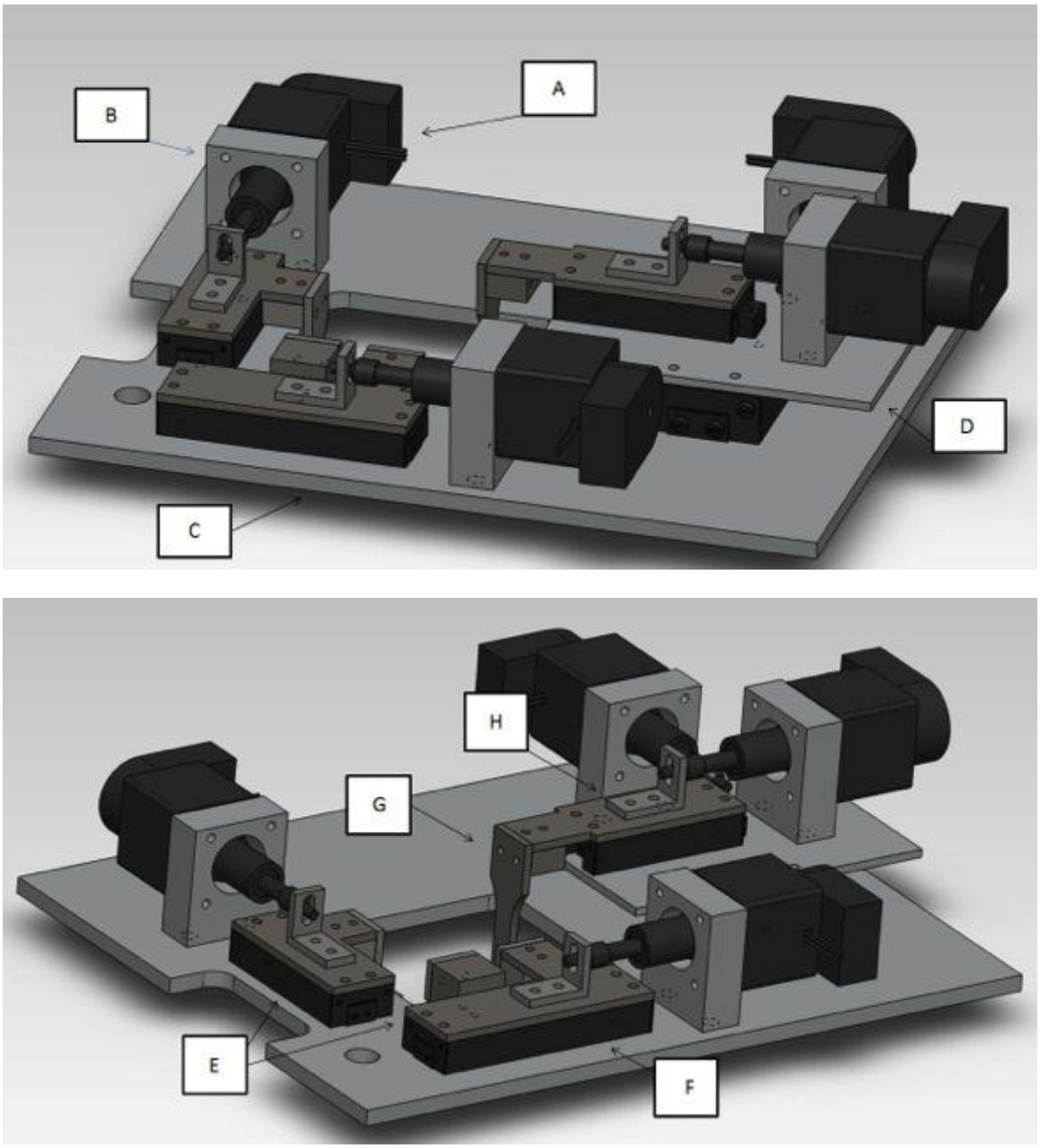

Figure 18. CAD of four motor design with stacked motors in two different views

The heart of the design is the four linear actuators with encoders (A.) strategically placed atop a subplate (D.) and baseplate (C.). The motors are secured to the baseplate via motor mounts (B.). Due to the dimensional constraints presented by the microscope and its mechanical stage, all components of the design are placed very snug with limited flexibility. Three of the

four motors are attached to metal hooks (E and G.) that sit on linear ball slides (F.). The motors are secured to the hooks with L-mounts (H). The forth motor is attached to the subplate. At the ends of the hooks where they dip down into the baseplate is where the PDMS well attaches for real-time microscope viewing. Drawings of individual components are attached in Appendix B.

The design utilizes four linear ball slides, four hooks, four linear actuators with encoders, one subplate all mounted to a single baseplate. The baseplate, subplate and hooks will be CNC machined for proper precision, along with any other additional high-precision parts. Motors, encoders, linear ball slides and hardware will be ordered from various retailers.

Final Design

In order to successfully accomplish the client statement, the team divided the project into two parts. The first part, which is the device development, comprises of motors, motor controls and other mechanisms to apply mechanical stretch to the substrate. The second part, which is the substrate development, includes designing and developing a PDMS substrate which will translate mechanical stretch applies on it to the cells seeded.

Device Design

Feasibility tests were performed in order to assess whether or not experiments can be carried out or the design can be built with its desired functions. For example, the cells seeded well that will be stretched must allow viewing of the cells through the microscope. Feasibility study will determine whether or not the well planned to be used in the design allow such viewing capability. Additionally, different motors can facilitate stretching desired by this design project. However, in order to determine whether commercially available motors can provide the capacity to stretch the well at 30% strain (maximum) at 1Hz (maximum), the well must be tested in

simpler mechanical stretching system to determine the maximum force needed for said 30% strain. The force calculated can then be used in motor selection in the design process. In short, these feasibility tests are performed to decide the practicability of the project itself and whether certain aspects of the project will succeed.

Motors

Three types of motors have been considered in the designing of this device: servomotors, stepper motors, and linear motors. Servomotors are DC motors with a servomechanism. A DC motor converts electric energy from DC current electricity into mechanical energy by creating torque. DC motors use stationary magnets to rotate a rotor in the form of an electric current supplied wire, thus generating torque due to the principle of Lorentz force [42]. The servomechanism controls the motor rotational position using negative feedback to find the difference between desired position and actual position, known as the error signal, which then drives the motor further to eliminate the error, and in doing so achieve the desired position [43].

A stepper motor also uses magnets to create torque, but is able to divide one full rotation into steps, the number of which depends on the design of the motor. A magnetic gear is attached to the shaft, and is driven by a number of toothed electromagnets, dependent on specifications of the individual motor. The gear is designed such that the teeth only align with one electromagnet per position. To rotate the gear, one electromagnet is activated, aligning the gear to itself. The next electromagnet in line is then activated, shutting off the previous, and the gear advances to align with the newly energized electromagnet. The process is continued to cycle through the electromagnets, thus driving the motor through a number of incremental steps, which allows the motor to be moved very precisely [44].

The third motor type considered, the linear motor, is a linear actuator, which translates the torque and rotational motion into linear thrust and motion via integrated mechanisms, often in the form of ball lead screw or roller screw units, attached to a motor. They are easily controlled using logic controllers or processors, and so have become popular options in applications requiring precise motion control [45].

After comparing various commercially available motors and through deliberation, the team decided that linear actuator motors were the fit best for the final device for a multitude of reasons. Firstly, linear motors have a small and compact form factor which met the design's space constraints. Additionally, linear motors reduced the complexity of the design by eliminating the need to translate the rotational motion of common motors to linear motion. Moreover, stretching cells require very fine positional control, thereby making linear motors with high precise motion controlling ability very desirable. Consequently, the team performed extensive market research to elect the best linear motor available for the final device.

Determining Force Requirement of the Motor

In order to select the motor that will efficiently stretch the well at the desired rates but at minimal cost, a Strex® well, ST-CH-04.0-XY well, was stretched uniaxially using Instron 5544 Uniaxial Mechanical Testing Device. The well was stretched at 25% strain at 1Hz. Three separate experiments were carried out to average the maximum loads required to achieve 25% strain. The team did not strain the well at 30% since the Strex® well manual specifies the maximum strain allowed to be 20%. The dimensions of the well were input as 40mmx20mmx10mm. The thickness used, 10mm, was the thickness of the walls of the well but not the membrane. However, that value was used so that the force calculated will be more than the actual required force. The results are shown below:

Table 4. Three experiments showing maximum loads required for each maximum extension and strain

Experiment #	Maximum load (N)	Extension at maximum load (mm)	Maximum strain (%)
1	34	11	28
2	33	11	27
3	30	10	25
Average	**32**	**11**	**27**

The average maximum load was calculated to be 32N. In order to make an estimate of required force for 30%, linear interpolation was performed. Therefore, for 30% strain, 39 N forces is required. However, load and strain may not be linearly proportional due to properties of the PDMS well, the team decided to assume 45 N maximum load would be required for 30% strain. This assumption allows choosing a motor with power that slightly exceeds actual requirement. Doing so will prevent motor failures since our device may potentially exceed usage and undergo experiments that require continuous operation for 6-24 hrs.

Motor Selection for Chosen Design

Due to the amount of constraints associated to building an electronic motor-driven device to be fitted on a microscope, the MQP's success was largely dependent on finding quality motors with a high degree of functionality. As per the client's desired design specifications, the well would have to be stretched from 5-30% with a frequency of 0.01-1Hz with accuracy within 10%. In addition, the final device needs to operate for at least 6 hours. In order to build a device that meets these specifications, compact and powerful motors with accuracy and durability is required. The majority of linear actuators on the market today consist of high speed, low force actuators with large form factors, with only a small percentage of companies advertising precision movement. Among these companies is Haydon-Kerk, which provides a variety of stepper-driven linear actuators with the capacity for precision control.

The most important aspect of the motor being considered for the design was its capacity to apply a load and the rate at which it was applied. Although the PDMS well's mechanical properties could be modulated through a variety of methods, the well in possession by the team required 40N to be stretched 30%. This, accompanied by the client's desire for a device that could stretch cells cyclically at up to 1Hz, required the motor to pull at least 40N at 12mm/s. Therefore, any motor taken into consideration for use in the MQP had to meet these specifications. Haydon-Kerk provides multiple versions of the same motors, with larger form factors for more powerful motors. They also provide a variety of differently threaded models for different force/speed curves. Fig. 19 illustrates the variety of force/speed profiles for one size of motor as advertised by the company.

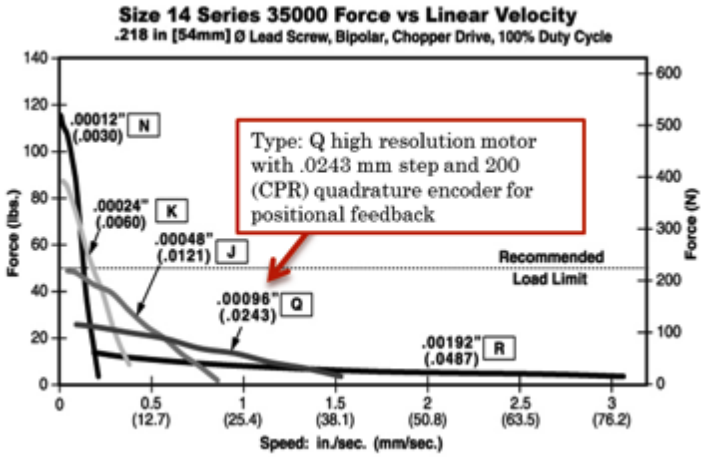

Figure 19. Force vs. speed graph for Haydon-Kerk Size 14 Thread Models (Reprinted with permission)

As seen in Fig. 19, the Q model provides a force ~22lbs at a speed of 12.7mm/s, which is faster and stronger than what the team estimated would need for the final device. In addition, Haydon-Kerk provides their motors in 200 step/revolution configuration. In the Q model, the thread has a lead pitch of 0.0243mm. Ultimately, this means that the motor would move

.0243mm per step, which is well within the desired range of error. Also, any force applied to the Q model motor if used in the device would be well under the recommended load limit as shown in the graph. Another consideration to take into account in the choice of the motor was stroke length. The client expressed interest in a total of 30% strain with the device. Using a 40x40mm well, that would amount to 12mm in either direction. Therefore, a total thrust of one inch was decided to be sufficient for this application.

In order to validate the necessity for such a powerful motor, and to better understand the basics of motor control, the team created a mock prototype to test the stretching capabilities of a single motor attached to the side of a test well. A Firgelli L12 motor with gearing option 100, obtained for testing, was used to stretch the Strex well in order to validate the calculations. Hook fixtures for the Strex well were mounted, one to a wooden block and another fixed to the clevis rod end of the Firgelli motor. The Firgelli was fixed with screws to a separate wood block, and both blocks were clamped to a board. The motor was connected to a function generator and a multimeter, and was powered using a current of 250 mA. The voltage range used to power the motor was used to control speed, from 3.5 – 12V, slowest to fastest respectively. Position was controlled by a separate voltage, over a range of 0V at start position to 5V for full extension. The Strex well was placed on the hooks, and the motor was run to stretch the well. The mock prototype and test setup can be seen in Fig. 20.

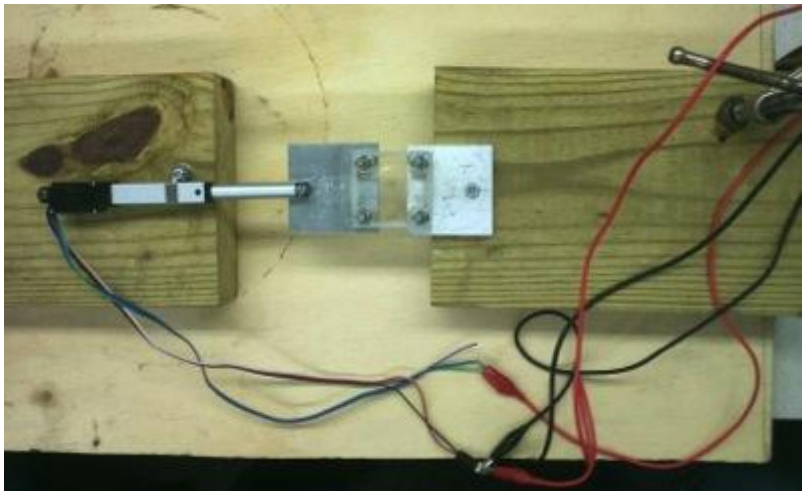

Figure 20. Mock Prototype

By using the mock prototype, it was determined that the well could be strained 30% and that the motor was capable of applying this strain. However, this came at the cost of speed, as the motor with the highest rated voltage (12V) was only able to stretch the well at ~5mm/s.. The Firgelli motor would be a suitable candidate for the design, but the force required to stretch the STREX hindered its speed to the extent that it would not be useful for the application. As seen in Fig. 21, Firgelli L12 with gear option 100 and 210 meet the force requirement of 30 N. However, as per client's request, the maximum frequency at which the substrate will be strained requires to be at 1 Hz, translating to speed requirement of 24 mm/s to strain 40x40x10 mm Strex well at 30% strain. However, both Firgelli L12 only allow ~4mm/s at 30 N (shown by black arrow in Fig. 21), failing to meet the specification requirements. In contrast, Haydon-Kerk Size 14 type Q allows approximately 4 times the speed required at maximum force required at 30N (~7lbs) (Fig. 19). These experiments served to further solidify the choice in the Haydon-Kerk motors, as they could apply a greater force than the Firgelli motor while maintaining an adequate speed.

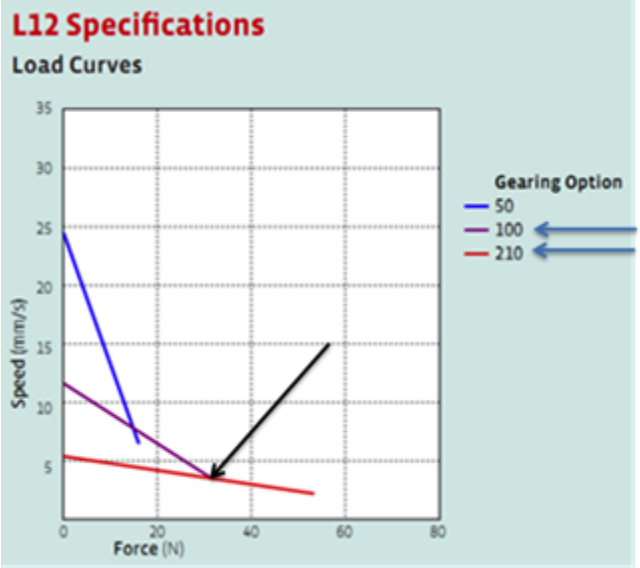

Figure 21. Force vs. speed graph for Firgelli L12 with different gear option (Reprinted with permission)

Another important factor to consider was the overall size of the motor. Due to the microscope the device will be used on, size was one of our most limiting constraints. Specifically, the microscope arm and head restricted the device axially and vertically with regards to size, respectively. When in place, the head of the microscope became the largest constraint, only allowing 7.2cm vertically for the device. Haydon-Kerk size 14 motors have a surprisingly small form factor compared to other similar motors on the market. Having a height of only 3.2cm, the motors would fit on the microscope stage with enough space for other components of the design (Fig.22).

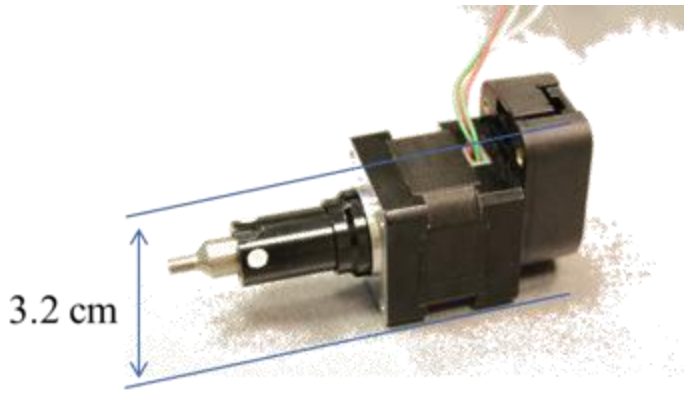

Figure 22. Haydon-Kerk Size 14 Type Q motor with encoder

In addition to having a motor tailored by the manufacturer for specific applications requiring different forces, thrust, and thread pitch, Haydon-Kerk also allows their motors to be fitted with precision add-ons that are encoders. The quadriture encoders provided by Haydon-Kerk would allow the monitoring of steps taken by the motor in either direction and provide the data as an input for programming purposes. This would allow precision control of the motors as well as allow the creation of safeguard and therefore providing preventative means against damaging either the device or the microscope.

Motor Controls

Motor controllers, drivers and user interfaces for command delegation were extensively researched in order to successfully operate the Haydon-Kerk Series 14 linear actuators. For a motor controller, the Arduino Mega 2560 was chosen due to its versatility and potential troubleshooting support. Four Big Easy Drivers from www.sparkfun.com were chosen to drive the four linear actuators because of their proven reliability and low-cost. Tying everything together will be a LabVIEW interface focused on easy utility and user friendliness.

Motor controllers, drivers and user interfaces for command delegation were extensively researched in order to successfully operate the Haydon-Kerk Series 14 linear actuators. For a

motor controller, the ChipKit Max32 was chosen due to its versatility and potential troubleshooting support. Four Big Easy Drivers from www.sparkfun.com were chosen to drive the four linear actuators because of their proven reliability and low-cost. Tying everything together is the software user interface, MPIDE.

The ChipKit Max32 microcontroller board is based on the PIC32MX795F512 chip as seen in Fig. 23 below. Functioning at a clock speed of 80 MHz, the ChipKit utilizes 83 digital input/output pins to send and receive commands; more than enough to support four linear actuators and digital encoders. The board can be powered by either a 6 to 20 volt external power supply via the power jack or through the micro-USB port parallel to the power jack. Communication with the ChipKit is accomplished through the USB port and MPIDE software that can be downloaded for free from https://github.com/chipKIT32/chipKIT32-MAX/ downloads. MPIDE is used to create programs which can be uploaded and saved to the board's 512K of flash memory and 128K RAM[46].

Figure 23: ChipKit Max32 Controller (Reprinted with permission)

The Easy Driver from www.sparkfun.com is a cheap and popular solution to drive a variety of stepper motors (Fig. 24). Primarily for bi-polar stepper motors, the Easy Driver has the capabilities to drive motors up to .750Amp/phase, which is over the 570mA/phase needed to operate the Haydon-Kerk Series 14 linear actuator. Because the driver acts as a chopper microstepper, it defaults to a 8 step microstepping mode that needs to be compensated for when programming the user interface. Lastly, the driver can take a maximum motor driver voltage of 35V, ample enough voltage to accustom the 5V motors [47].

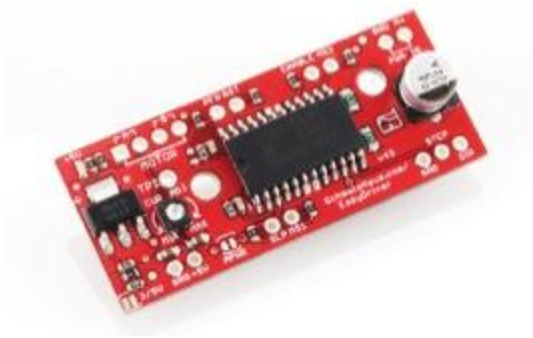

Figure 24: Easy Driver (Reprinted with permission)

In order to test the feasibility of the proposed motor control setup, a prototype was constructed as depicted in the schematic shown in Fig. 25. First, a 12V power supply (Fig. 25, A) is used to supply power to the motor (Fig. 25, E). The ChipKit Max32 micro-controller (Fig. 25, B) receives programs from a computer (Fig. 25, D) and transmits the commands to the Easy Driver (Fig. 25, C). These drivers, in turn, translate commands into electric pulses to the motor.

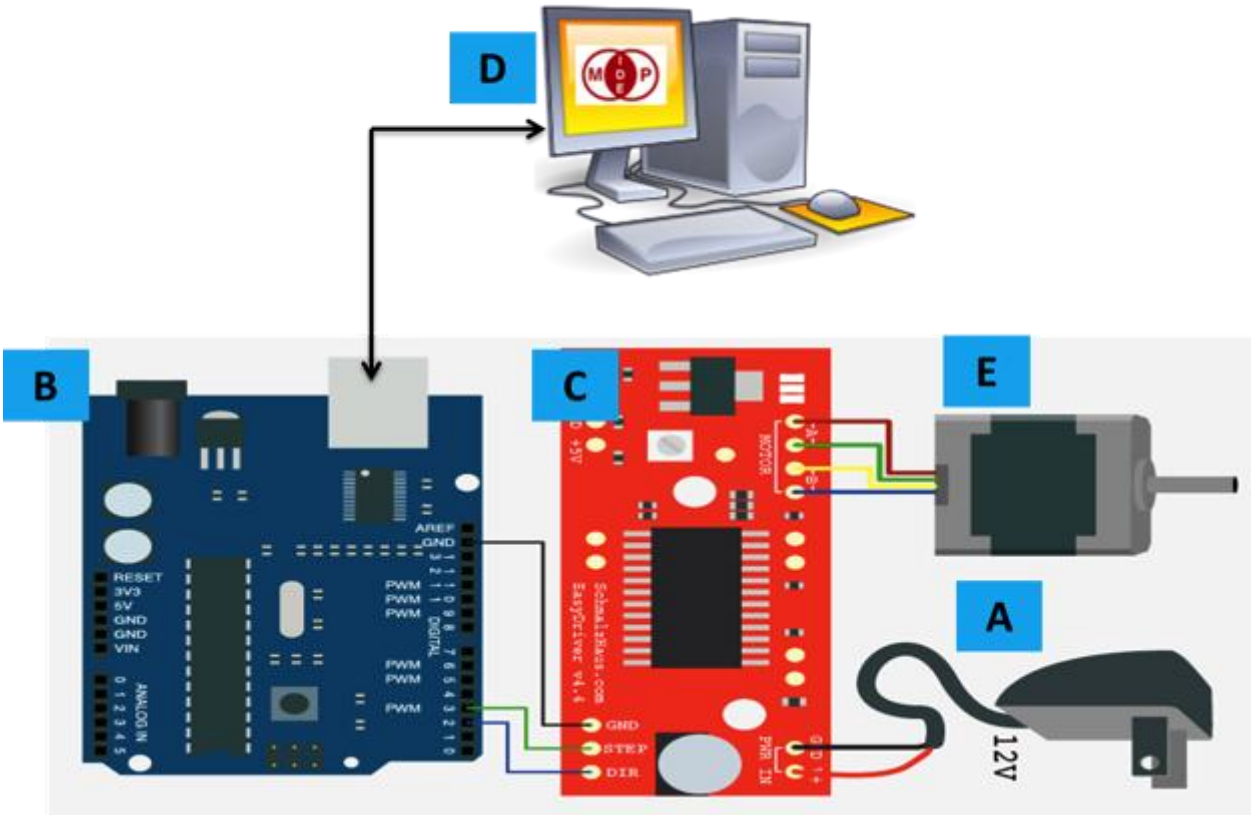

Figure 25. Schematic of motor controller and driver (Reprinted with permission)

Prototype construction started with the soldering of the four wire leads of the linear actuator to the motor pins of the Easy Driver in their appropriate locations. Next, the two wires to the power supply (V+ and GND) were soldered to the driver along with the three wires (GND, step and direction) for the ChipKit Max32. The controller pins were connected to the ChipKit at their appropriate pins and the microcontroller USB was plugged into the computer. For initial testing of the prototype, MPIDE was installed and the following code was written to operate the motor:

```
#define DIR_PIN 2
#define STEP_PIN 3

void setup() {
```

```
  pinMode(DIR_PIN, OUTPUT);
  pinMode(STEP_PIN, OUTPUT);}
void loop(){
//rotate a specific number of microsteps (16 microsteps per
step)
  rotate(5400, .5);
  delay(10);

  rotate(-5400, .25); //reverse
  delay(10);}

void rotate(int steps, float speed){
  //rotate a specific number of microsteps (16 microsteps per
step) - (negitive for reverse movement)
  //speed is any number from .01 -> 1 with 1 being fastest -
Slower is stronger
  int dir = (steps > 0)? HIGH:LOW;
  steps = abs(steps);

  digitalWrite(DIR_PIN,dir);

  float usDelay = (1/speed) * 70;

  for(int i=0; i < steps; i++){
    digitalWrite(STEP_PIN, HIGH);
    delayMicroseconds(usDelay);

    digitalWrite(STEP_PIN, LOW);
    delayMicroseconds(usDelay);}}
```

By changing the code slightly, the speed of the motor was modified as well as the length extended and retracted by the actuator arm (number of steps). More elaborate programs utilizing the Accelstepper Library were developed to provide a more defined speed control. See Appendix G for more information.

Linear Ball Slides

The success of this design relies upon the ability to apply constant strain to the cells. The mechanical strain is applied to the cells when the elongation and retraction of the motor arms

stretches and contracts the substrate on which the cells are attached. However, in our design, there are concerns of moments acting on the motor arms. The effects of moments may lead to undesirable strain patterns on the cells. Therefore, the team decided to arrange the motors in such a way that the arms of the motors are attached on and guided by linear ball-bearing slides. Doing so removes the moments affecting on the arms and place them instead on the ball slides.

As a result of removing the moment from the motor, the moment is transferred to the linear bearings themselves, which must be accounted for. The Del-tron crossed roller slides were incorporated in the design for their compact form factor and their ability to withstand relatively large loads. A quick verification was done to determine which model slide would be able to withstand the load generated by pulling the well. From these calculations, the following linear ball slides were chosen for use in the final design: RS2-1, RS2-2 and RN-3. The RS2-2 is depicted in the figure below. The calculations for the largest hook as well as the specifications for the RN series are shown below (Fig. 26 A).

The equation used to calculate the moments was M=F*d, where F is the load applied to the hook and d is the moment arm. The loads for both M1 and M2 were estimated to be 11 lb-in, well below the max recommended load for each parameter. The moment arm for both loads is the length of the hook in the y-axis, which is 1.1in. The force caused by the well resisting stretch, was estimated to be 10lbs.

A

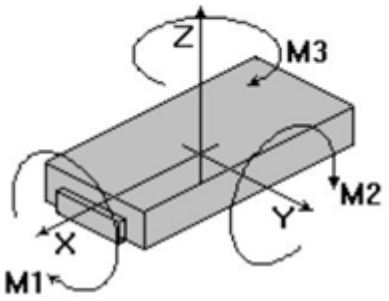

Moment	Estimated load (lb-in)	Max recommended load (lb-in)
M1	11	31.29
M2	11	68.32
M3	-	71.74

B

Figure 26. A. Moment calculation for the linear slide attaching the largest hook. B. Del-tron RS2-2 linear ball slide (Reprinted with permission)

Design Materials

To hold and transfer strain to the cell culture wells, four hook assemblies are used. In order to ensure that the desired strain (requested of the motors) is equivalent to that present on the wells, these hooks must not absorb much strain. This means they must be very stiff and deflect minimally. Stainless steel is chosen to construct the hooks. There are a number of advantages to using stainless steel. Most importantly, it is very strong and stiff, which is critical for this design, as any deflection in the structure will negatively affect the stretching of the well. To verify the structural integrity of the hooks, finite element analysis is performed on the longest hook, as it will endure the greatest stresses and strains. The hook is designed and drafted in SolidWorks, then imported to ANSYS Workbench. A bearing load of 10 Newtons, greater than

the force required to stretch the wells 10%, is applied to the hook end of the arm. Deformation in both x (Fig. 27) and y (Fig. 28) direction are analyzed using ANSYS.

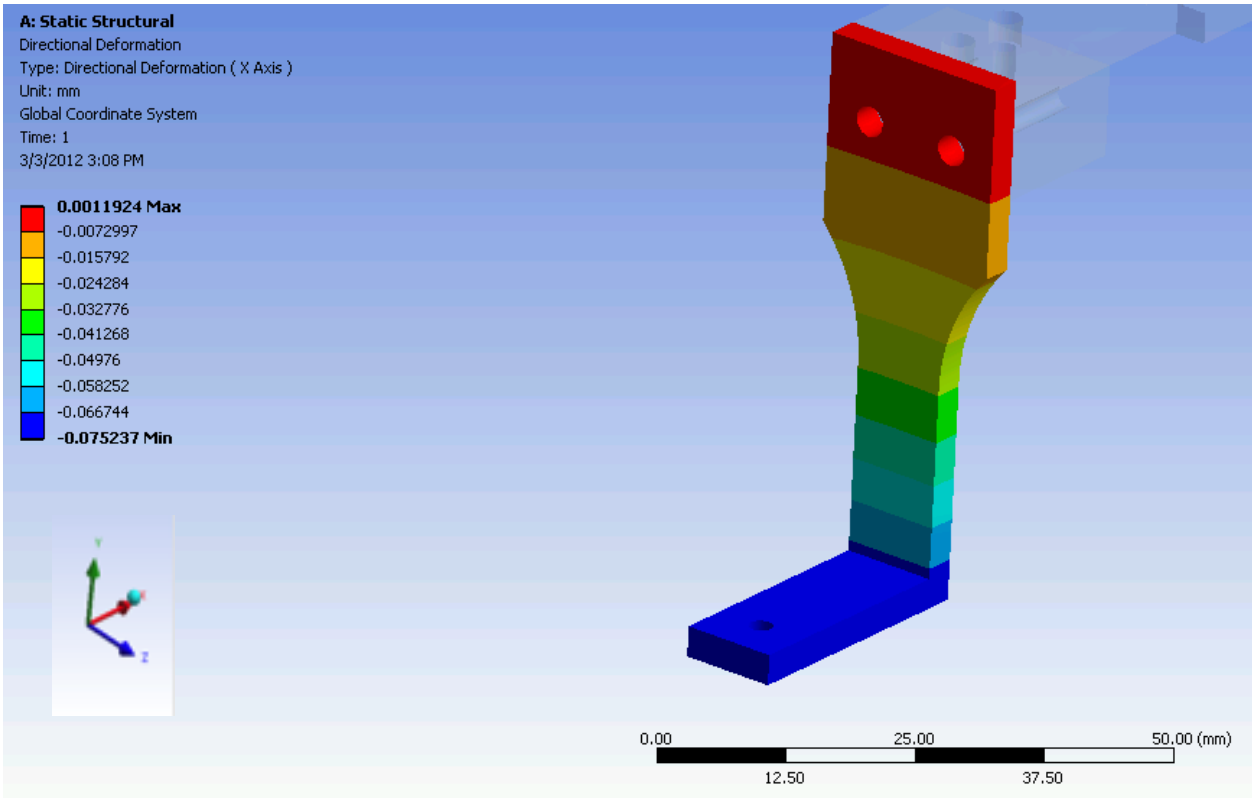

Figure 27. FEA of arm and hook: x-axis deformation

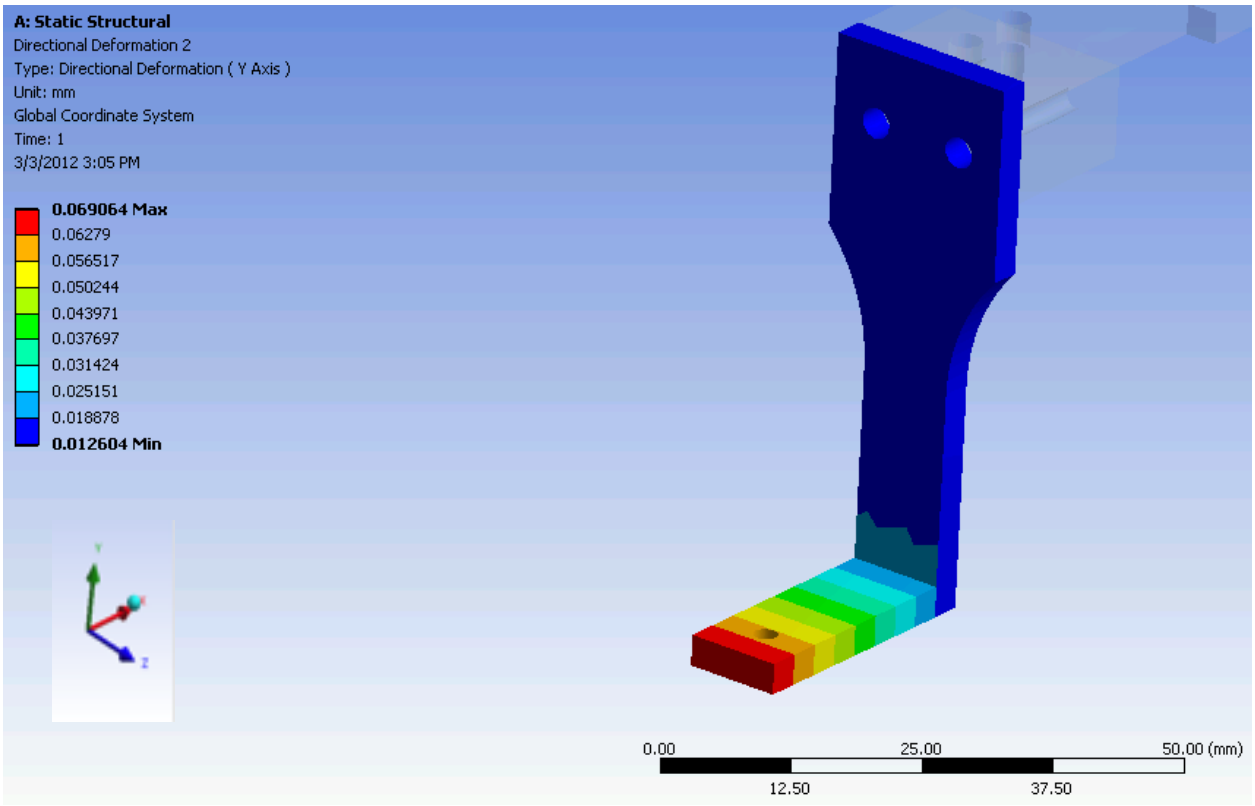

Figure 28. FEA of arm and hook: y-axis deformation

From Fig. 27 and 28, it can be seen that x-directional deformation does not exceed 0.075 mm and y-directional deformation does not exceed 0.069 mm, which are both less than 0.1% of the allowed error of 1mm at 10N. This is very small and the team considers it insignificant, and therefore these arm and hook connections are sufficient to translate strain from the motors to the wells. These analyses demonstrate that stainless steel is both strong enough to withstand the forces and stiff enough to ensure the precision of the device. In addition to meeting mechanical requirements, stainless steel is ideal for any part of this device because it is corrosion resistant, important as the device may be exposed to high humidity. Stainless steel can also be feasibly machined by the resources available. All hardware, such as screws, are stainless steel. It is again important that they do not corrode. Their strength is still favorable, and stainless steel hardware is standard and readily available.

The baseplate for the device as well as the subplate onto which the raised hook and third motor is mounted are made of 1100 aluminum. A quarter-inch aluminum plate is sufficient to support the weight of the motors and other device components, and it is stiff enough to prevent deflection. The aluminum will not rust or corrode, and because it is lightweight, the overall weight of the device can be minimized. Lastly, rubber feet are added on the bottom of the plate. This is a standard material for motion-resistant, surface-preserving feet for most devices, and they can be easily obtained and attached to the baseplate.

Final Design Prototype

In order to check the final design's dimensions, a prototype of the CAD model was materialized and fit to a Zeiss inverted microscope with motorized stage. The design's hooks, motor mounts and motors were created from rapid prototyping the exact parts that were defined in the SolidWorks model of the final design. Next, using a CAD drawing of the baseplate, a piece of 6.35mm wood composite was accurately cut to size using a table saw and a file to smooth the edges. The same process was used to create the subplate from a piece of 3.175mm wood composite. Lastly, using a jig saw, a 70mm x 60mm hole was cut in the baseplate and all components were prepared for assembly.

Assembly of the prototype was accomplished by following the conditions set forth by the SolidWorks model. First, three of the four linear ball slides were strategically fixed to the baseplate with double sided tape. The rapid prototyped motor mounts were pasted to the plastic motors and then glued to their proper locations on the baseplate and subplate. Subsequently, the fourth linear ball slide was taped to the subplate which was then adhered to the largest of the four slides on the far right of the baseplate as seen in Fig. 29. Finally, the four rapid prototype hooks

were fixed on top of the linear slides and the fully assembled prototype was placed on the motorized stage of the microscope for dimensional analysis.

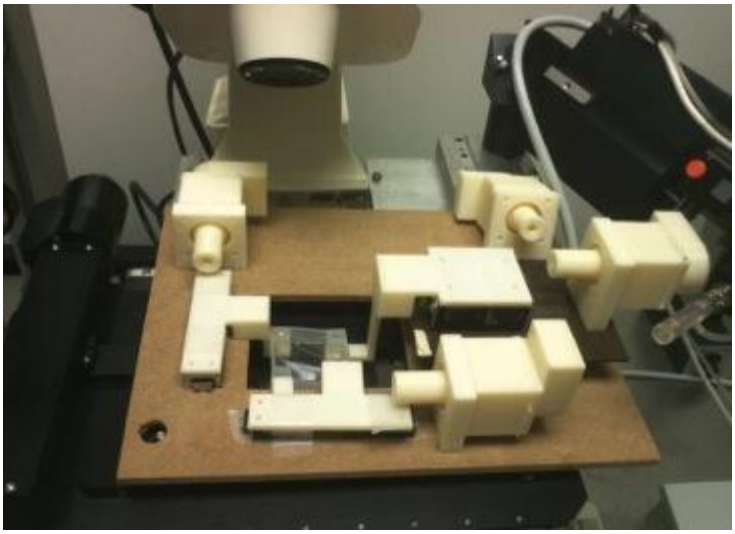

Figure 29. Prototype on microscope stage with light up

As seen in Fig. 30 below, assessment of the prototype's arrangement was carried out while positioned on the motorized microscope stage. First, the prototype was checked for clearance issues. The main concern of the design was centered around the elevated hook on top of the subplate. Though close, the hook managed to miss colliding with the light of the microscope (Fig. 30). To make this less of an issue, alternative designs were evaluated. Secondly, lower hook clearances (where the well sits) were examined. The subplate hook and the far left hook faintly grazed the top of the motorized stage. To fix this, the hooks were shortened by 1mm. Lastly, the decision was made to slightly lower the sitting height of the design by cutting around a small elevated portion of the motorized stage. This allowed for better positioning of the device and more leeway for subplate clearances.

Figure 30. Prototype on microscope stage with light down

Substrate Design

While testing the mechanical properties of the STREX well, it was observed that the well would "twist" at the corners when strained uniaxially, as seen in the figure below (Fig. 31). This reorientation of the corners create strain concentrations around the edge of the well that, combined with the inward deflection of the walls due to Poisson's Effect, would decrease the amount of area useful for data collection. In order to examine if this is actually the case, simulation models were run using ANSYS software.

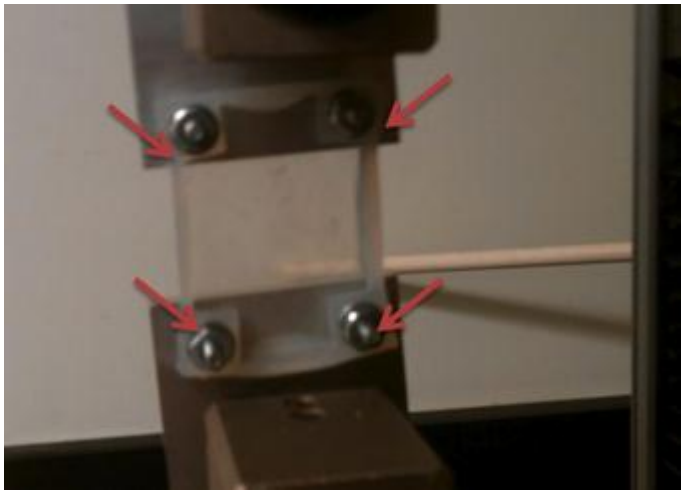

Figure 31. Strex well being stretched uniaxially (twisted corners are shown in red arrows)

Finite Element Analysis of PDMS Well

In order to effectively apply mechanical force to the cells, a soft substrate onto which the cells will be cultured is needed to translate the mechanical forces from the motors to the cells. However, it is essential to investigate the strain field in the area of interest in which the cells are seeded to understand the actual strains the cells experience on the substrate. Such knowledge will enable investigators to determine the relation between strain produced by the motors and the strain suffered by the cells. Additionally, the designs of the substrate on which the cells will be seeded depend largely on its ability to provide uniform strain field for a specific area of interest. Only when cells are seeded onto the uniform strain field region of the substrate will the experiments be accurately controlled. Therefore, before fabricating a specific cell culture well, simulation models are required to determine if it can provide sufficient area of constant strain field.

The team chose to use cell culture well similar to Strex® well since it is a commercially available PDMS well. In addition, the well was readily available to the team in Prof. Billiar's lab. FEA of the well was performed using ANSYS Workbench. The local strain, which is related to the global strain, of the well surface onto which the cells will be seeded under mechanical stimulation was investigated. A solid model was first constructed by the team using SolidWorks, and this model was then uploaded to ANSYS. PDMS was created as a new material in ANSYS, using a linear elastic model with an elastic modulus of 2.5 MPa and .45 Poisson's ratio. Simulation forces and constraints were then defined for 10% equibiaxial strain. At each corner, a displacement load was applied using both x and y components. The top-left corner displacement was defined to be -2mm along the x-axis and 2 mm along the y-axis. The top-right corner displacement was 2mm along the x-axis and along the y-axis, the bottom-right corner

displacement 2mm along the x-axis and -2mm along the y-axis, and the bottom-left corner displacement -2mm along the x-axis and -2mm along the y-axis. In order to ensure the forces would accurately represent the forces created by the posts of the hooks, the cylindrical faces of the hook holes were divided into two sections using small extrusion defects added in SolidWorks. The faces were broken such that the division was perpendicular to the direction of the applied forces. The geometry and setup were then transferred to ANSYS Mechanical APDL and strain fields were generated.

X-directional as well as y-directional strain fields were generated and are shown in Fig. 32 and Fig. 33. The scale for each of the results was made identical for comparison.

A uniaxial simulation was also performed. Stretch was applied along the x-axis, and in Fig. 34 and 35, resultant strain along the x-axis and the y-axis are examined.

Since the wells were strained 10%, acceptable area was defined as 10% strain with 10% error, meaning strain between 9 and 11%. Areas colored in green and yellow correspond to this 9 to 11% area.

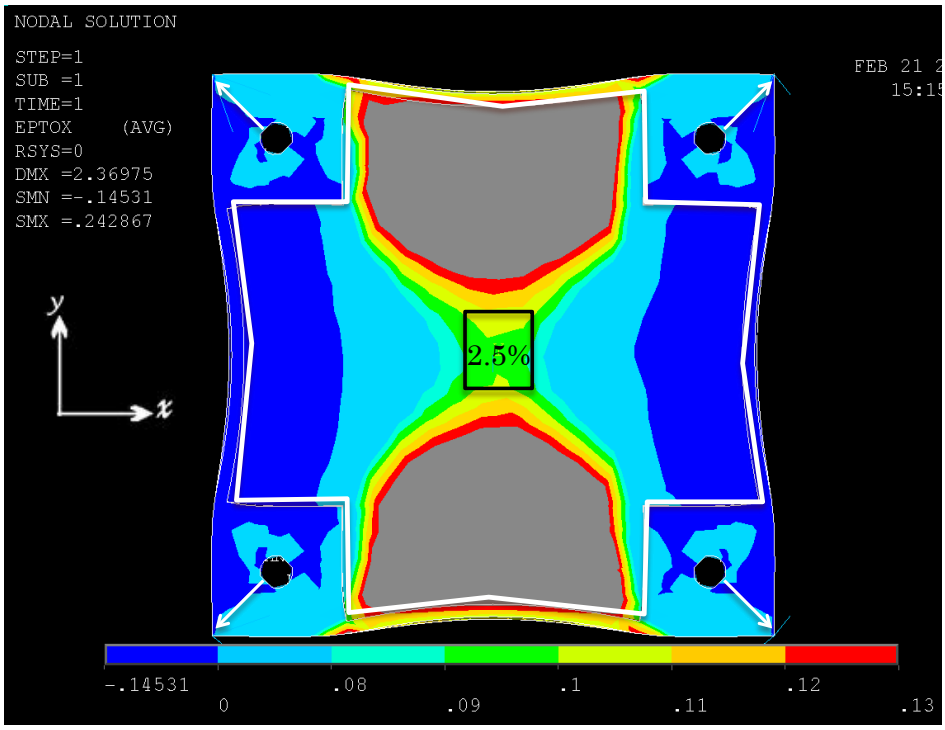

Figure 32: FEA: Axial strain field of Strex Well, 10% equibiaxial, x-directional

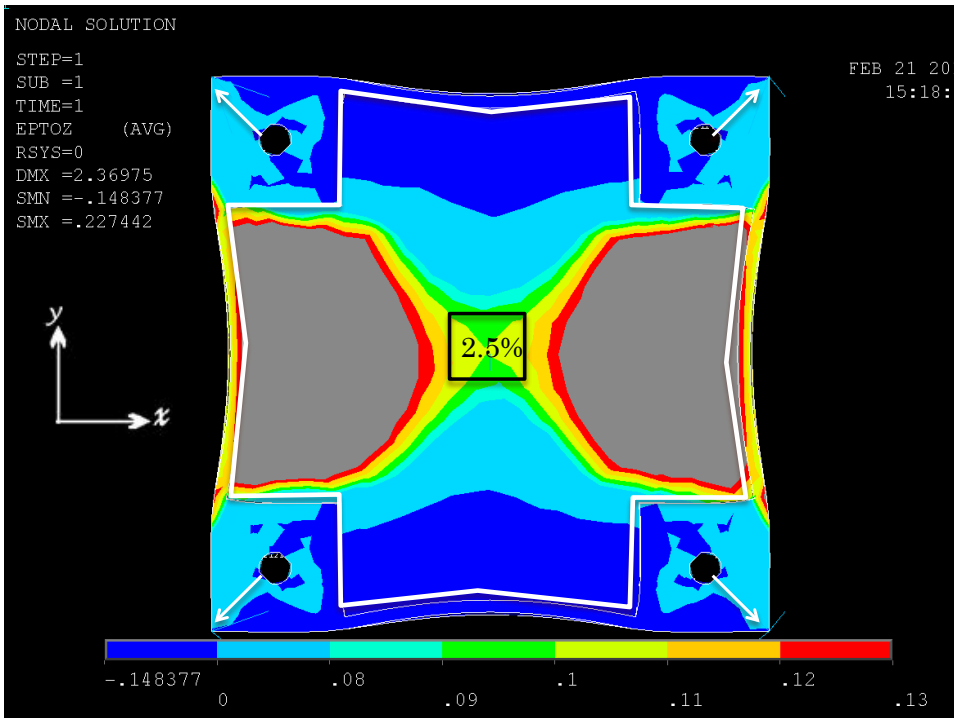

Figure 33: FEA: Transverse strain field of Strex Well, 10% equibiaxial, y-directional

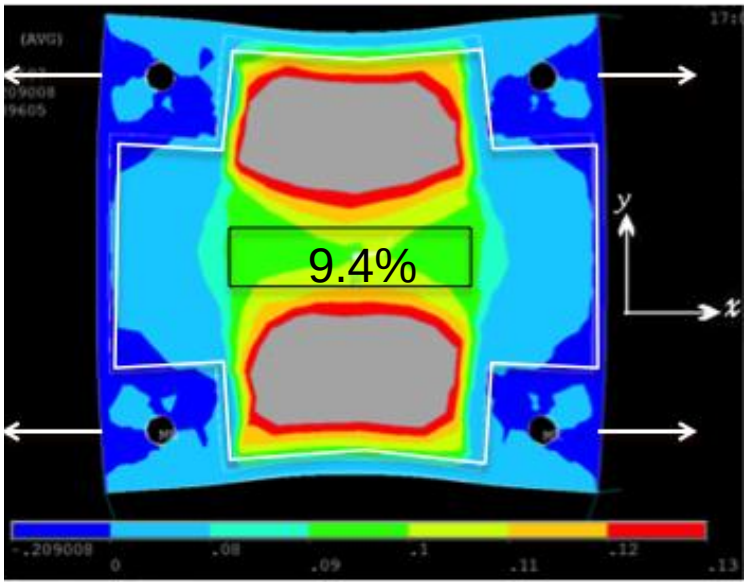

Figure 34: FEA: Axial strain field of Strex Well, 10% uniaxial, x-directional

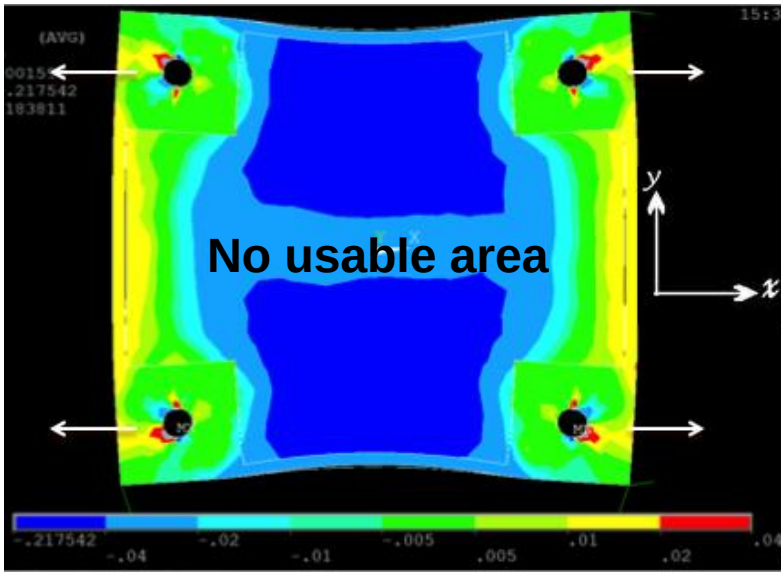

Figure 35: FEA: Transverse strain field of Strex Well, 10% uniaxial, y-directional

It can be seen from the figures that there is a relatively small area in the center of the well with a uniform strain field compared to total area of the well, and when the axial strain is superimposed over the transverse strain, the overlapping usable area was about 2.25%. This means that cells must be seeded in the small area of uniform strain in order for them to

experience the same strain, resulting in a larger area of interest, which will burden imaging of the cell behavior. It must be noted that outside this area there are stress concentrations, greatly increasing strain. Therefore, these areas should be avoided when seeding or observing cells.

After the strain field of the Strex® well had been analyzed, it was evident that during equibiaxial stretch, the uniform strain field area was actually small compared to the total area of the well. In addition, the equibiaxial Strex® well provides almost no uniform strain field when the well is stretched uniaxially (Figs. 34 and 35). Only 9.4% uniform area is observed in x-directional (Fig. 34) and no usable area was obtained in y-directional (Fig. 35) since strains in the middle region are much less than 10% strain simulated. Since this project requires the device to stretch uniaxially and equibiaxially, it is important for the soft substrate to provide considerably large and consistent uniform strain field whether it is stretched uniaxially or equibiaxially.

Custom made PDMS well

As noted earlier, the inconsistent strain field of the equibiaxial Strex well may due to the twisting of the corners when the well is stretched uniaxially. In order to minimize this effect with the intent to create a more uniform strain field, a new well was created. In the new well, the thin walls were aligned with the posts, thereby preventing the reorientation of the corners when stretched uniaxially.

This custom well was then analyzed using ANSYS through the same procedure as for the Strex® well. These results are shown below (Fig. 36, 37, 38, 39).

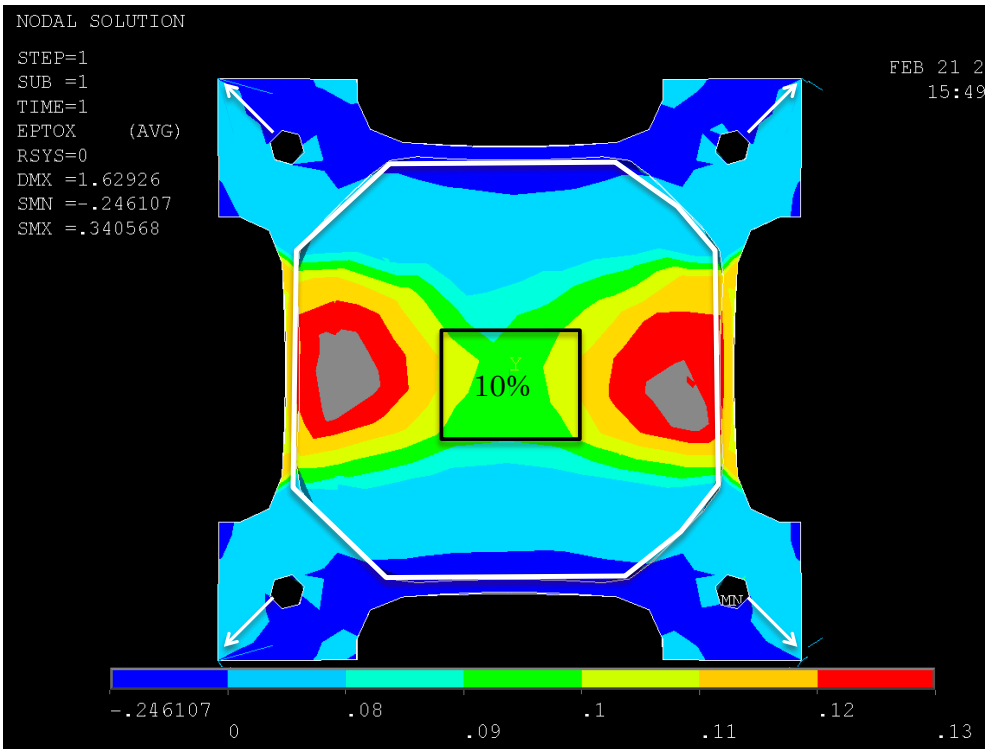

Figure 36: FEA: Axial strain field of Custom Well, 10% equibiaxial, x-directional

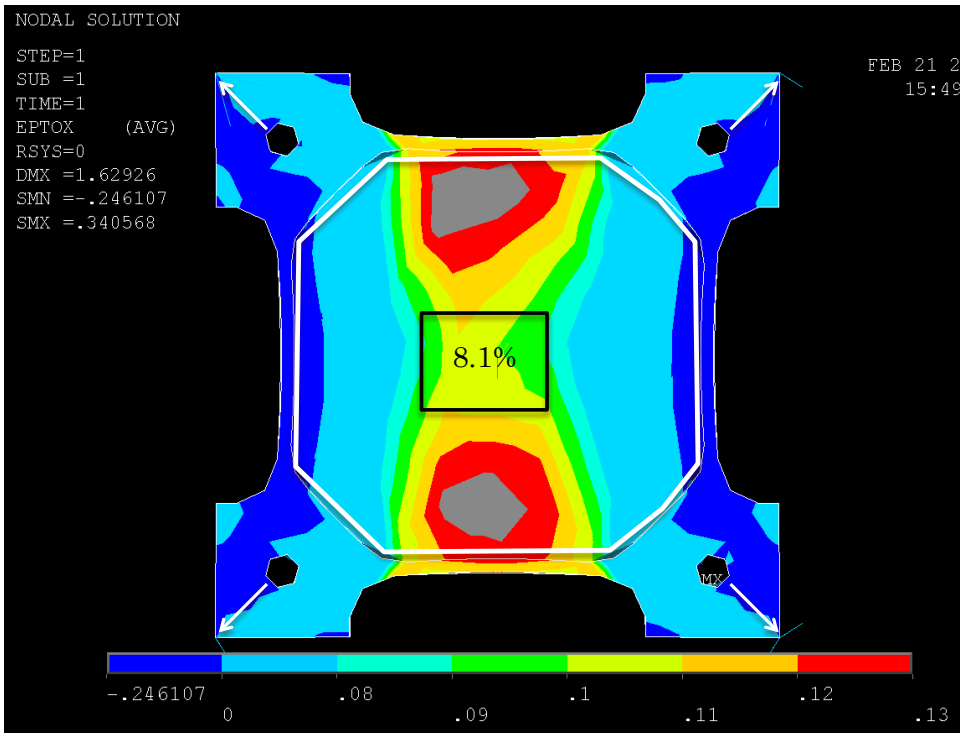

Figure 37: FEA: Transverse strain field of Custom Well, 10% equibiaxial, y-directional

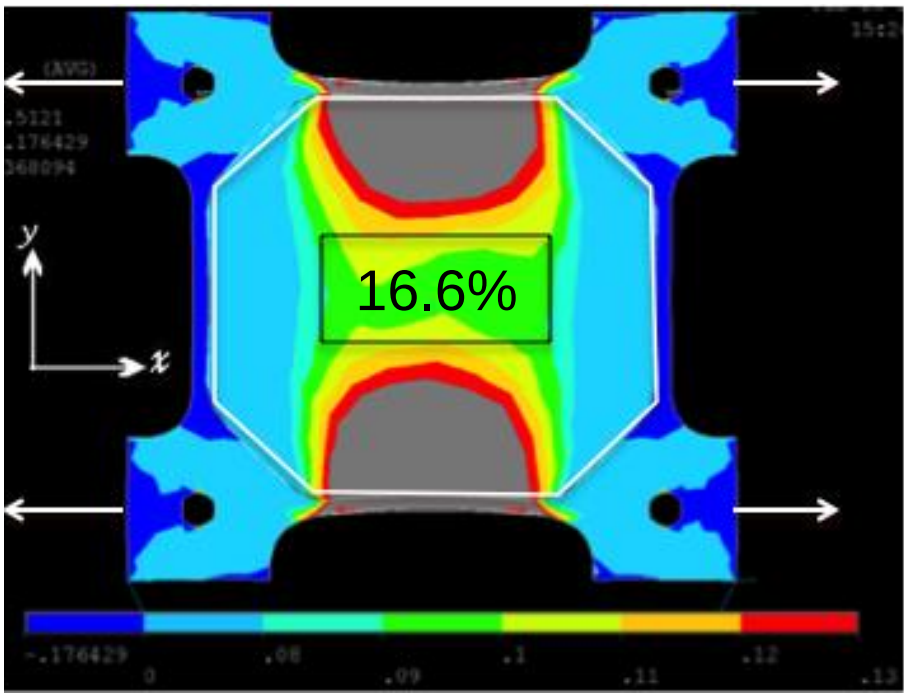

Figure 38: FEA: Axial strain field of Custom Well, 10% uniaxial, x-directional

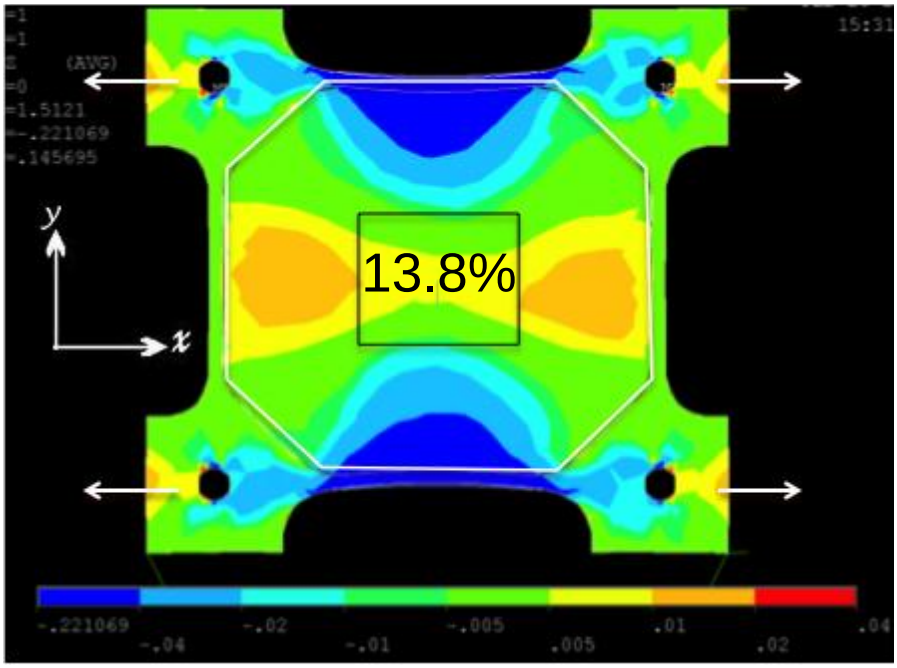

Figure 39: FEA: Transverse strain field of Custom Well, 10% uniaxial, y-directional

It was observed that the usable area of the custom well is a vast improvement on the Strex® well. When the axial and transverse strain fields were superimposed, overlapping usable equibiaxial area was about 9% and uniaxial about 12%. It was calculated that the usable area of the custom well is 300% larger during equibiaxial stretch and during uniaxial stretch the Strex® well did not have any usable area.

With this analysis as verification of the custom PDMS well design, the well was next constructed.

Final Design Construction

Device Construction

The purpose of this section is to provide a brief overview of each part used in the final assembly of the device, including how each was created, and how it fits into the assembly.

All parts and subassemblies are secured to the base plate (Fig. 40), which contains mounting points for three linear slides, three motor mounts, stationary hook, and connector mount via clearance and tapped holes. The plate, made of 1/4 in. thick 1060 alloy, was manufactured through water jetting, with various clearances and tapped holes made manually as the design progressed.

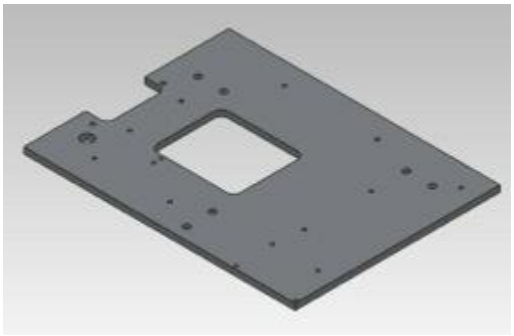

Figure 40: Baseplate

The motor mounts (Fig. 41) were created simply to secure the motors to the baseplate while providing ample clearance between the motor arm and the linear slide subassembly. Made of 5/8 in. thick 1060 alloy, the motor mounts were created on campus through the use of CNC machining.

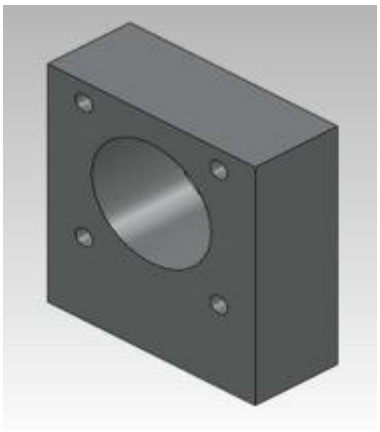

Figure 41: Motor Mount

The subplate (Fig. 42), which is secured atop the Del-tron linear slide RS2-2, contains mounting points for one motor mount, one Del-tron RN2 slide, and one subplate L-bracket. The subplate, created from 1/8in. thick 1060 alloy, was created manually and tapped.

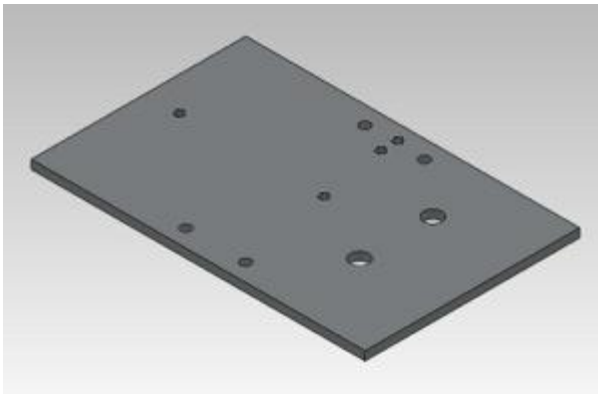

Figure 42: Subplate

The L-brackets (Fig. 43, A) and hooks (Fig. 43, B) were all created from 304 alloy for corrosion resistance and strength. All angles pieces were created from 3/16in thick angle stock, which was cut down to shape through water jetting. This was done to limit the deflection in the parts caused by machining relatively thin material. The three L-mounts are secured to the hook assembly via screws, while also securing the motor arm to the hook assembly via a nut. The subplate L-mount connects one motor arm to the subplate. All hooks are connected to stainless steel blocks which contain tapped threads.

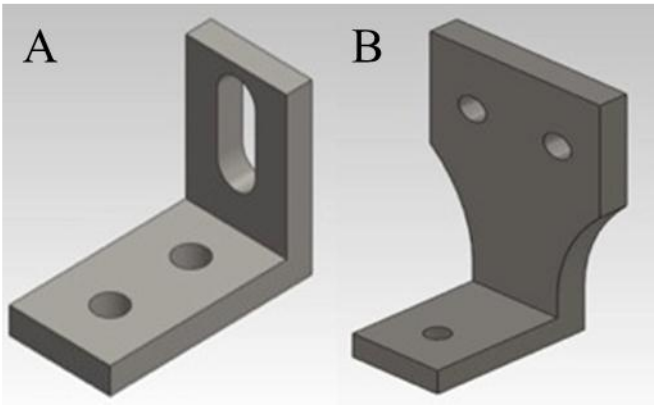

Figure 43: (A) L-Bracket and (B) Hook

The hook mounts (Fig. 44) were also water jet parts, but were created from scrap 1/8in. thick 304 alloy material. The hook mounts function to secure the blocks and hooks to the linear slides via screws. These parts were created through water jetting.

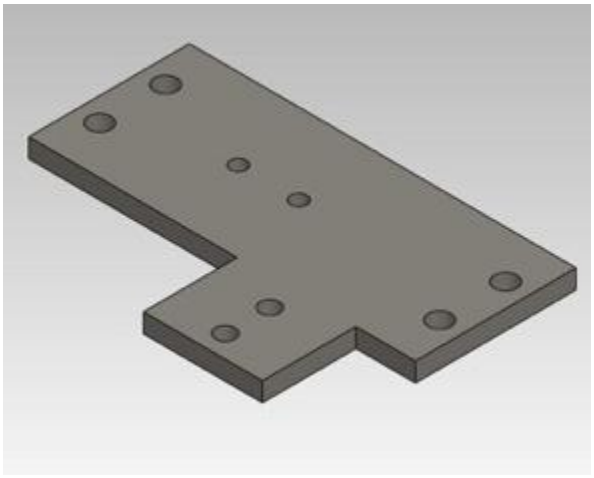

Figure 44. Hook Mount

The connector mount (Fig. 46), made from 1/4in thick 1060 alloy, was created to secure the female connectors for the motors and encoders to the baseplate. This part was created through water jetting.

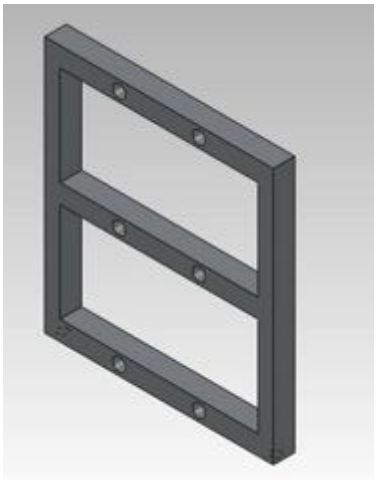

Figure 45: Connector Mount

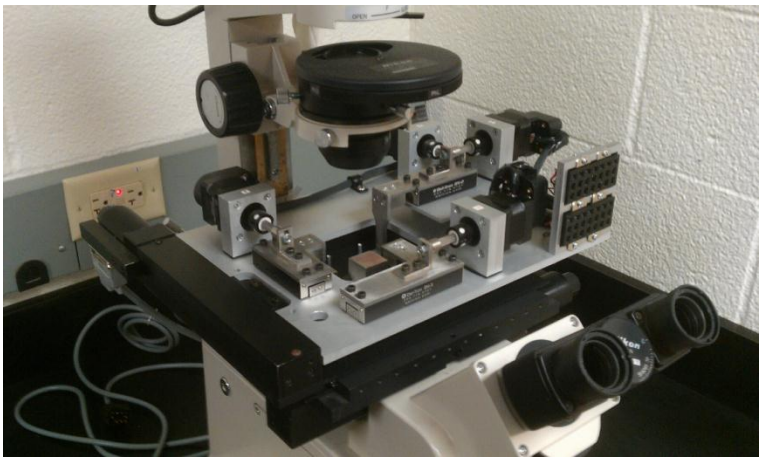

Figure 46. Final Device Placed on an Inverted Microscope

The final design of the device is shown in Fig. 46, which displays all of the components depicted above assembled together and mounted on a Nikon inverted microscope. All 1060 alloy components were anodized for increased wear and corrosion resistance.

Housing Unit

A housing unit was created to hold all of the communication and driving components associated with the device, as seen in Fig. 47 below. A 12V DC power supply (D) was used to power the device. From here, the 12V power went to a 5 Amp voltage regulator (C) where it was adjusted down to 8V through an onboard potentiometer. Dialing the voltage to 8V was confirmed using a multimeter. Next, the 8V power was soldered in parallel on a shield unit which sits atop the ChipKit Max32 controller (A). Power was distributed to each of the Easy Drivers (B) through the P+ and P- (Gnd.) pins and to a small green LED on the front of the housing unit (two 150 ohm resistors were used for LED). Refer to Appendices D-F for Easy Driver, ChipKit 32Max controller and voltage regulator schematics.

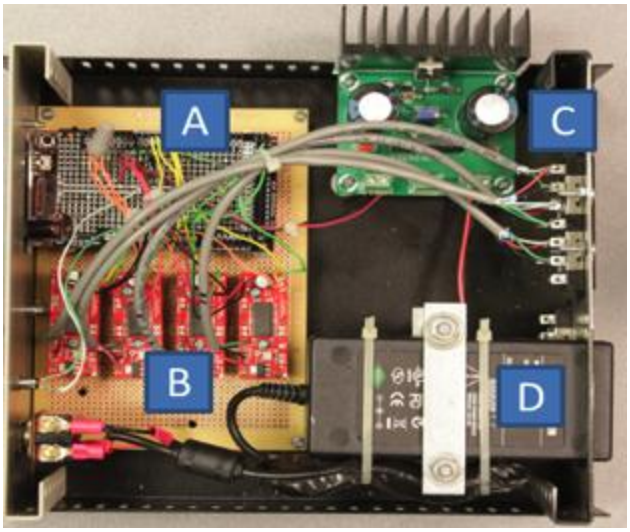

Figure 47: Instrumentation Housing Unit – (A) Chipkit Max32 Controller (B) Four Easy Drivers (C) Voltage Regulator (D) 12V DC Power Source

Figure 48: Housing Unit

Communicating with the motors was done in a three part process. In part one, MPIDE software was used to write programs that would then be uploaded and executed by the motors through a micro USB jack on the front of the ChipKit Max32 controller. The coding library used was called accelstepper. Refer to Appendix G for software downloads and code examples. Part two included the controller's relay and translation of the programs made in MPIDE to the motor

drivers. This was executed by calling step and direction pins in the program and making the physical connections of the corresponding pins to the desired driver (Ex. If step pin 4 was claimed in the program, step pin 4 on the controller is the called pin). The current setup for step and direction pins for each motor can be seen in Table 5 below.

Table 5: Step and Direction Pins Associated with each Motor

Motor	Step Pin	Direction Pin
1	3	25
2	2	31
3	4	23
4	5	29

Part three involved the transmission of current/voltage signals from motor drivers to stepper motors. The device utilizes the 5 volt version of the Haydon Kerk size 14 motors (Type Q). These are bipolar motors that operate at .56 Amps/phase (NOTE: the motors are currently running at .2 Amps/phase which is adjustable by the potentiometers located on each Easy Driver). The motor drivers (Easy Drivers) have four motor pins: two A pins and two B pins. Connections from the housing unit to the device were made utilizing beau power connectors and following the correct wiring diagram for the size 14 motors found in Appendix C. In Fig. 49 below, a complete wiring schematic of the housing unit can be found.

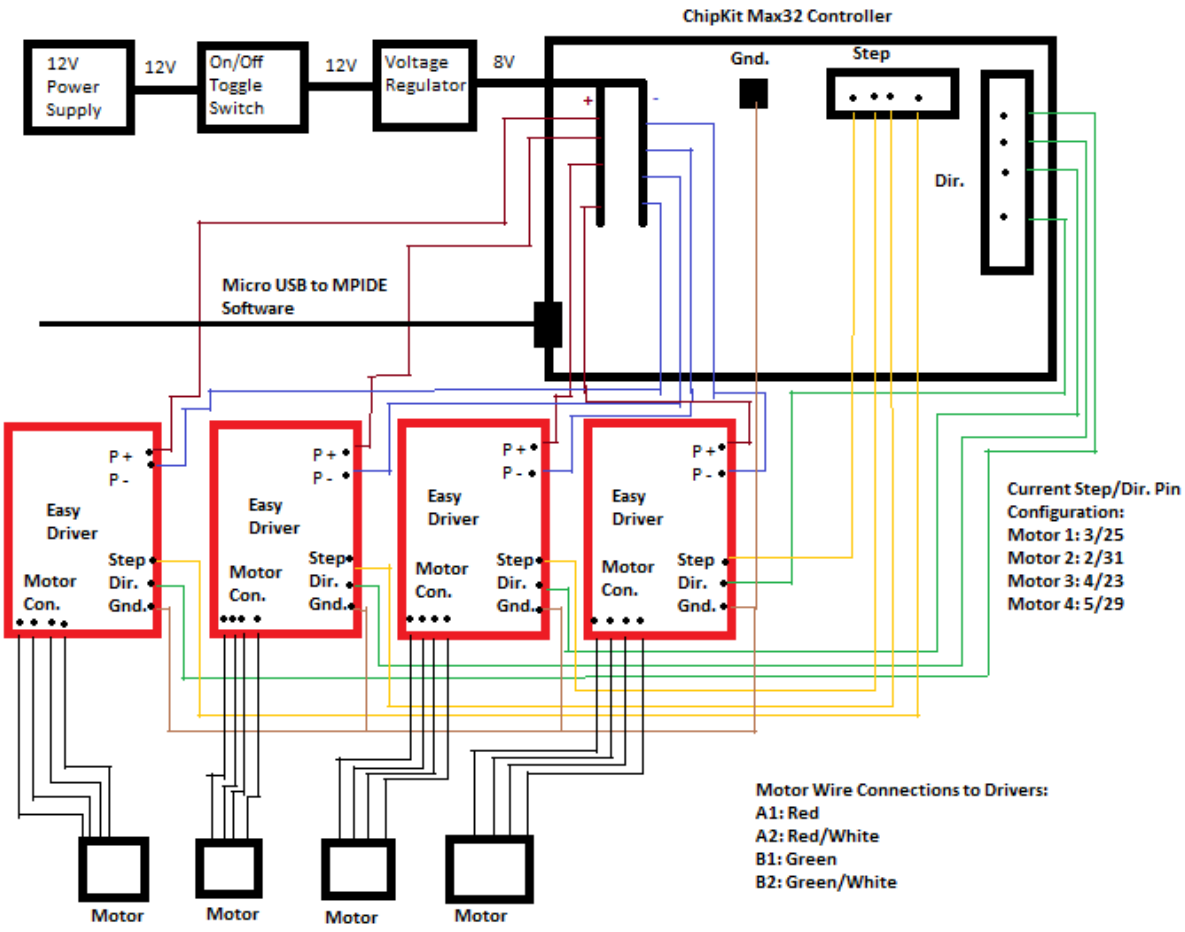

Figure 49: Schematic of Housing Unit

Substrate Development

In order to fabricate the new well, the material of which the well will be made of was chosen first. Since cells need to be seeded on the elastic substrate to apply mechanical forces, polydimethylsiloxane (PDMS) was chosen due to its elastomeric, optically transparent, and chemically inert properties. Additionally, PDMS can be fabricated easily and efficiently [45]. Furthermore, the same material was used in Strex well. Afterwards, a solid works CAD model of the mold for was drawn for manufacturing purposes (Fig. 50). Laser cutting machine at WPI was used to machine the mold. The machined components can be seen in Fig. 51.

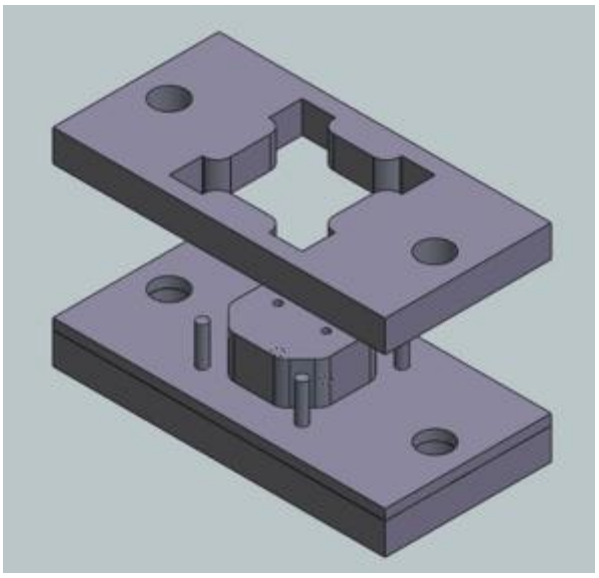

Figure 50: CAD drawing of PDMS well mold

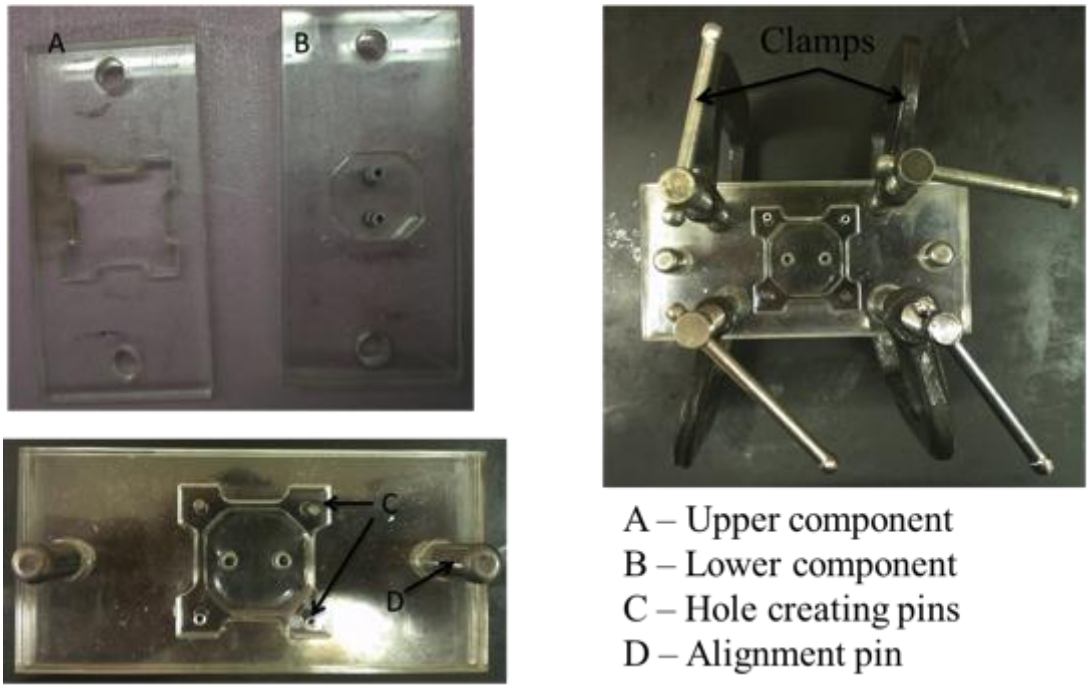

Figure 51: Components of the PDMS well mold

As seen in Fig. 51, components A and B are aligned with large pins D. Small pins C are placed in the mold to create holes in the cured PDMS well frame. These holes will attach well to

the hooks of the final device. To prevent leakage from the mold, external clamps are used to tighten the component A and B.

PDMS well fabrication

PDMS is molded into square-like shape well with a thin PDMS film of 0.004" thick (Thin silicone membrane, SSP-M823, Specialty Silicone Products) glued to the bottom for seeding cells. PDMS culturing well was fabricated using the protocol established in Dr. Billiar's lab. Sylgard 184 silicone elastomer base is mixed with Sylgard 184 silicone elastomer crosslinker in 20:1 ratio (Sylgard elastomer kit, Dow Corning). After the base and corsslinker are very well mixed, the mixture is placed in the vacuum chamber for 5 minutes to degas. After 5 minutes, remaining excess bubbles are removed by using nitrogen gas. The mixture is then poured evenly into the mold show in Fig. 51. The PDMS with the mold is then incubated in the oven at 50^{o}C for overnight, after which the PDMS mold is taken out. The mold and PDMS film are then sterilized with 70% ethanol and exposed under ultraviolet rays for 15 min. The mold and film are glued together by medical grade silicone adhesive (Silbione MED ADH 4100 RTV, Bluestar Silicones) under the biosafety hood in sterilized conditions. The flowchart of PDMS well fabrication is shown in Fig. 52.

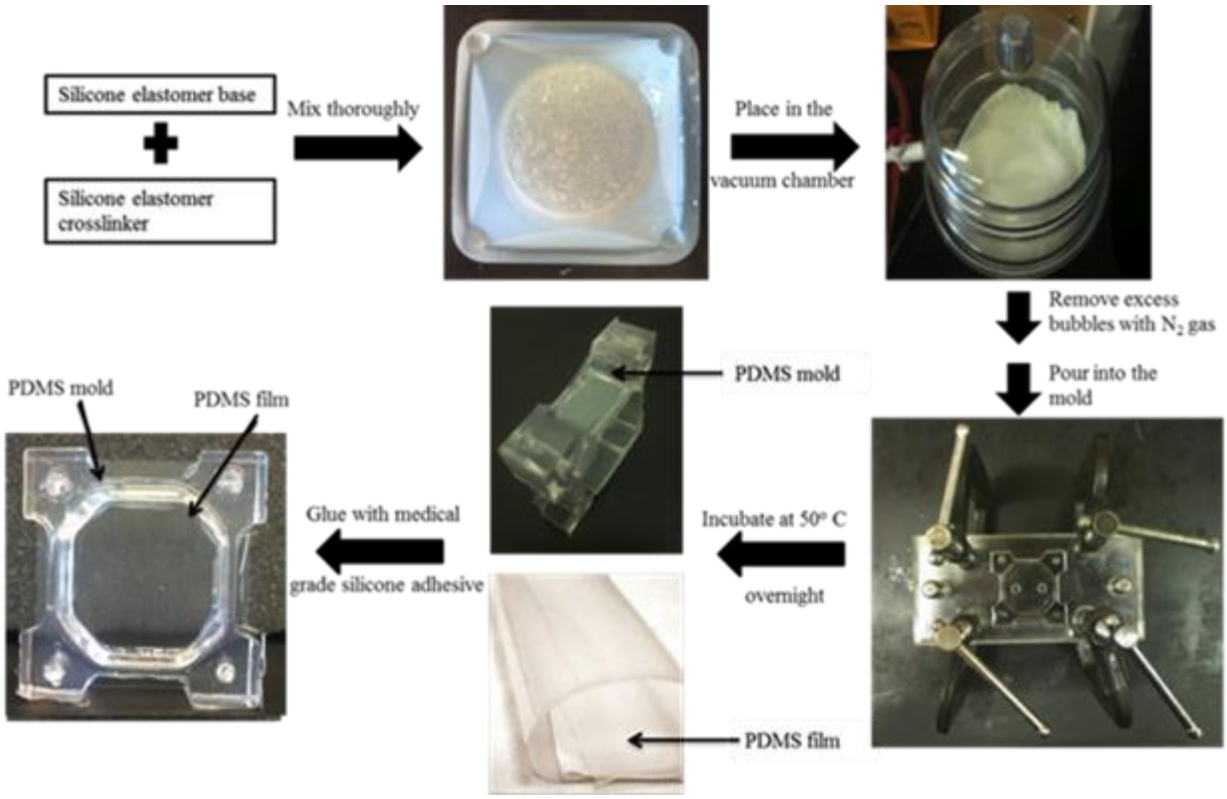

Figure 52: Process of making PDMS cell culture well

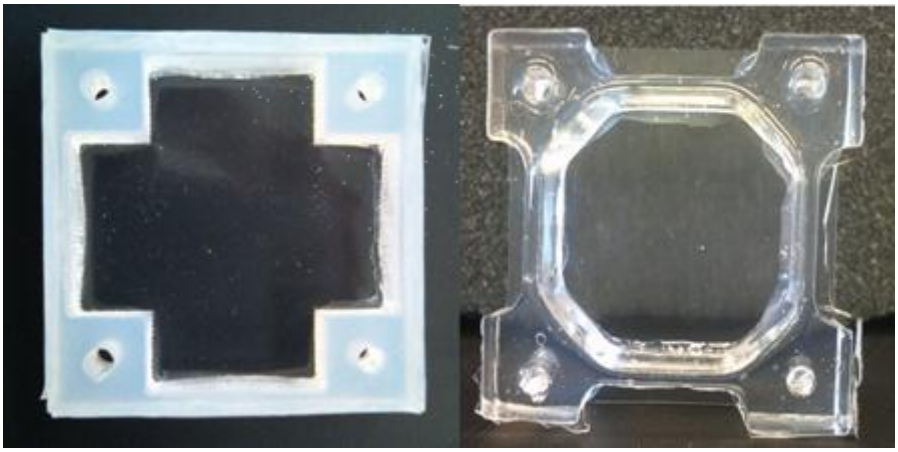

Figure 53: Strex well (left) and custom well (right)

Final Device Validation

In order to ensure that the final device works properly and meets the expectations of clients, validation tests were conducted on the device as well as the substrate. High Density Mapping (HDM) technique was used to map the strain fields in the well. Operating time was

validated by measuring motor temperature. Max frequency requirement was confirmed by measurements obtained from HDM strain data.

Well Validation

Additional analysis was performed to confirm the superiority of the custom designed well using HDM Both wells were dusted with highly reflective particles and then stretched using the team's device while a digital video recording was made to capture the deformation. HDM analysis was performed for cyclical uniaxial stretch at 1 Hertz and at 10%, 20%, and 30% strain for the Strex® well and the custom well using both the 20:1 and 15:1 PDMS ratios. The videos were analyzed using a special HDM computer program that tracks the reflective particles, and these results were further analyzed in Matlab to create graphical strain field maps. The results for the Strex® well and the 15:1 custom well at 10% strain can be seen below in Figures 54 and 55. Additional HDM results can be found in Appendix I.

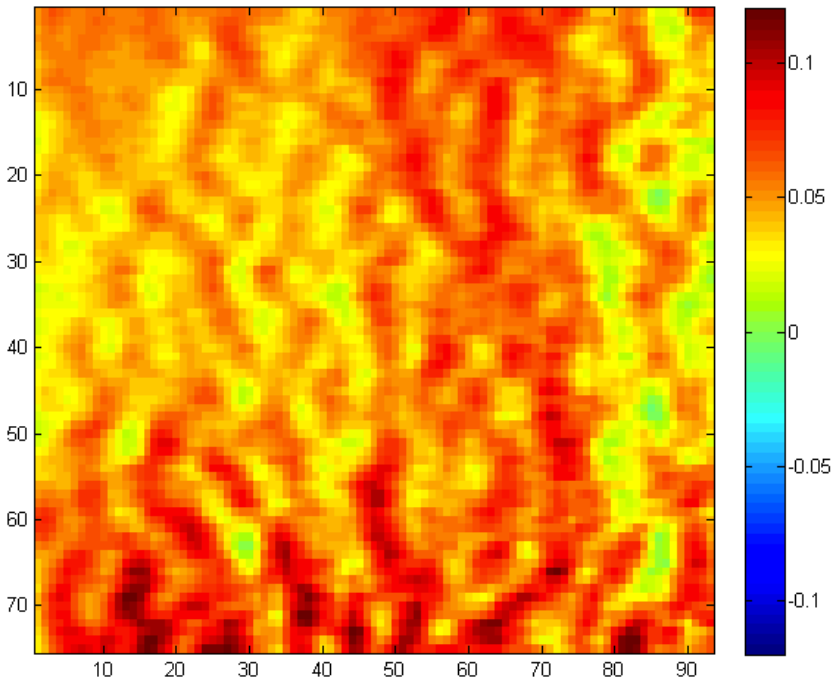

Figure 54: HDM: 15:1 Custom well, 10% uniaxial stretch, x-directional strain

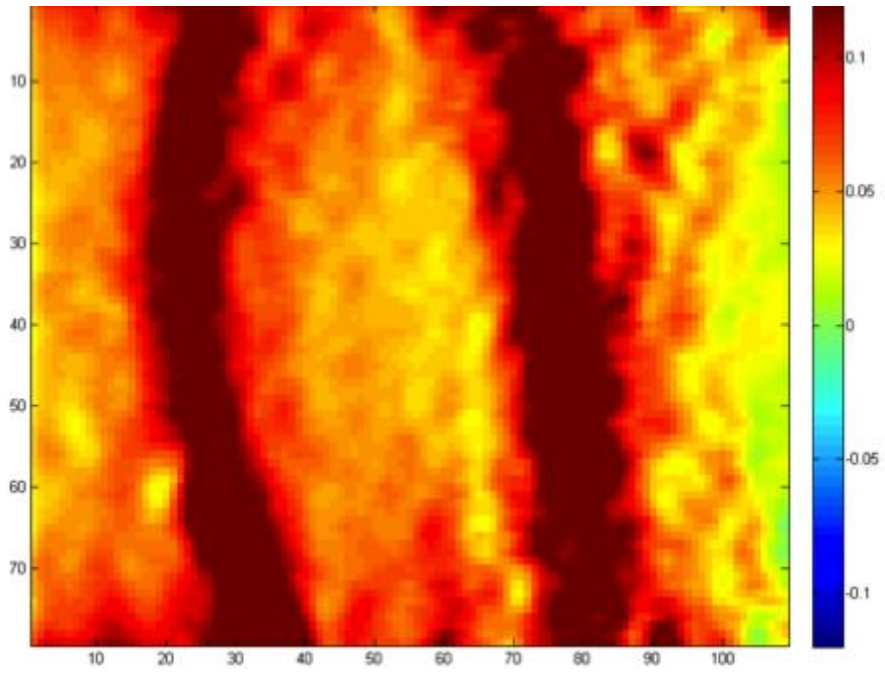

Figure 55: HDM: Strex® well, 10% uniaxial stretch, x-directional strain

It was observed that the variance of the strain field is much more drastic for the Strex® well than the custom well. Since the program run with the device was to achieve 10% strain, the strain fields should show some area of 10% strain. However, the Strex® well exhibits a large area of only about 4% strain in the center and the two red vertical regions indicate strain of over 12%. The custom well exhibits a general range of 3-10% scattered throughout the surface, averaging to about 6% strain across the surface. Though these results are not consistent with the FEA results, they show that the custom well has a less varied strain field than the Strex® well. More HDM data can be found in Appendix I.

Device Validation

Operation Time

Operation time was validated by running the motors for 6.5 hours and measuring the temperature using a thermocouple. A LabVIEW VI (see Appendix H) was written to obtain temperature measurements over 6.5 hours and the results were plotted as seen in Fig. 56. It can be observed that the temperature of the motor remained fairly constant at 27^{o}C, thereby confirming that the device can operate at a minimum of 6.5 hours without overheating.

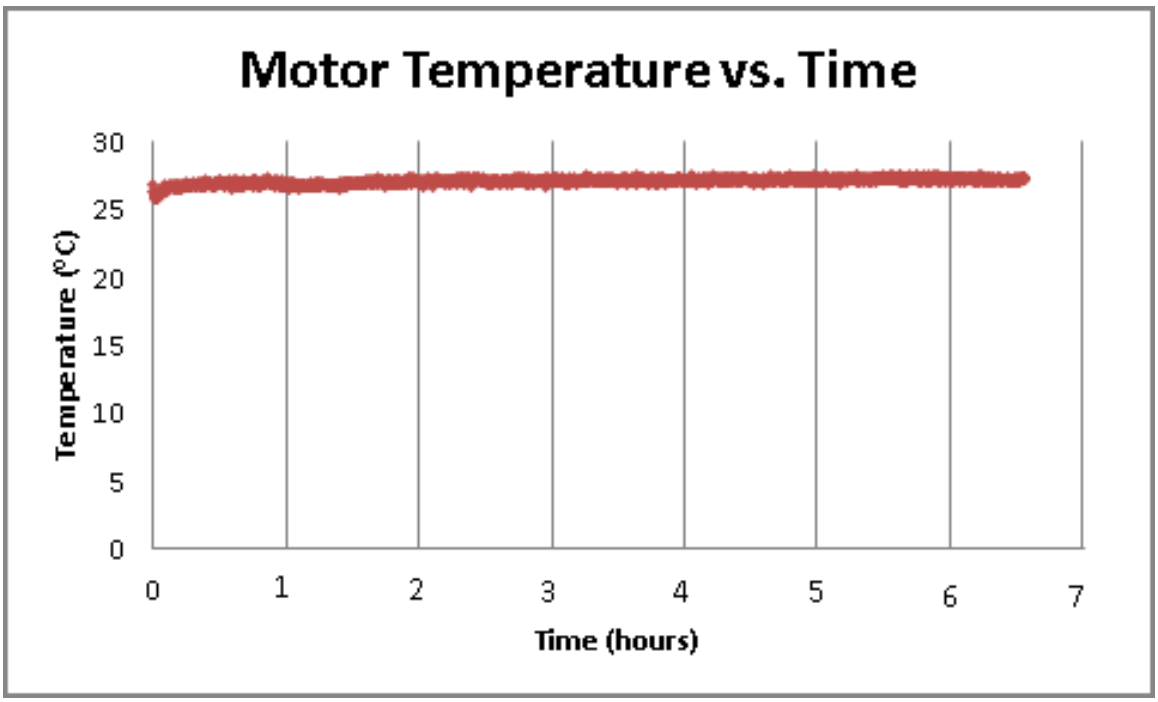

Figure 56: Motor temperature vs. time for 6.5 hrs

Cell Seeding and Viewing

In order to confirm cell attachment on the PDMS film and visibility through the film with a microscope, GFP labeled human fibroblasts were seeded. Firstly, the PDMS substrate is cleansed and sterilized with 70% ethanol. The well is then exposed to UV light for 15 minutes for further sterilization. Pepsin extracted collagen was then coated onto the well to promote cells attachment. After 30 minutes, the well is rinsed with PBS and dried. GFP labeled fibroblasts were then seeded at 2800 cells/cm^2 and incubated in 5% CO_2 at 37^{o}C. After one day, the cells can be viewed via an inverted microscope under fluorescence and were observed to be attaching well (Fig. 57). This confirms not only visibility of cells through custom PDMS substrate but also that PDMS substrate does not provide harmful conditions for the cells seeded. However, the team observed that cells were not clearly visible. This may be due to the thickness of PDMS sheet that is obstructing the light source. Another cause may be due to dirt particles adhered to the PDMS

sheet. Utilizing commercially available sterilized PDMS sheet in the PDMS well may eliminate this problem.

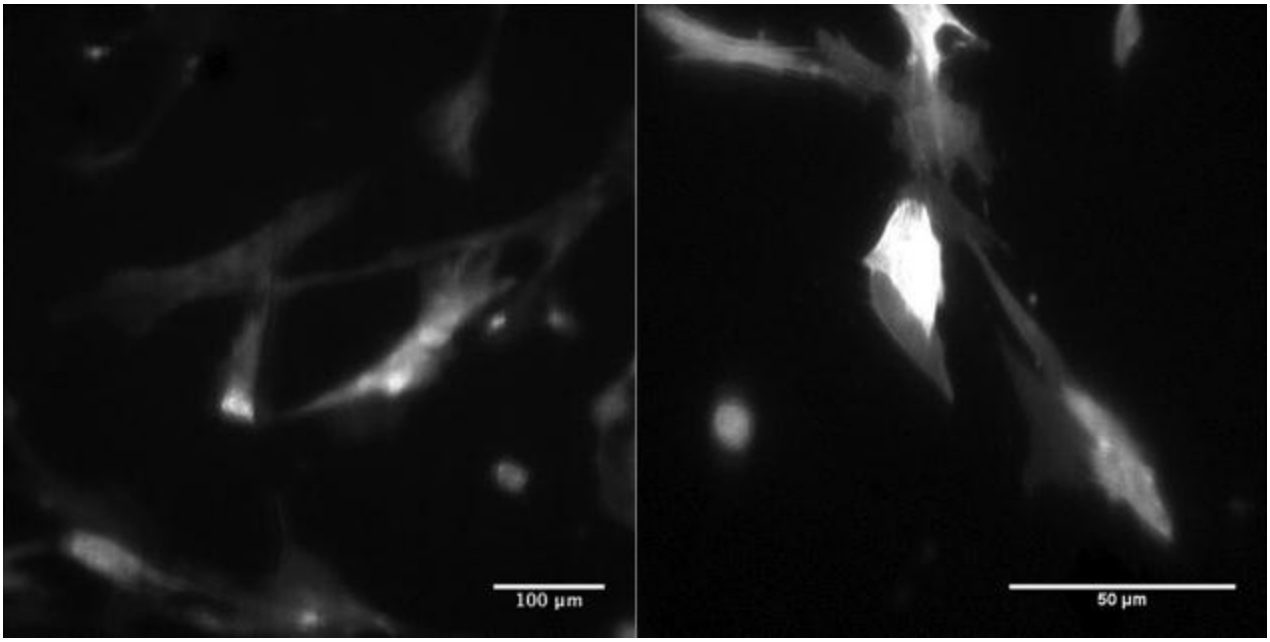

Figure 57: Fluorescence images of GFP labeled human fibroblasts seeded after one day

Discussion

The primary goal of this project was to create a device that surpassed some of the limitations of current biaxial stretching devices while also enabling real time viewing of cells under an inverted microscope. Through testing, it was determined that the device can stretch a 40mm x 40mm PDMS well at a range from uniaxial to equibiaxial at a frequency from 0.01Hz to 1 Hz. Our device allows users to apply various profiles of mechanical strain in each experiment. While performing cyclic motion, the device has a duty cycle resembling a sawtooth waveform, ensuring that strain is applied at a near-linear rate to the well. The motors are capable of operating for an extended period of time (>6 hours), compared to the 20 minute operating time of similar industry devices. Such increase in operation time extends the capabilities in studying in-depth mechanobiology that requires long straining of cells. Although the team went over budget

for this design, the final device is market ready and cost twenty fold less than commercially available Strex device. Additionally, our final device successfully addresses major limitations associated with current devices including the inability to provide "real-time" analysis of cellular responses, non-uniform uniaxial and equibiaxial strains and limited operation time. Therefore, the team determines that exceeding of budget is justified.

Sustainability and Hazard Issues

The device created in this project was built to provide a utility for researchers to study the effects of mechanical strain on cells. Devices similar to the one created in this project are commercially available in the market to study mechanobiology. This device will not have a direct effect on the economy of everyday living, but further understanding of mechanobiology may ultimately lead to useful biomedical applications that could have an effect on economics of everyday living, specifically in health care services or treatments.

This device was created using mostly spare metallic parts obtained through junk yards. Therefore, the creation of our device had a negligible impact on the environment, regarding the use of natural resources. In addition, the production of the device described in this report had no effect on the biology or ecology regarding renewable energy.

The device, built solely for academic purposes, will not influence or have an impact on the "ordinary" person. If brought to the market, the device would primarily be used in both private and public laboratories, but will never be marketed toward the general populace. Additionally, our device will not have any effect on the global market. Likewise, the device will have no influence on any ethical issues.

The prototype built during the duration of our project poses no issue with respect to the health and safety of people. The device's main purpose is to assist in research and will not be

used outside of a laboratory setting. The design will not pose a health risk to the individual using it if the device is operated accordingly to the instructions provided.

The device was designed in a fashion that allows it to be replicated in its entirety in the future. The parts used in the design were modeled using SolidWorks, which allows the creation of engineering drawings used to accurately replicate modeled items. All engineering drawings used to create custom parts are included in Appendix B. The parts modeled using CAD software were manufactured using a combination of CNC machining and water jetting, both of which are standard machining processes. In addition, all electronic items used in this project are commercially available on the market, and can be purchased in order to manufacture the device.

Conclusion and Recommendations

Conclusion

Validation tests confirmed that the final device fully accomplish the client statements. The device fits very well with the Zeiss Microscope allowing "real-time" visualization of cells under stretch. Additionally, the device can perform uniaxial stretch in either X or Y direction as well as equibiaxial stretch with strain rates ranging from 0.1-30%. Moreover, the device can achieve strain at a frequency of .01-1 Hz in sinusoidal sawtooth waveform as confirmed by HDM data. Overheating was not observed and the device was confirmed to be able to operate for at least 6.5 hrs. Better uniformity of strain in the custom PDMS substrate compared to commercially available Strex® was also confirmed by HDM data. Lastly, the final market-ready device was constructed under a budget of $1,200 (See Appendix J for Bill of Materials).

Recommendations

Although the final device successfully achieved all the objectives set forth by the client and design team, a few modifications can be made to facilitate easier and more efficient use. Firstly, the team would like to suggest implementation of LabVIEW program to command the device. Using LabVIEW will increase user-friendliness due to its intuitive user interface.

Additionally, an incubation chamber which provides physiological conditions need to be constructed to successfully perform mechanobiology studies. The chamber needs to provide 37^{o}C and 5% CO_2 to better simulate the living conditions for the cells being stretched. This incubation chamber, however, must be designed in a way to avoid damaging the motors or any components of the final device as well as the microscope being used.

Each size 14 linear actuator was ordered with a two channel quadrature TTL squarewave encoder with optional index as a third channel. Their primary application is for positional feedback. In short, the encoders' main purposes are to count the number of steps each motor makes and relay this information back to the software interface. This information will help provide an absolute home position for the motors, greatly expanding the number of different programs the device can run. For example, if a user desired to run the motors that stretch the substrate in the y direction for a set amount of time and then switch to the motors that will stretch it in the x direction mid-test, the device will need a home position to retreat back to before commencing the second task. Currently, this cannot be achieved without the encoders.
The group recommends programming the encoders to be used in conjunction with the rest of the device. The encoders have already been wired to the beau connector on the plate. The group will need to terminate the wiring within the housing unit and figure out how to incorporate the encoders in the MPIDE code. Additional information about the encoders can be found at:

http://www.haydonkerk.com/LinearActuatorProducts/StepperMotorLinearActuators/LinearActuatorEncoders/tabid/200/Default.aspx

Future works include determining the current the encoders draw and resisting the 8V main power down to the 5V needed to power the encoders using resistors. Then, each of the encoders are needed to be wired to the input pins on the ChipKit Max32 controller. Lastly, a program needs to be generated to properly utilize the encoders.

References

1. Wang J, Li B. Mechanics rules cell biology. Sports Medicine, Arthroscopy, Rehabilitation, Therapy & Technology 2010;2(1):16.

2. Dartsch PC, Betz E. Response of cultured endothelial cells to mechanical stimulation. Basic Res Cardiol 1989;84(3):268-81.

3. Ghazanfari S, Tafazzoli-Shadpour M, Shokrgozar MA. Effects of cyclic stretch on proliferation of mesenchymal stem cells and their differentiation to smooth muscle cells. Biochem Biophys Res Commun 2009 10/23;388(3):601-5.

4. Sumanasinghe RD, Bernacki SH, Loboa EG. Osteogenic differentiation of human mesenchymal stem cells in collagen matrices: Effect of uniaxial cyclic tensile strain on bone morphogenetic protein (BMP-2) mRNA expression. Tissue Eng 2006 12/01; 2011/09;12(12):3459-65.

5. Zhang L, Kahn CJF, Chen H, Tran N, Wang X. Effect of uniaxial stretching on rat bone mesenchymal stem cell: Orientation and expressions of collagen types I and III and tenascin-C. Cell Biol Int 2008 3;32(3):344-52.

6. Rath B, Nam J, Knobloch TJ, Lannutti JJ, Agarwal S. Compressive forces induce osteogenic gene expression in calvarial osteoblasts. J Biomech 2008;41(5):1095-103.

7. W. DM. Mechano-potential etiologies of aortic valve disease. J Biomech 2010 1/5;43(1):87-92.

8. Choi K, Seo Y, Yoon H, Song K, Kwon S, Lee H, Park J. Effects of mechanical stimulation on the proliferation of bone marrow-derived human mesenchymal stem cells. Biotechnology and Bioprocess Engineering 2007;12(6):601-9.

9. Nomura S, Takano-Yamamoto T. Molecular events caused by mechanical stress in bone. Matrix Biology 2000;19(2):91-6.

10. Goodman CA, Mayhew DL, Hornberger TA. Recent progress toward understanding the molecular mechanisms that regulate skeletal muscle mass. Cell Signal 2011 12;23(12):1896-906.

11. Ishijima M, Rittling SR, Yamashita T, Tsuji K, Kurosawa H, Nifuji A, Denhardt DT, Noda M. Enhancement of osteoclastic bone resorption and suppression of osteoblastic bone formation in response to reduced mechanical stress do not occur in the absence of osteopontin. J Exp Med 2001;193(3):399.

12. Throm Quinlan AM, Sierad LN, Capulli AK, Firstenberg LE, Billiar KL. Combining dynamic stretch and tunable stiffness to probe cell mechanobiology *in vitro*. PLoS ONE(8):e23272.

13. Wang J, Thampatty B. An introductory review of cell mechanobiology. Biomechanics and Modeling in Mechanobiology 2006;5(1):1-16.

14. Hsu H, Lee C, Kaunas R. A dynamic stochastic model of frequency-dependent stress fiber alignment induced by cyclic stretch. PLoS ONE(3):e4853.

15. sub Kwon Y, Kravitz L. How do muscles grow? Physiol Rev 2010;84:209-38.

16. Leung DYM, Glagov S, Mathews MB. Cyclic stretching stimulates synthesis of matrix components by arterial smooth muscle cells in vitro. Science 1976 Feb. 6;191(4226):pp. 475-477.

17. Lee I, Wang J, Lee Y, Young T. The differentiation of mesenchymal stem cells by mechanical stress or/and co-culture system. Biochem Biophys Res Commun 2007 1/5;352(1):147-52.

18. Hsu H, Lee C, Locke A, Vanderzyl SQ, Kaunas R. Stretch-induced stress fiber remodeling and the activations of JNK and ERK depend on mechanical strain rate, but not FAK. PLoS ONE(8):e12470.

19. Pietramaggiori G, Liu P, Scherer SS, Kaipainen A, Prsa MJ, Mayer H, Newalder J, Alperovich M, Mentzer SJ, Konerding MA, Huang S, Ingber DE, Orgill DP. Tensile forces stimulate vascular remodeling and epidermal cell proliferation in living skin. Ann Surg 2007;246(5):896,902 10.1097/SLA.0b013e3180caa47f.

20. Chin MS, Lancerotto L, Helm DL, Dastouri P, Prsa MJ, Ottensmeyer M, Akaishi S, Orgill DP, Ogawa R. Analysis of neuropeptides in stretched skin. Plast Reconstr Surg 2009;124(1):102,113 10.1097/PRS.0b013e3181a81542.

21. Langrana NA, Alexander H, Strauchler I, Mehta A, Ricci J. Effect of mechanical load in wound healing. Ann Plast Surg 1983;10(3):200-8.

22. Balestrini JL, Billiar KL. Equibiaxial cyclic stretch stimulates fibroblasts to rapidly remodel fibrin. J Biomech 2006;39(16):2983-90.

23. Sommerlad BC, Creasey JM. The stretched scar: A clinical and histological study. Br J Plast Surg 1978 1;31(1):34-45.

24. Arem AJ, Madden JW. Effects of stress on healing wounds: I. intermittent noncyclical tension. J Surg Res 1976 2;20(2):93-102.

25. McCullen SD, Haslauer CM, Loboa EG. Musculoskeletal mechanobiology: Interpretation by external force and engineered substratum. J Biomech 2010 1/5;43(1):119-27.

26. Butcher JT, Nerem RM. Valvular endothelial cells and the mechanoregulation of valvular pathology. Philosophical Transactions: Biological Sciences 2007 Aug. 29;362(1484, Bioengineering the Heart):pp. 1445-1457.

27. Weston MW, LaBorde DV, Yoganathan AP. Estimation of the shear stress on the surface of an aortic valve leaflet. Ann Biomed Eng 1999;27(4):572-9.

28. Gupta V, Tseng H, Lawrence BD, Jane Grande-Allen K. Effect of cyclic mechanical strain on glycosaminoglycan and proteoglycan synthesis by heart valve cells. Acta Biomaterialia 2009 2;5(2):531-40.

29. Ku C, Johnson PH, Batten P, Sarathchandra P, Chambers RC, Taylor PM, Yacoub MH, Chester AH. Collagen synthesis by mesenchymal stem cells and aortic valve interstitial cells in response to mechanical stretch. Cardiovascular Research 2006 August 01;71(3):548-56.

30. Grande-Allen KJ, Griffin BP, Ratliff NB, Cosgrove III DM, Vesely I. Glycosaminoglycan profiles of myxomatous mitral leaflets and chordae parallel the severity of mechanical alterations. J Am Coll Cardiol 2003 7/16;42(2):271-7.

31. Koike M, Shimokawa H, Kanno Z, Ohya K, Soma K. Effects of mechanical strain on proliferation and differentiation of bone marrow stromal cell line ST2. J Bone Miner Metab 2005;23(3):219-25.

32. Rangappa S, Wechsler AS, Yasha Kresh J. 1068-125 cyclic stretch of adult human mesenchymal stem cells induces expression of early cardiac and neuronal genes. J Am Coll Cardiol 2004 3/3;43(5, Supplement 1):A177.

33. Guan J, Wang F, Li Z, Chen J, Guo X, Liao J, Moldovan NI. The stimulation of the cardiac differentiation of mesenchymal stem cells in tissue constructs that mimic myocardium structure and biomechanics. Biomaterials 2011 8;32(24):5568-80.

34. Qi M-, Hu J, Zou S-, Chen H-, Zhou H-, Han L-. Mechanical strain induces osteogenic differentiation: Cbfa1 and ets-1 expression in stretched rat mesenchymal stem cells. Int J Oral Maxillofac Surg 2008 5;37(5):453-8.

35. Thomas D B. Techniques for mechanical stimulation of cells in vitro: A review. J Biomech 2000 1;33(1):3-14.

36. B-Bridge International. 2009 STREX mechanical cell strain instrument, microscope-mountable, uni/bidirectional stretch. <http://lifesciences.b-bridge.com/products/detail/885/STREX_Mechanical_Cell_Strain_Instrument,_Microscope-

mountable,_uni_and_bidirectional_stretch>. Accessed 2011 10/06.

37. Hsu H, Lee C, Kaunas R. A dynamic stochastic model of frequency-dependent stress fiber alignment induced by cyclic stretch. PLoS ONE 2009 03/25;4(3):e4853.

38. Park JS, Chu JSF, Cheng C, Chen F, Chen D, Li S. Differential effects of equiaxial and uniaxial strain on mesenchymal stem cells. Biotechnol Bioeng 2004;88(3):359-68.

39. Cell Lines Service. 2011 S1 cell stretcher <http://www.cell-lines-service.de/content/e8/e155/index_ger.html>. Accessed 2011 10/06.
40. Flexcell International Corporation. 2011 Flexcell® FX-5000™ Tension System<http://www.flexcellint.com/slideshow2.htm>. Accessed 2011 10/06.

41. Ahmed WW, Kural MH, Saif TA. A novel platform for in situ investigation of cells and tissues under mechanical strain. Acta Biomater 2010; 6 (8): 2979-2990.

42. Nave CR. 2010 Hyperphysics. <http://hyperphysics.phy-astr.gsu.edu/hbase/hph.html>. Accessed 2011 5 October.

43. Lipták BG, Lipták BG. Instrument engineers' handbook: Process control and optimization. CRC; 2005.

44. Machine Design magazine. 2011 <http://www.electricmotors.machinedesign.com/guiEdits/Content/bdeee4/bdeee4_1.aspx>. Accessed 2011 5 October.

45. Gieras JF. Permanent magnet d.c. commutator motors. In: Permanent magnet motor technology. CRC Press; 2009. p 119-169.

46. Arduino. 2011. <http://www.arduino.cc/en/Main/ArduinoBoardMega2560>. Accessed 2011 13 December.

47. Sparkfun Electronics. 2011.< http://www.sparkfun.com/products/10735>. Accessed 201113 December.

Appendices

Appendix A- Patented cell stretching devices

Patent ID	Description	Image
US 2007/0178584 A1	This device uses one stepper motor with a control unit and cell culture well (200um thick film). The walls (labeled 32 and 34) of the well are thicker than the rest. The thicker walls have 2 holes on each, which were attached to the pins of the stable plate (labeled 31) and moving plate (33). The uniaxial stretching is achieved by pulling or pushing the moving plate with the stepper motor through a linkage. Rotation of the motor is controlled by the control device (labeled 37).	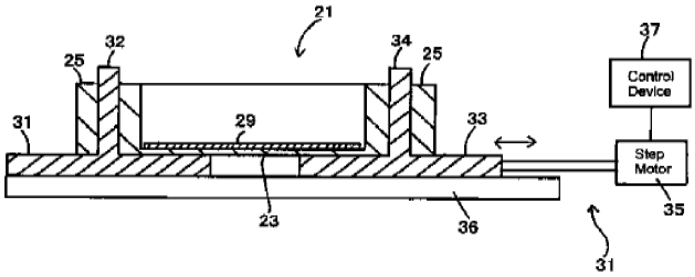
6,107,081	This device uses hydraulic pressure to stretch cells linearly. Cells (labeled 11) are seeded on the silicone membrane (labeled 8). The silicone is attached to the ram (labeled 7). The left end of the ram is fixed while right end is movable. The right end is attached to hydraulic compression chamber (labeled 4). Stretching is achieved by increasing or decreasing the hydraulic pressure generated by the pump (labeled 3) within the hydraulic compression chamber (labeled 4). This induces uni-directional movement of the right end of the ram, thereby extending/distending the silicone and cyclically stretching the cells)	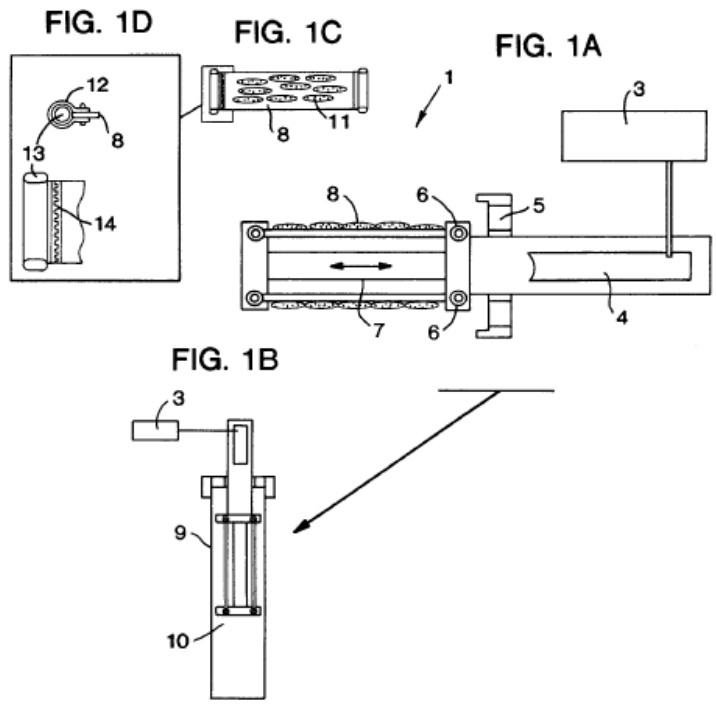

5,217,899	The device uses electric motor (labeled 38) to actuate a cam (labeled 40) which rotates about the axis (labeled 41). The rotation of the cam causes the rod (labeled 32) and displacement applicator (labeled 24) to move upward or downward. The silicone sheet, on which cells are seeded, is placed right above the displacement applicator. The sheet is circular shape and attached firmly around the rim. When the motor drives the cam and moves the rod upward, displacement applicator deforms the silicone sheet by moving upward. At the end of upward stroke, the cam and the spring (labeled 34) will return the rod and displacement applicator to a lowered position. This returns the deformed silicone to initial position. Repetitive movement of such mechanism will apply cyclic biaxial stretch on the cells.	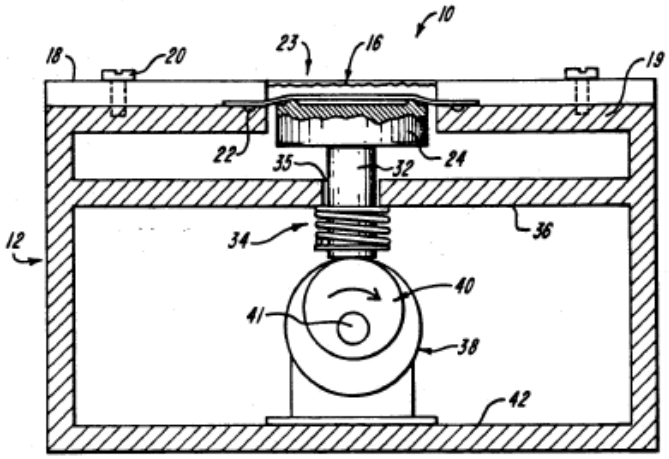 FIG. 1
US 2008/0166796 A1	In order to apply stretch to cells, they are seeded on the deformable culture surface (Fig.1 labeled 4). The membrane is attached to a series of posts (Fig.1 labeled 5) by bending the membrane around the post and secured by an elastic band (Fig.1 labeled 2). The posts are connected to arms (Fig.1 labeled 1) which extend in the direction away from culture surface. The arms, in turn, are connected to pivot points (Fig.2 labeled 7) which are fixed in an outer ring ((Fig.2 labeled 6) near the outer boundary of the device. Rotation of the arms about the pivot points will stretch the membrane biaxially (Figure 2a to Figure 2b), applying mechanical force to the cells. The movement of the arms	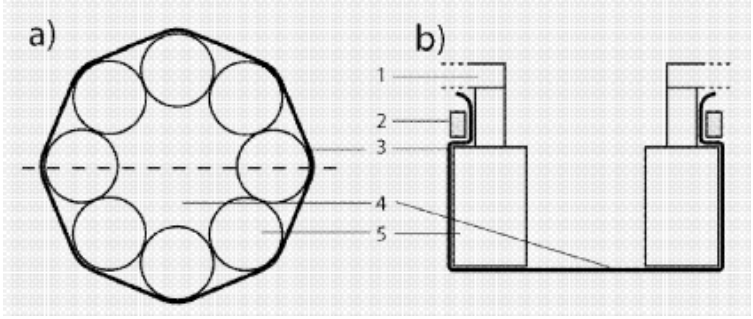 Figure 1 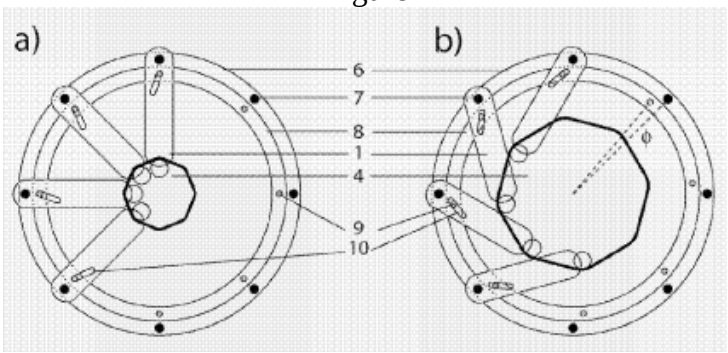

	from position shown in Figure 2a to Figure 2b back and forth will translate cyclic stretch. The patent, however, did not describe how the arm movement will be achieved. It does claim that the device will be compact enough to allow viewing of cells while being stretched.	Figure 2

Appendix B- Drawings of individual components of the device

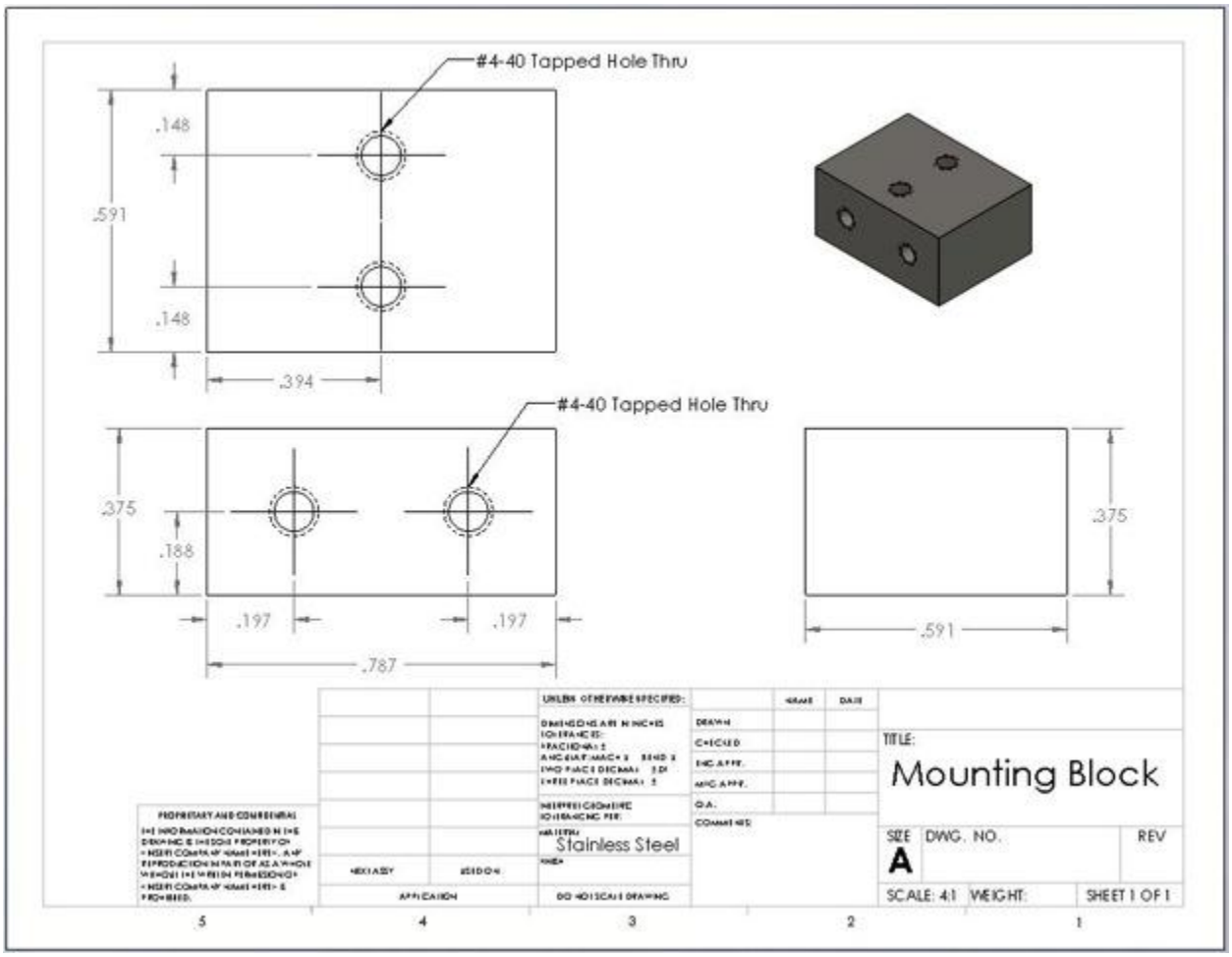

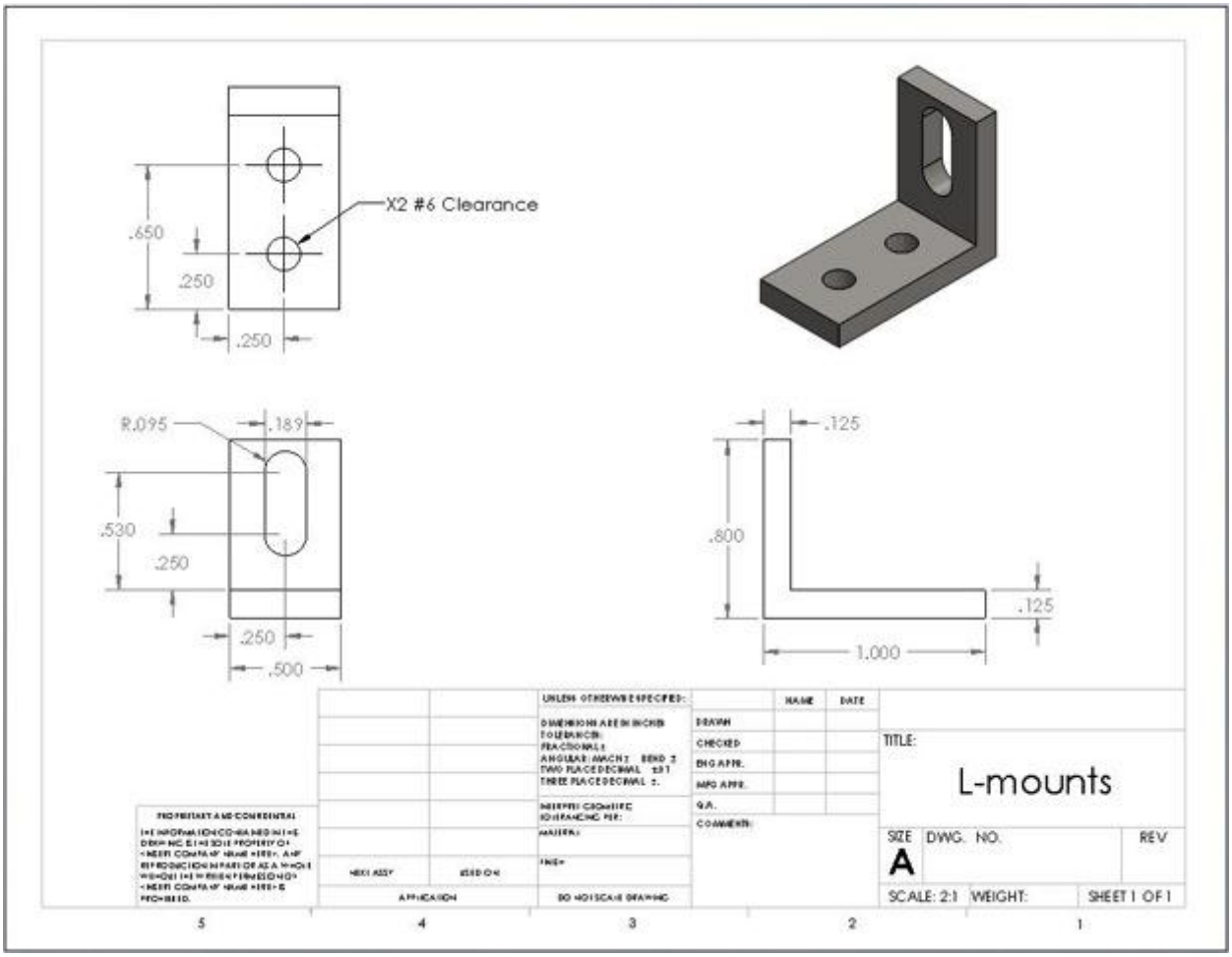
X2 #6 Clearance
.650
.250
.250
R.095
.189
.530
.250
.250
.500
.125
.800
.125
1.000
UNLESS OTHERWISE SPECIFIED:
NAME
DATE
DRAWN
CHECKED
ENG APPR.
MFG APPR.
Q.A.
COMMENTS:
TITLE:
L-mounts
SIZE
A
DWG. NO.
REV
SCALE: 2:1
WEIGHT:
SHEET 1 OF 1

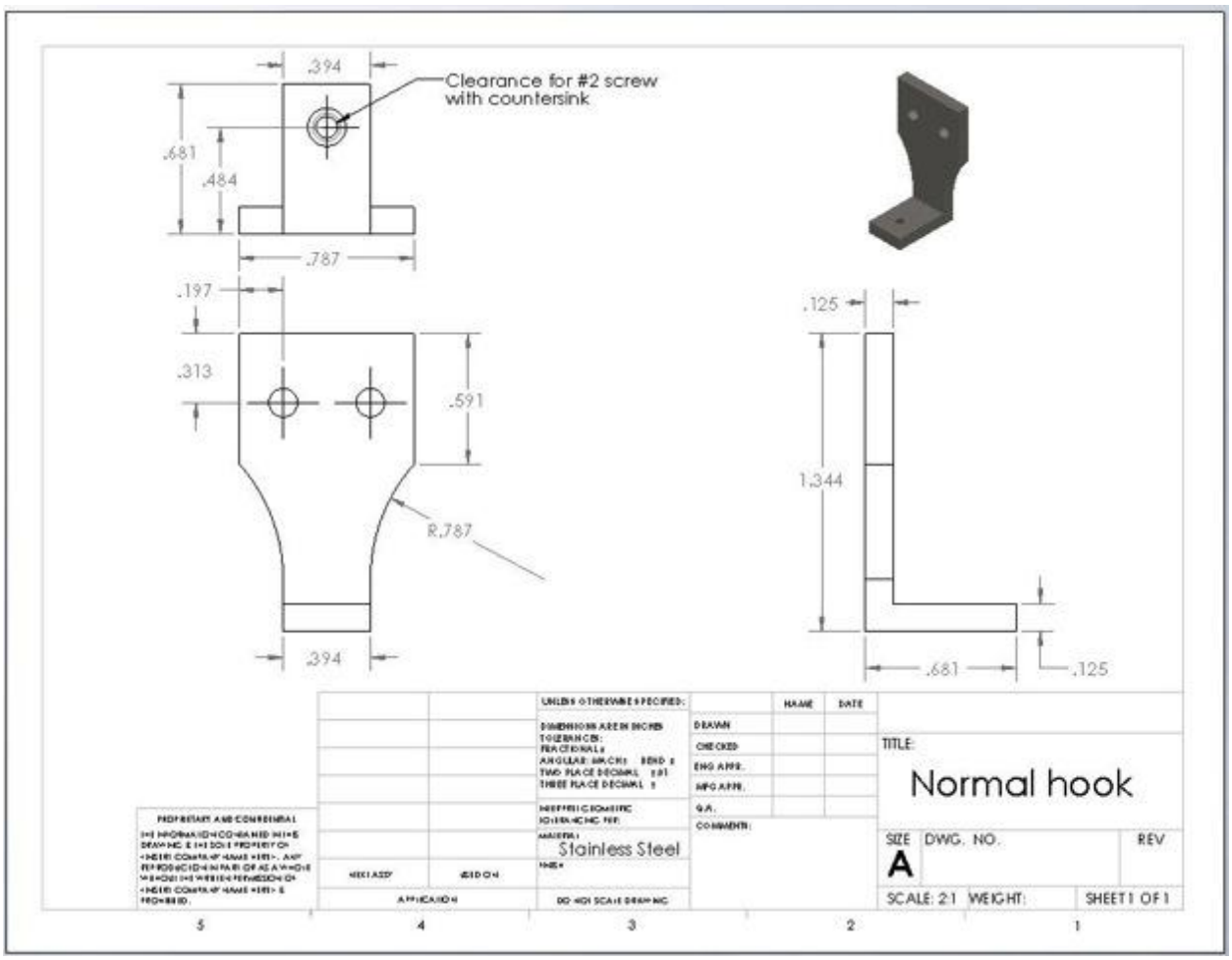
.394
Clearance for #2 screw with countersink
.681
.484
.787
.197
.313
.591
R.787
.394
.125
1.344
.681
.125
UNLESS OTHERWISE SPECIFIED:
NAME
DATE
DRAWN
CHECKED
ENG APPR.
MFG APPR.
Q.A.
COMMENTS:
Stainless Steel
TITLE:
Normal hook
SIZE
A
DWG. NO.
REV
SCALE: 2:1
WEIGHT:
SHEET 1 OF 1
5
4
3
2
1

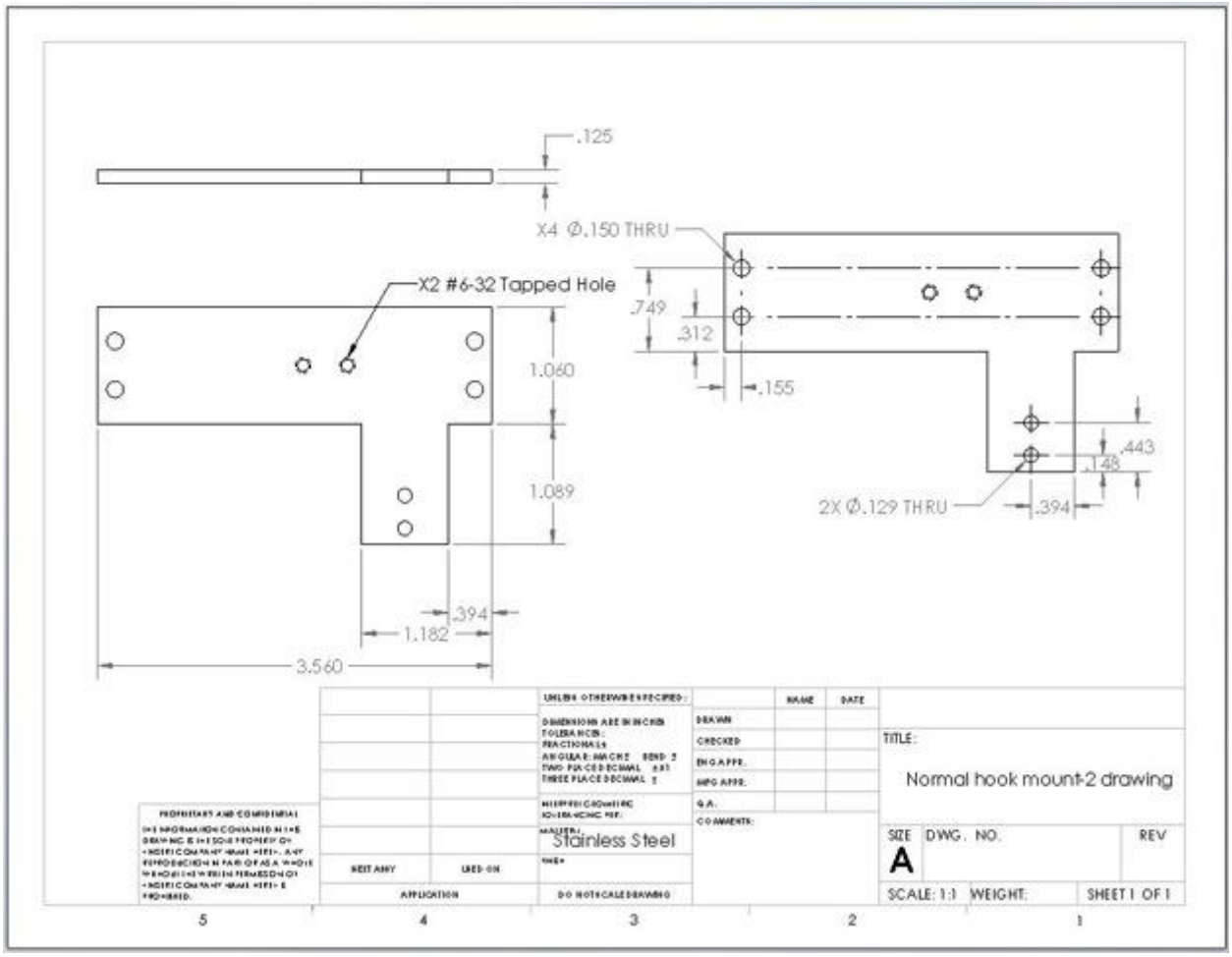
.125
X4 Ø.150 THRU
X2 #6-32 Tapped Hole
.749
.312
.155
1.060
1.089
.443
.148
2X Ø.129 THRU
.394
.394
1.182
3.560
UNLESS OTHERWISE SPECIFIED:
NAME
DATE
DRAWN
CHECKED
ENG APPR.
MFG APPR.
Q.A.
COMMENTS:
TITLE:
Normal hook mount-2 drawing
Stainless Steel
SIZE
A
DWG. NO.
REV
SCALE: 1:1
WEIGHT:
SHEET 1 OF 1
NEXT ASSY
USED ON
APPLICATION
DO NOT SCALE DRAWING
5
4
3
2
1

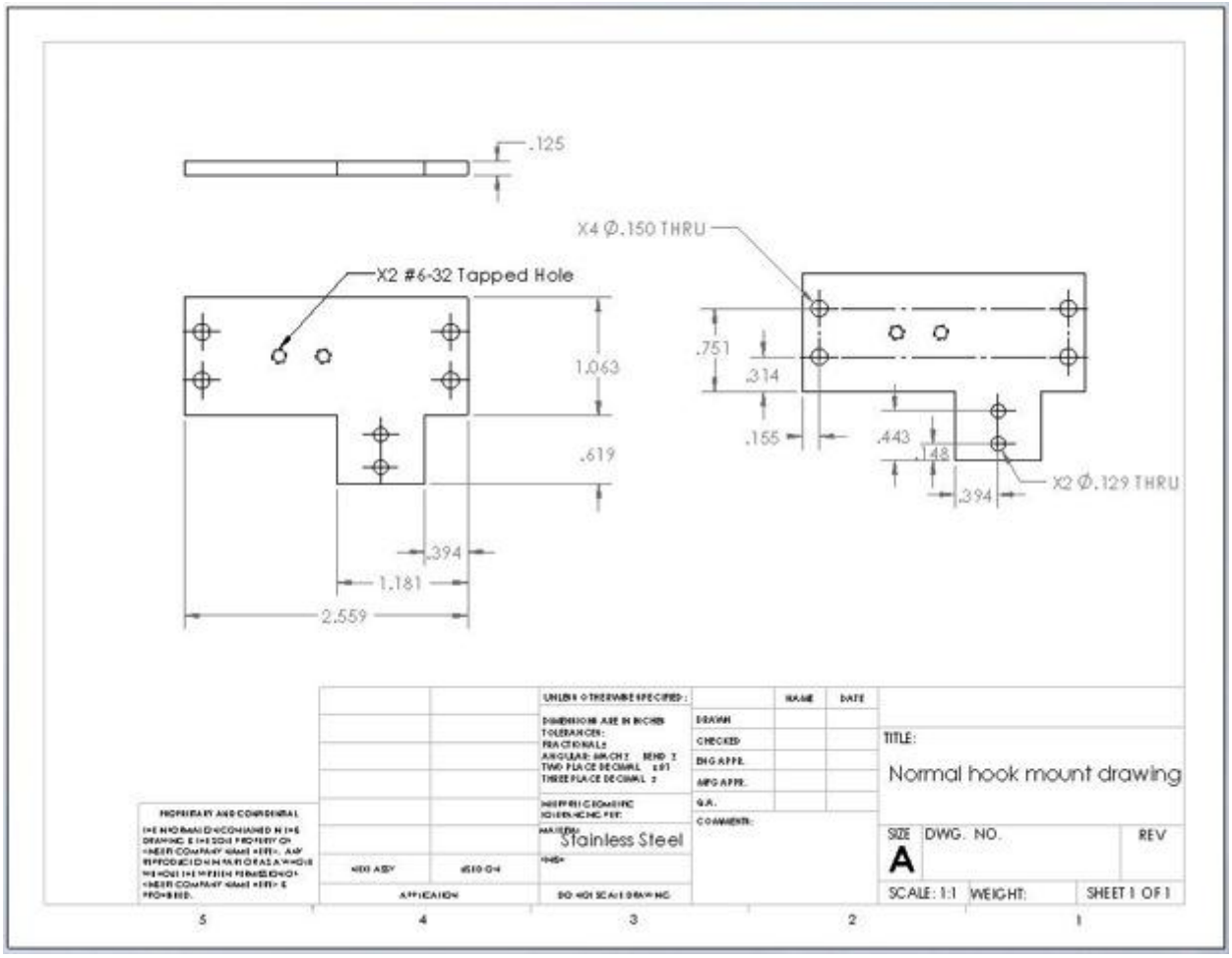
.125
X4 Ø.150 THRU
X2 #6-32 Tapped Hole
1.063
.619
.394
1.181
2.559
.751
.314
.155
.443
.148
.394
X2 Ø.129 THRU
UNLESS OTHERWISE SPECIFIED:
NAME
DATE
DRAWN
CHECKED
ENG APPR.
MFG APPR.
Q.A.
COMMENTS:
Stainless Steel
TITLE:
Normal hook mount drawing
SIZE
A
DWG. NO.
REV
SCALE: 1:1
WEIGHT:
SHEET 1 OF 1
5
4
3
2
1

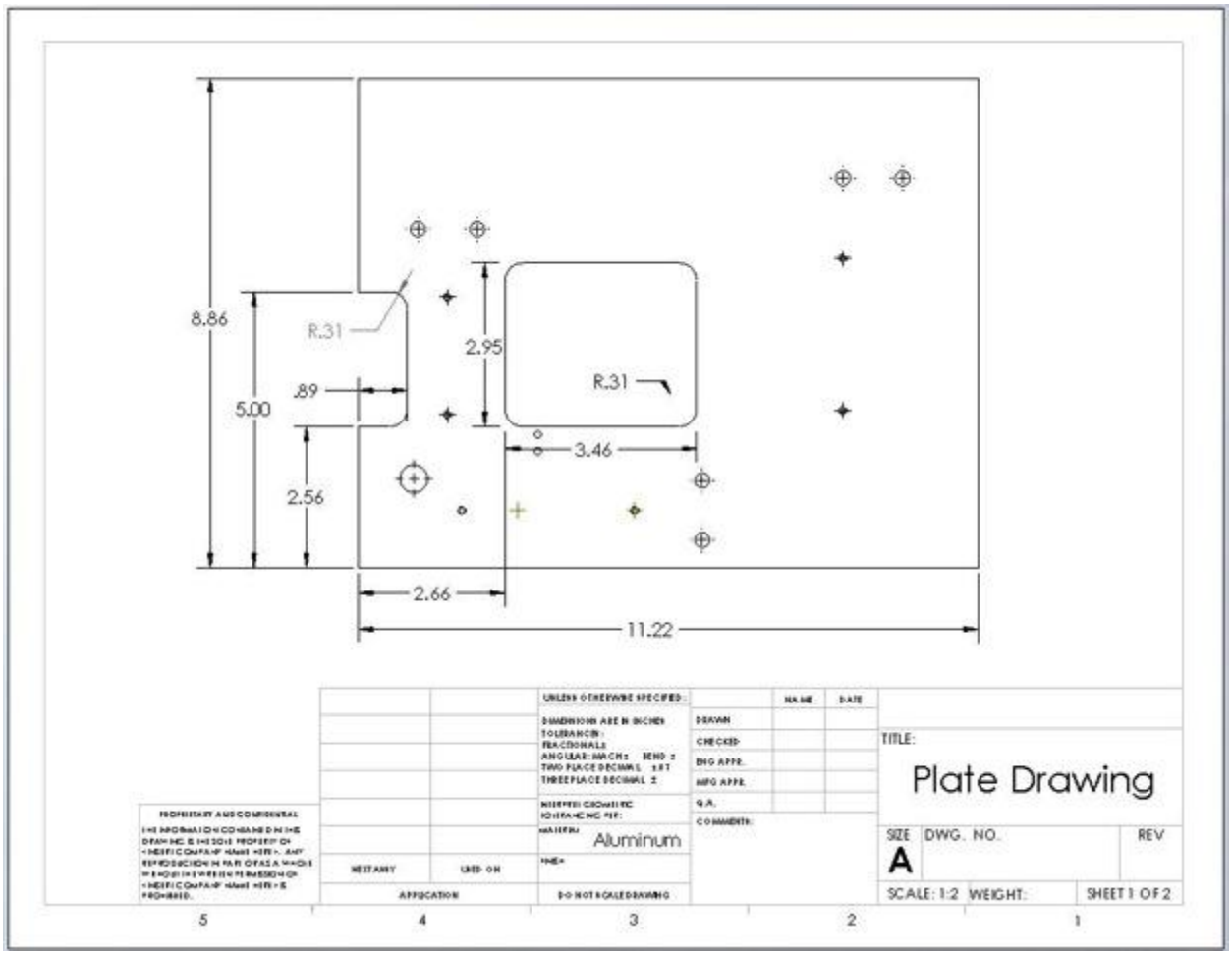
8.86
R.31
2.95
R.31
.89
5.00
3.46
2.56
2.66
11.22
UNLESS OTHERWISE SPECIFIED:
NAME
DATE
DRAWN
CHECKED
ENG APPR.
MFG APPR.
Q.A.
COMMENTS:
TITLE:
Plate Drawing
SIZE
A
DWG. NO.
REV
SCALE: 1:2
WEIGHT:
SHEET 1 OF 2
Aluminum
NEXT ASSY
USED ON
APPLICATION
DO NOT SCALE DRAWING
5
4
3
2
1

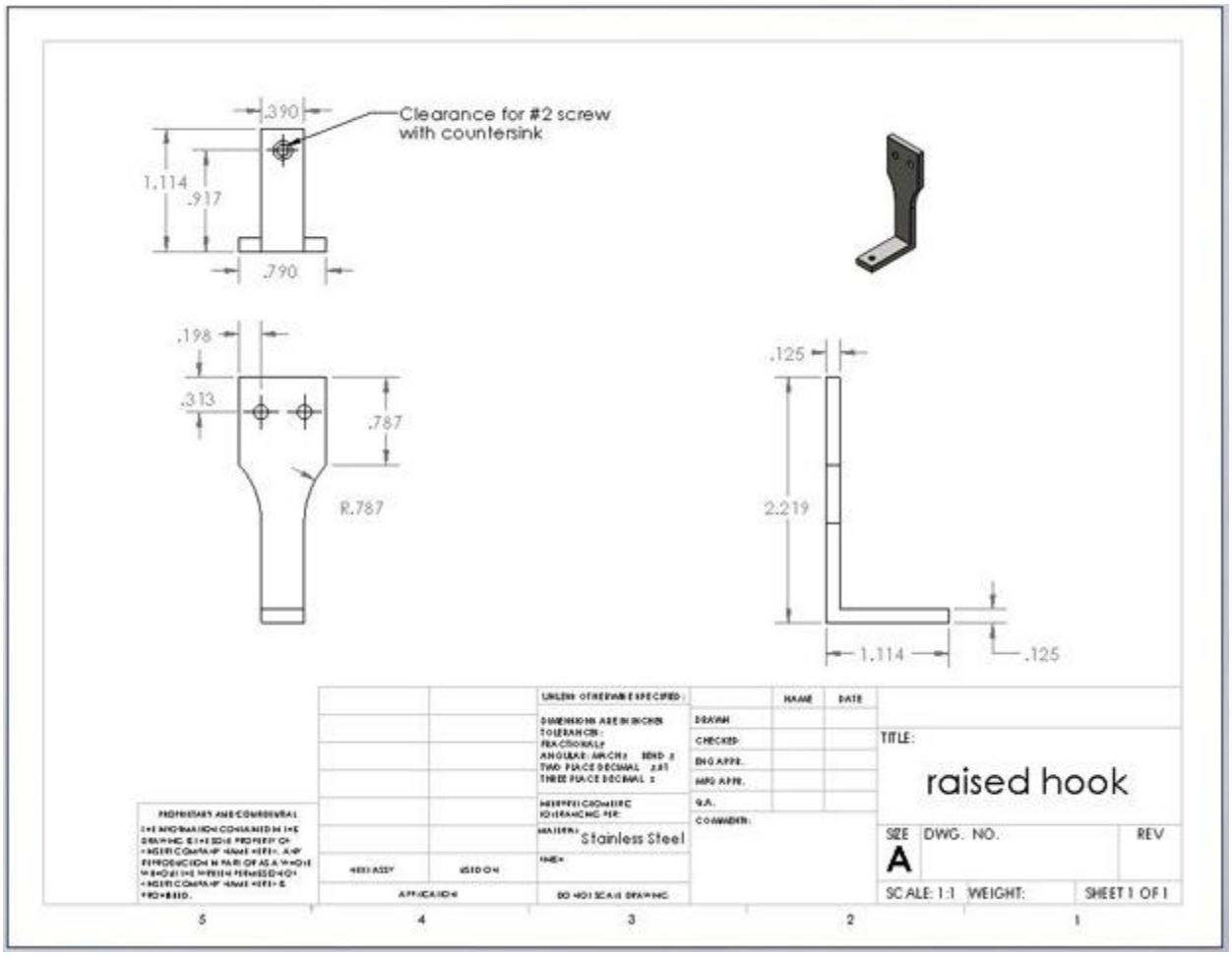
.390
Clearance for #2 screw
with countersink
1.114
.917
.790
.198
.313
.787
R.787
.125
2.219
1.114
.125
UNLESS OTHERWISE SPECIFIED:
NAME
DATE
DRAWN
CHECKED
ENG APPR.
MFG APPR.
Q.A.
COMMENTS:
TITLE:
raised hook
SIZE
A
DWG. NO.
REV
SCALE: 1:1
WEIGHT:
SHEET 1 OF 1
Stainless Steel

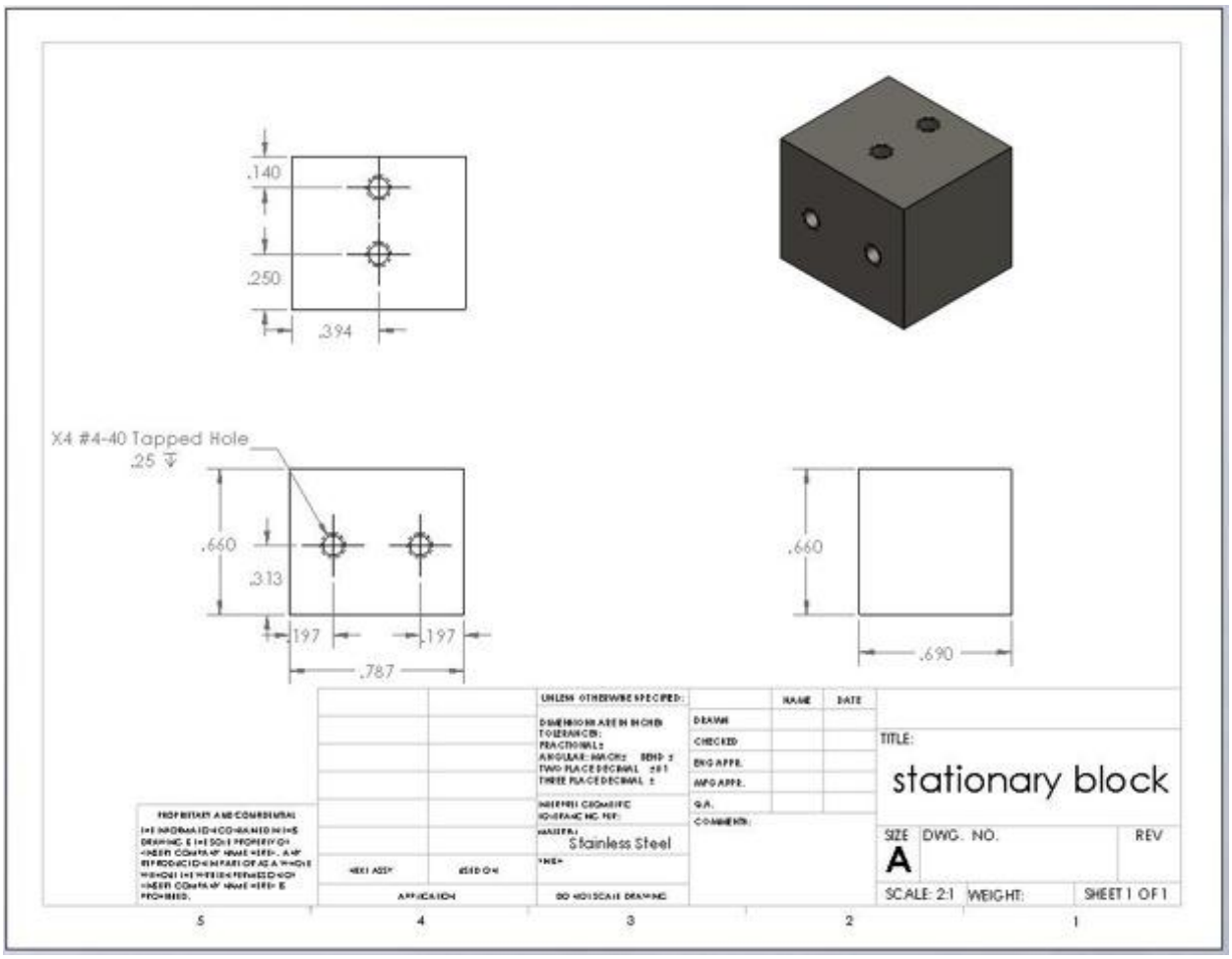
.140
.250
.394
X4 #4-40 Tapped Hole
.25
.660
.313
.197
.197
.787
.660
.690
Stainless Steel
stainless block
SIZE
A
SCALE: 2:1
WEIGHT:
SHEET 1 OF 1

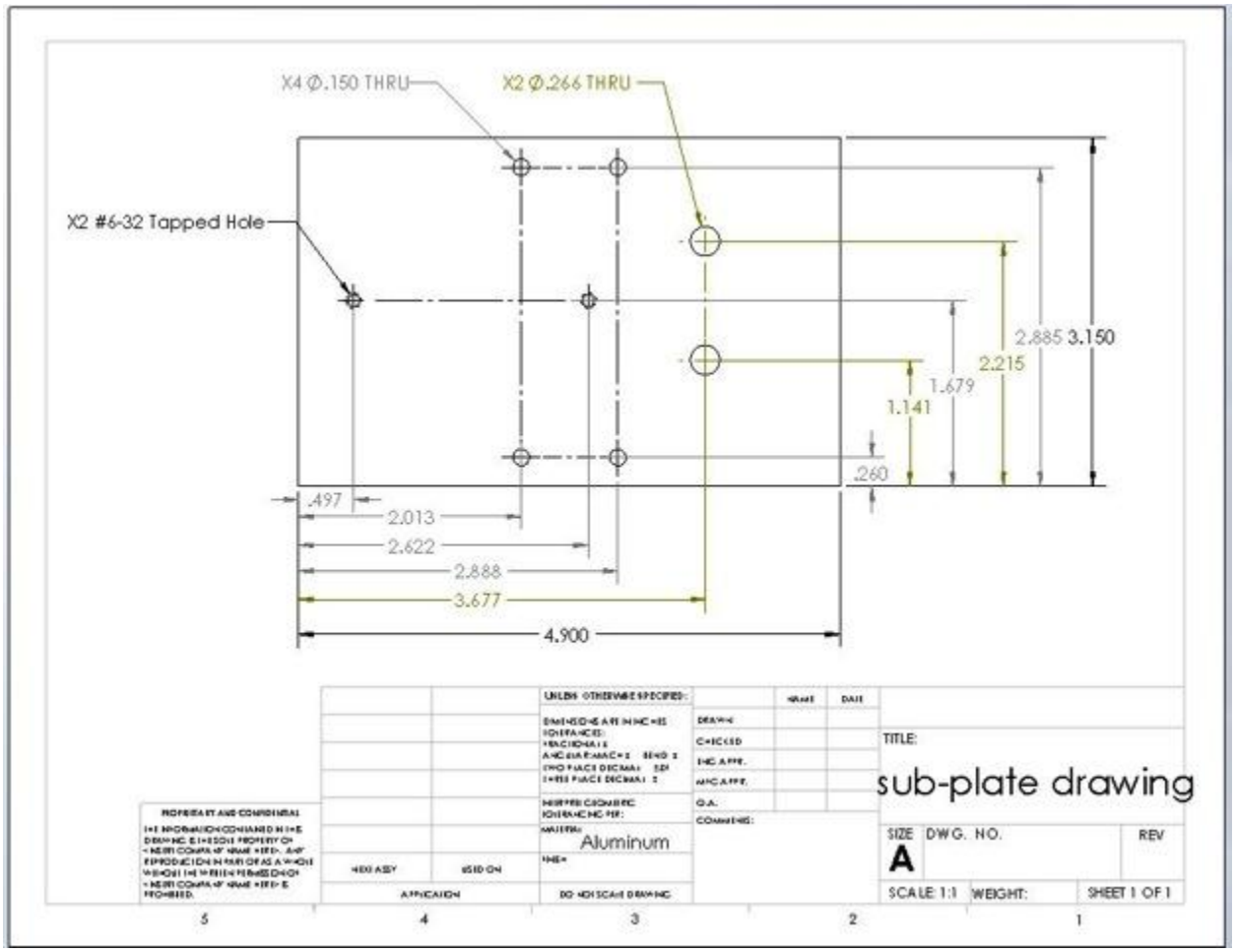
X4 Ø.150 THRU
X2 Ø.266 THRU
X2 #6-32 Tapped Hole
2.885
3.150
2.215
1.679
1.141
.260
.497
2.013
2.622
2.888
3.677
4.900
Aluminum
TITLE:
sub-plate drawing
SIZE
A
DWG. NO.
REV
SCALE: 1:1
WEIGHT:
SHEET 1 OF 1

Appendix C-Size 14 Linear Actuator Specifications

SERIES 35000 HYBRID LINEAR ACTUATOR (SIZE 14: 35mm (1.4") HYBRID LINEAR ACTUATOR 1.8 degree step angle)						
Part No.	**Captive**	35H4(X)-V			35H6(X)-V	
	Non-Captive	35F4(X)-V			35F6(X)-V	
	External Lin.	E35H4(X)-V			E35H6(X)-V	
Wiring		**Bipolar**			**Unipolar****	
Operating voltage		2.33 VDC	5 VDC	12 VDC	5 VDC	12 VDC
Current/phase		1.25 A	0.57 A	0.24 A	0.57 A	0.24 A
Resistance/phase		1.86Ω	8.8 Ω	50.5 Ω	8.8 Ω	50.5 Ω
Inductance/phase		2.8 mH	13 mH	60 mH	6.5 mH	30 mH
Power consumption		5.7 W				
Rotor inertia		27.0 gcm2				
Temperature rise		135°F (75°C) Rise				
Weight		5.7 oz (162 g)				
Insulation resistance		20 M Ω				

Screw 0.21 Linear Travel / Step 8" (5.54 mm)		Order Code I.D.
inches	**mm**	
0.00012	0.0030*	**N**
0.00024	0.0060*	**K**
0.00048	0.0121*	**J**
0.00096	0.0243*	**Q**
0.00192	0.0487*	**R**

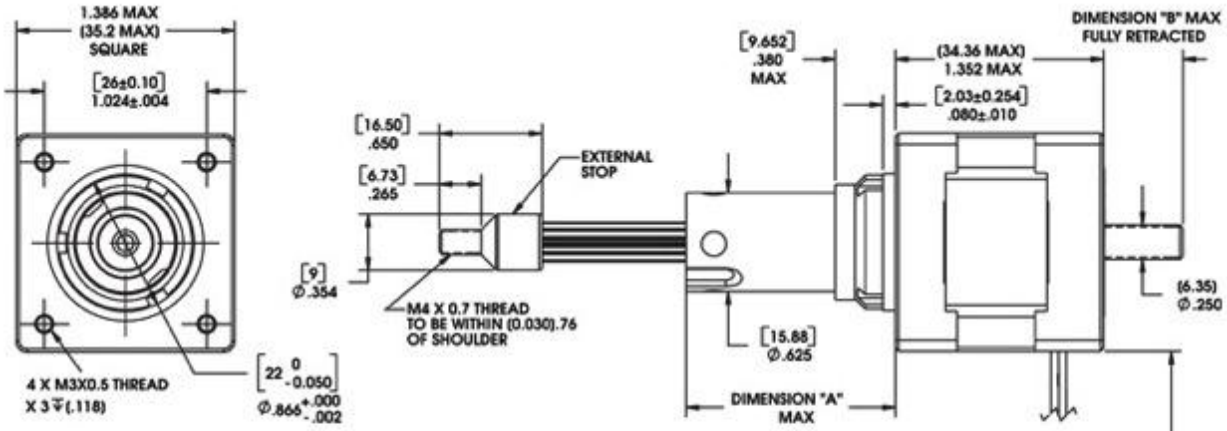

STROKE	DIM. "A"	DIM. "B"	SUFFIX #
0.50 (12.7)	0.82 (20.8)	0.04 (1.0)	– 905
0.750 (19.05)	1.07 (27.2)	0.29 (7.4)	– 907
1.00 (25.4)	1.32 (33.5)	0.54 (13.7)	– 910
1.250 (31.8)	1.57 (39.9)	0.79 (20.1)	– 912
1.500 (38.1)	1.82 (46.2)	1.04 (26.4)	– 915
2.00 (50.8)	2.32 (58.9)	1.54 (39.1)	– 920
2.500 (63.5)	2.82 (71.6)	2.04 (51.8)	– 925

Hybrid Actuator Wiring Diagram

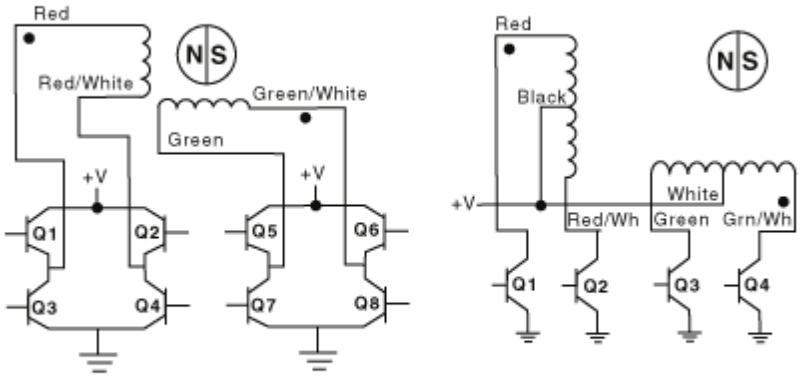

Appendix D- ChipKit Max32 Controller

For schematics and manual see:
http://www.digilentinc.com/Products/Detail.cfm?Prod=CHIPKIT-MAX32

Appendix E- Easy Driver

Specifications

Input voltage: 7-30V DC
Adjustable current control from 150 mA/phase to 750 mA/phase
MS1 and MS2 pins can be used to adjust microstepping

Schematic

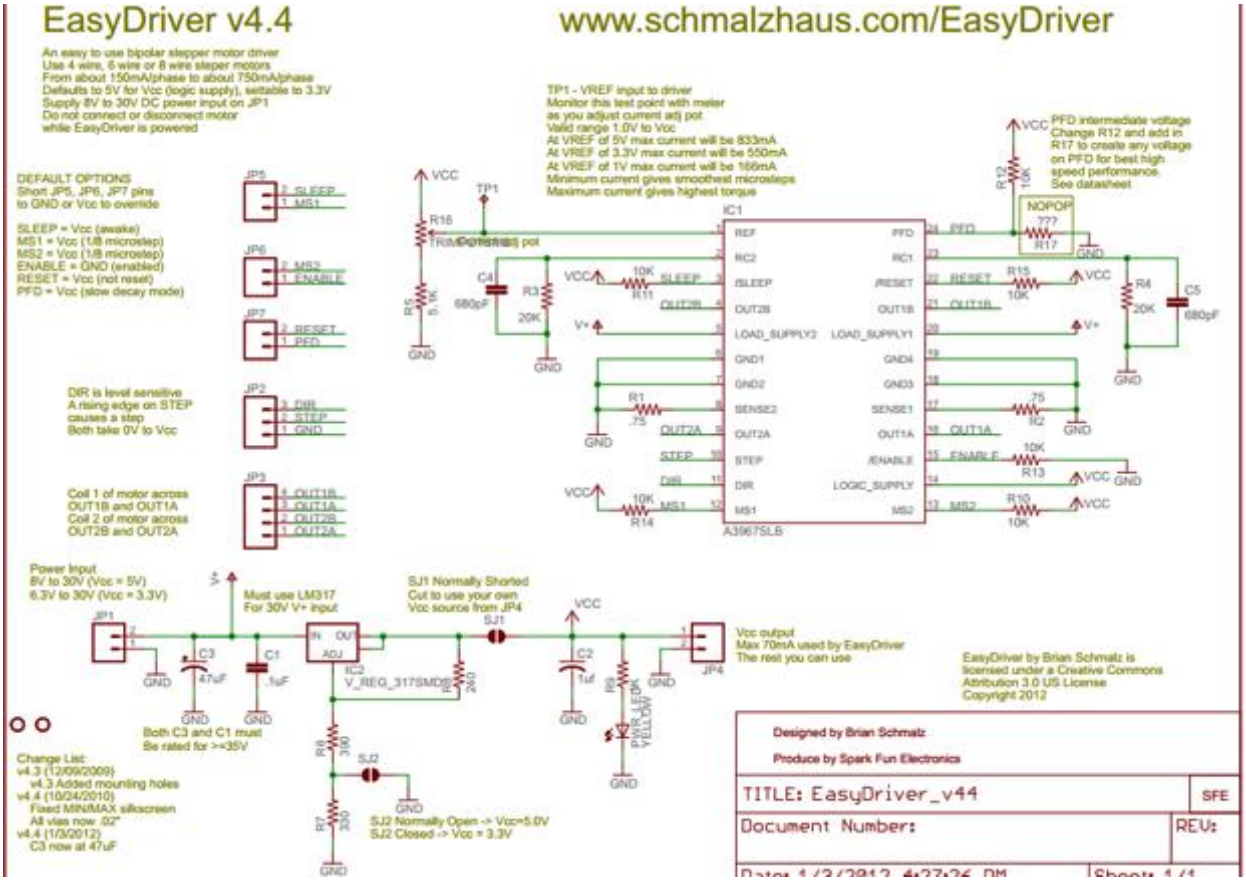

Appendix F- Voltage Regulator

Specifications

Maximum output current: 5 Amps
Input voltage: 4-35V DC or 4-26V AC
Output voltage range: 1.5-32V DC
Onboard potentiometer to vary voltage output
Uses the National Semiconductor voltage regulator model LM338T

Schematics

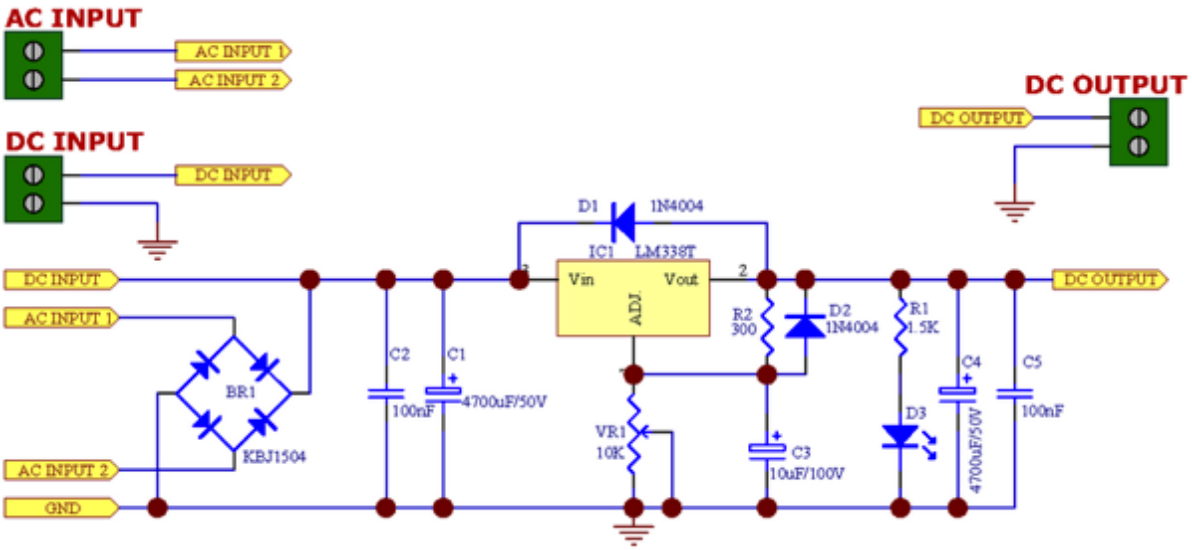

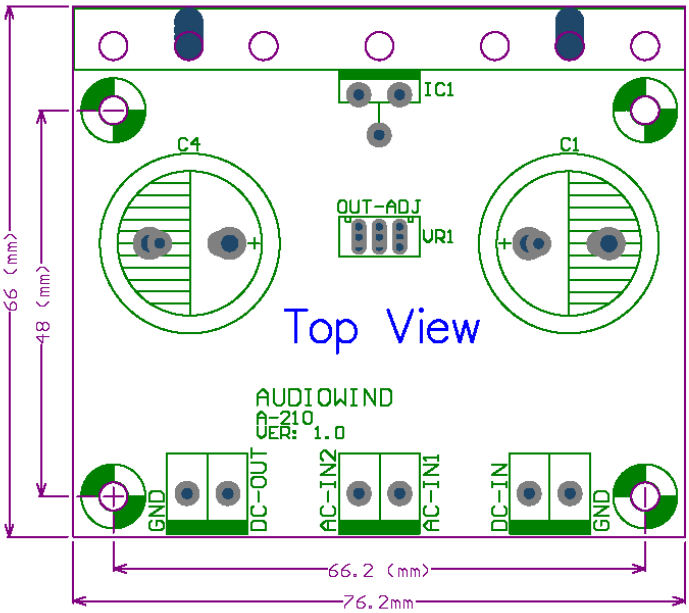
IC1
C4
C1
OUT-ADJ
VR1
Top View
AUDIOWIND
A-210
VER: 1.0
GND
DC-OUT
AC-IN2
AC-IN1
DC-IN
GND
66 (mm)
48 (mm)
66.2 (mm)
76.2mm

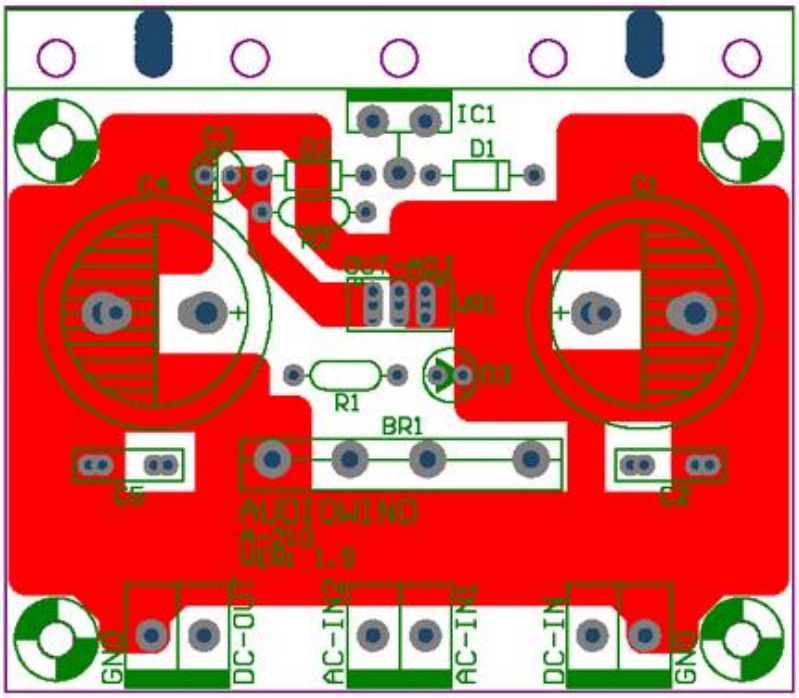
IC1
D1
C3
D2
C4
C1
R2
OUT-ADJ
VR1
D3
R1
BR1
C5
C2
AUDIOWIND
A-210
VER: 1.0
GND
DC-OUT
AC-IN2
AC-IN1
DC-IN
GND

Appendix G- Software Download and Program Examples

Software

MPIDE software can be downloaded from: https://github.com/chipKIT32/chipKIT32-MAX/downloads
Accelstepper Library can be downloaded from:
http://www.open.com.au/mikem/arduino/AccelStepper/

Save the Accelstepper library in the following two locations:

/mpide-0023-windows-20120122-test/hardware/pic32/libraries/AccelStepper
/mpide-0023-windows-20120122-test/libraries/AccelStepper

Make sure to select the proper controller (ChipKit Max32) and serial port from the Tools menu in MPIDE

Program Examples

Home Program: Used to home posts so well can be placed in device

```
#include <AccelStepper.h>

// Define some steppers and the pins the will use. The second number is the step pin and the third number is the direction pin. Leave the first number as 1
AccelStepper stepper1(1, 3, 25);
AccelStepper stepper2(1, 2, 31);
AccelStepper stepper3(1, 4, 23);
AccelStepper stepper4(1, 5, 29);

void setup()
{
   stepper1.setMaxSpeed(20000);
   stepper1.setAcceleration(20000);
   stepper1.runToNewPosition(4980);
   stepper1.setCurrentPosition(0);

   stepper2.setMaxSpeed(20000);
   stepper2.setAcceleration(20000);
   stepper2.runToNewPosition(5000);
   stepper2.setCurrentPosition(0);

   stepper3.setMaxSpeed(20000);
   stepper3.setAcceleration(20000);
```

```
    stepper3.runToNewPosition(4750);
    stepper3.setCurrentPosition(0);

    stepper4.setMaxSpeed(20000);
    stepper4.setAcceleration(20000);
    stepper4.runToNewPosition(5000);
    stepper4.setCurrentPosition(0);
}
void loop()
{
    stepper1.setMaxSpeed(20000);
    stepper1.setAcceleration(20000);
    stepper1.runToNewPosition(-4880);

    stepper2.setMaxSpeed(20000);
    stepper2.setAcceleration(20000);
    stepper2.runToNewPosition(-4900);

    stepper3.setMaxSpeed(20000);
    stepper3.setAcceleration(20000);
    stepper3.runToNewPosition(-4650);

    stepper4.setMaxSpeed(20000);
    stepper4.setAcceleration(20000);
    stepper4.runToNewPosition(-4900);
}
```

10% Strain at 1 Hz Program:

```
#include <AccelStepper.h>

// Define some steppers and the pins the will use
AccelStepper stepper1(1, 3, 25);
AccelStepper stepper2(1, 2, 31);
AccelStepper stepper3(1, 4, 23);
AccelStepper stepper4(1, 5, 29);

void setup()
{
    stepper1.setMaxSpeed(1978.0);
    stepper1.setAcceleration(20000);
    stepper1.moveTo(988);

    stepper2.setMaxSpeed(1978.0);
    stepper2.setAcceleration(20000);
```

```
    stepper2.moveTo(988);

    stepper3.setMaxSpeed(1978.0);
    stepper3.setAcceleration(20000);
    stepper3.moveTo(988);

    stepper4.setMaxSpeed(1978.0);
    stepper4.setAcceleration(20000);
    stepper4.moveTo(988);
}

void loop()
{
    if (stepper1.distanceToGo() == 0)stepper1.moveTo(0);
    if (stepper2.distanceToGo() == 0)stepper2.moveTo(0);
    if (stepper3.distanceToGo() == 0)stepper3.moveTo(0);
    if (stepper4.distanceToGo() == 0)stepper4.moveTo(0);

    stepper1.run();
    stepper2.run();
    stepper3.run();
    stepper4.run();

    if (stepper1.distanceToGo() == 0)stepper1.moveTo(988);
    if (stepper2.distanceToGo() == 0)stepper2.moveTo(988);
    if (stepper3.distanceToGo() == 0)stepper3.moveTo(988);
    if (stepper4.distanceToGo() == 0)stepper4.moveTo(988);

    stepper1.run();
    stepper2.run();
    stepper3.run();
    stepper4.run();
}
```

Appendix H- LabVIEW VI for Operation Time Validation

Block Diagram:

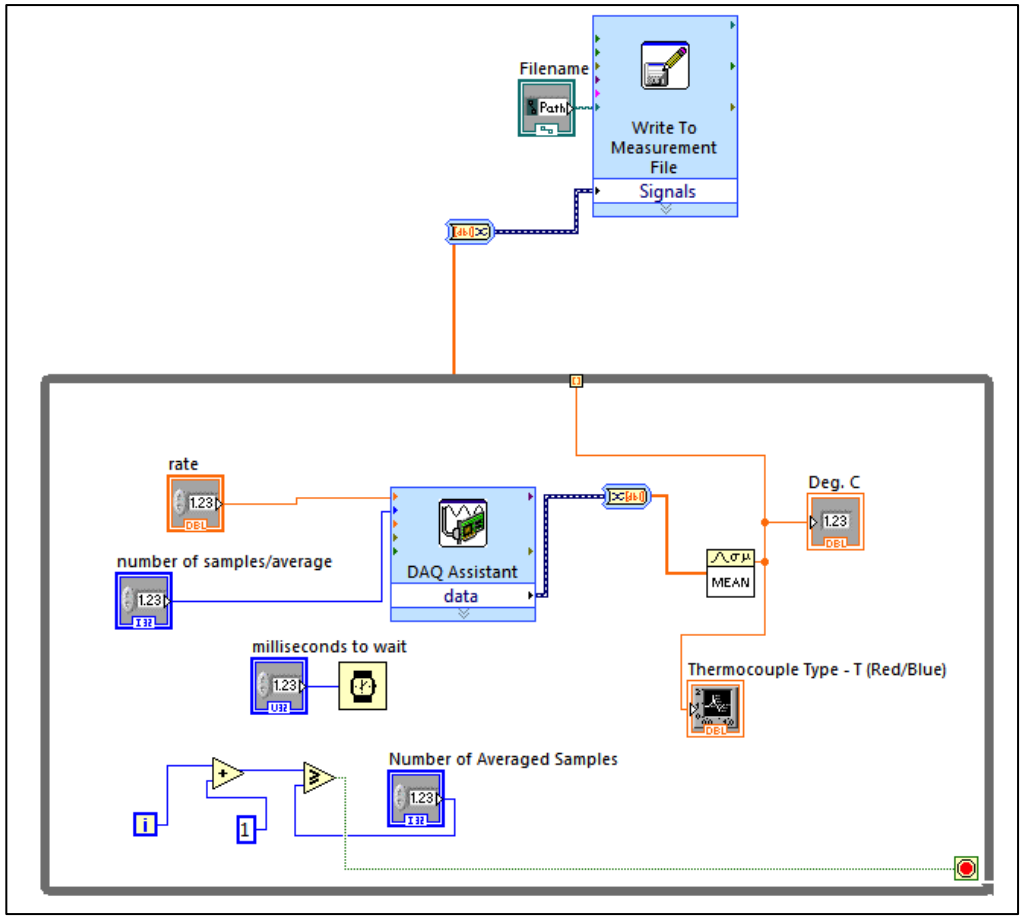

Front Panel:

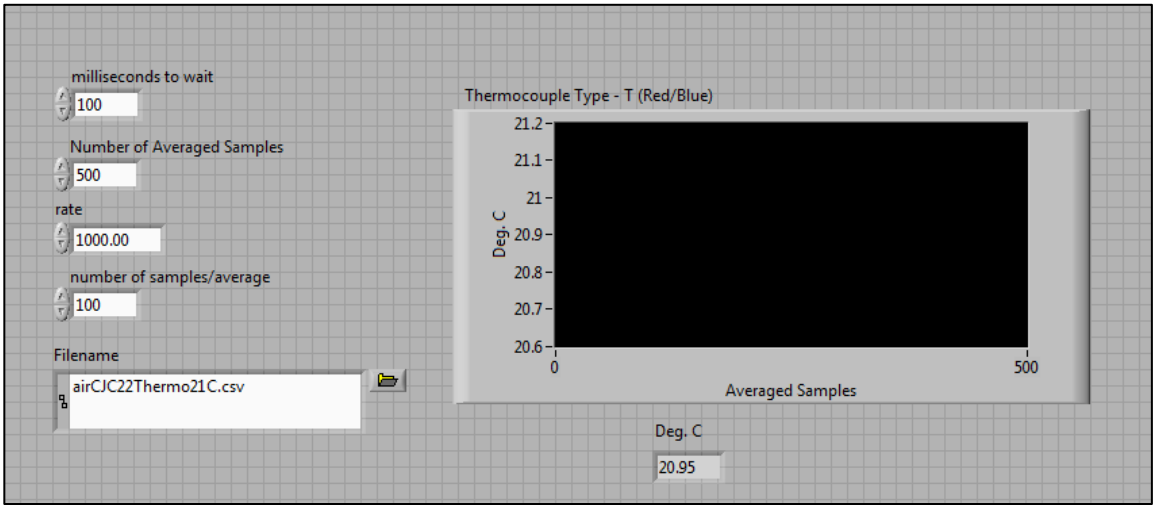

Appendix I: HDM Strain Fields of Strex and Custom Wells

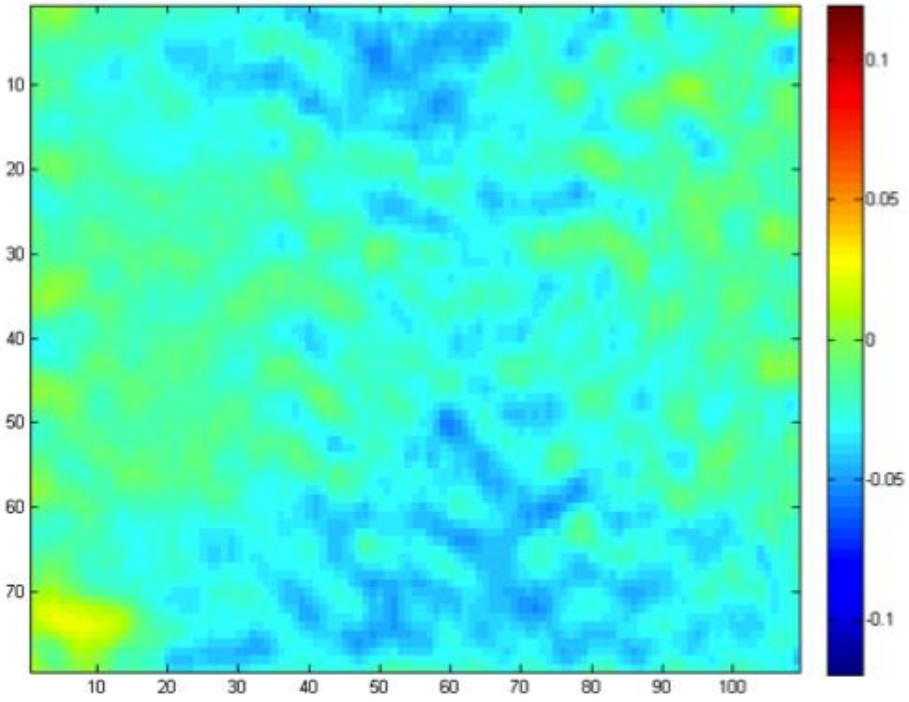

HDM: Strex® well, 10% uniaxial stretch, y-directional strain

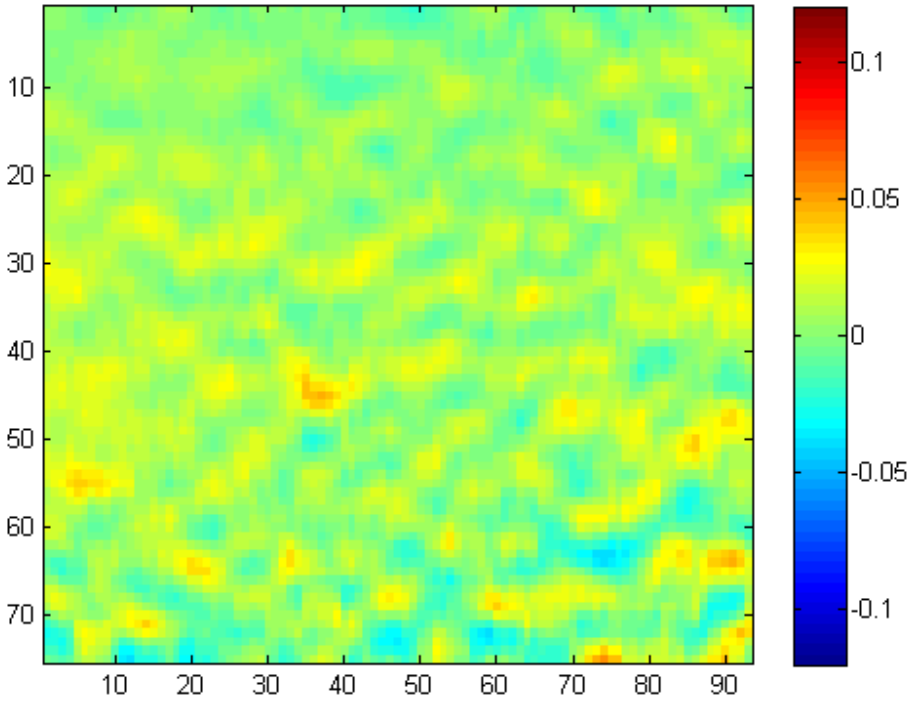

HDM: 15:1 Custom well, 10% uniaxial stretch, y-directional strain

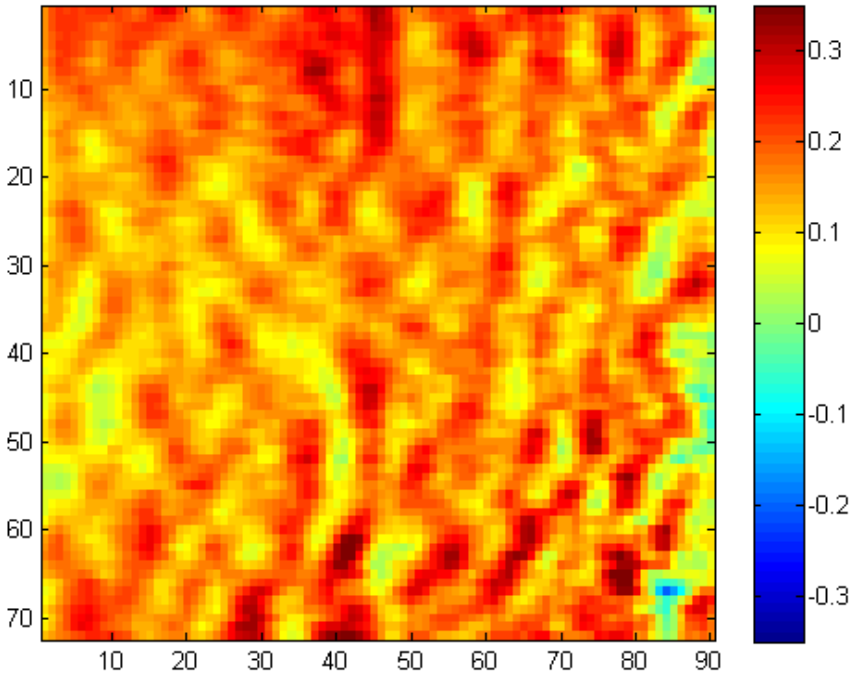

HDM: 20:1 Custom well, 30% uniaxial stretch, x-directional strain

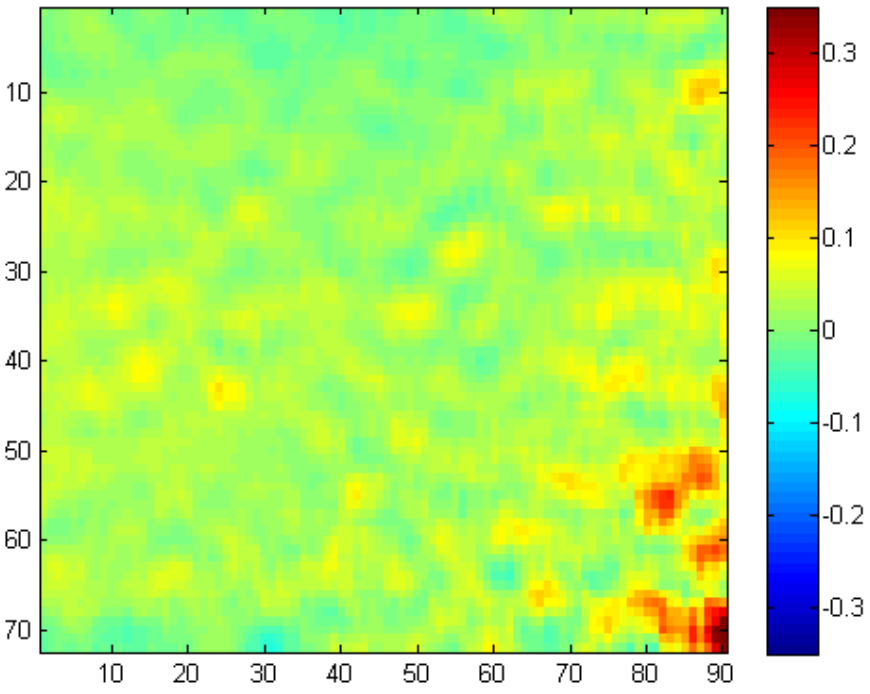

HDM: 20:1 Custom well, 30% uniaxial stretch, y-directional strain

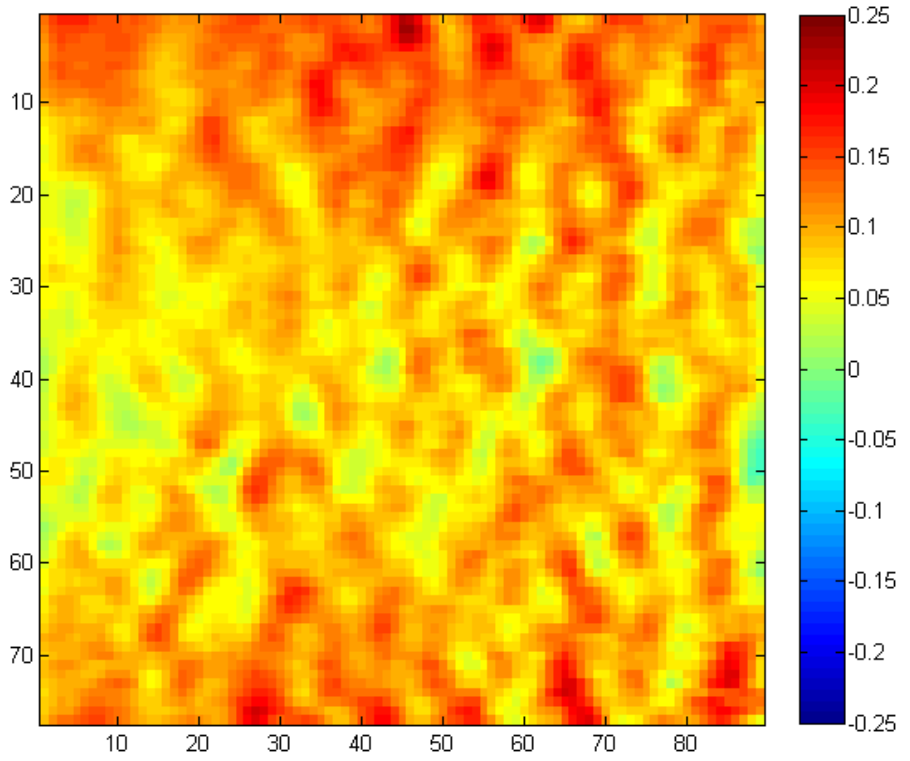

HDM: 20:1 Custom well, 20% uniaxial stretch, x-directional strain

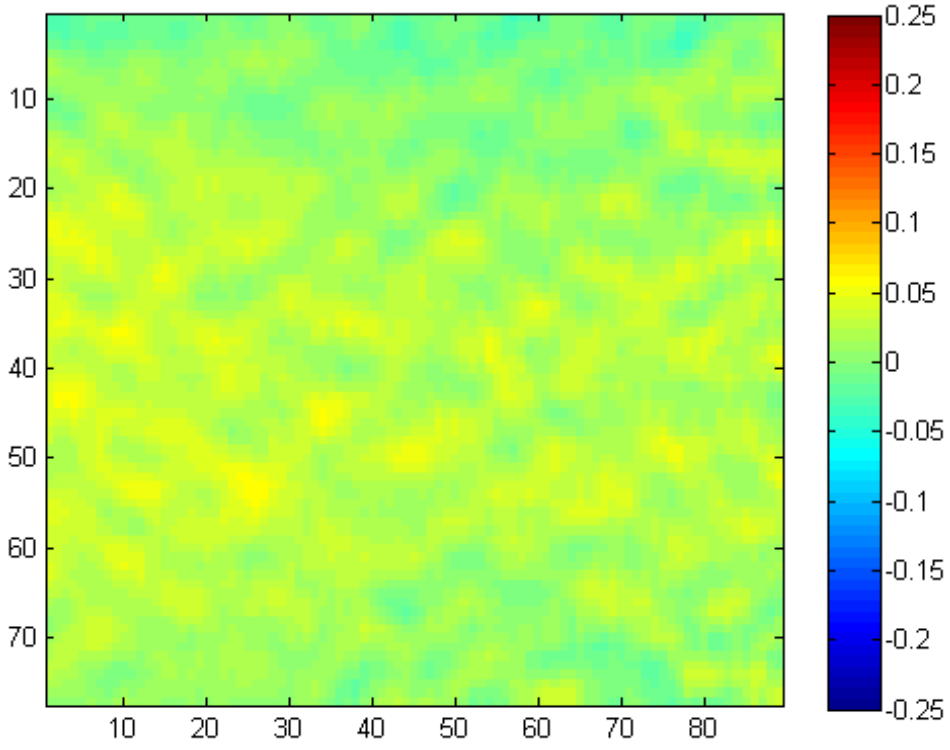

HDM: 20:1 Custom well, 20% uniaxial stretch, y-directional strain

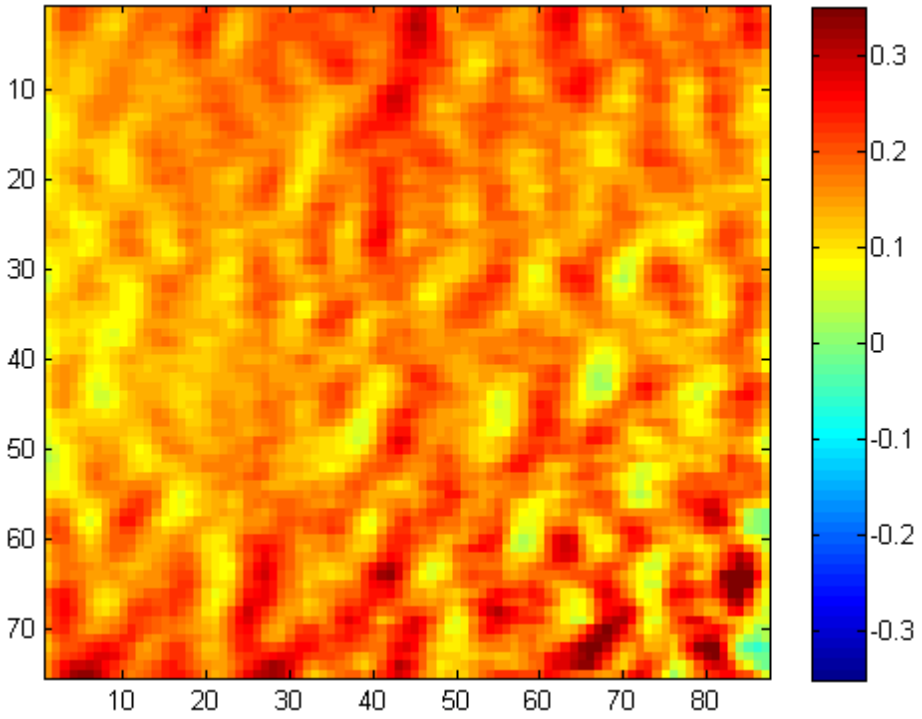

HDM: 15:1 Custom well, 30% uniaxial stretch, x-directional strain

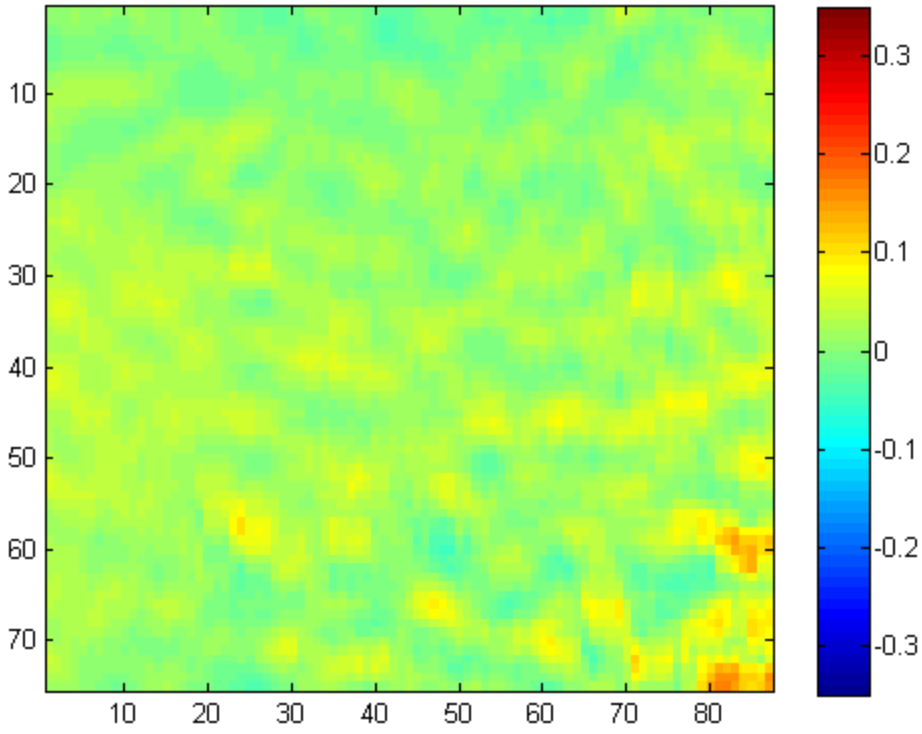

HDM: 15:1 Custom well, 30% uniaxial stretch, y-directional strain

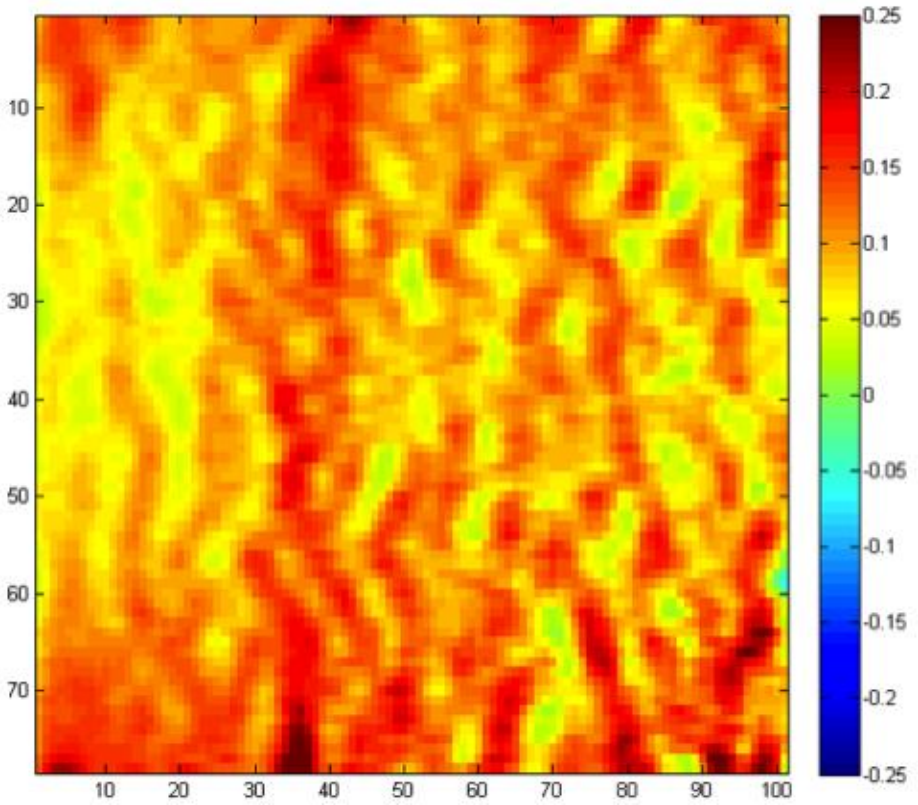

HDM: 15:1 Custom well, 20% uniaxial stretch, x-directional strain

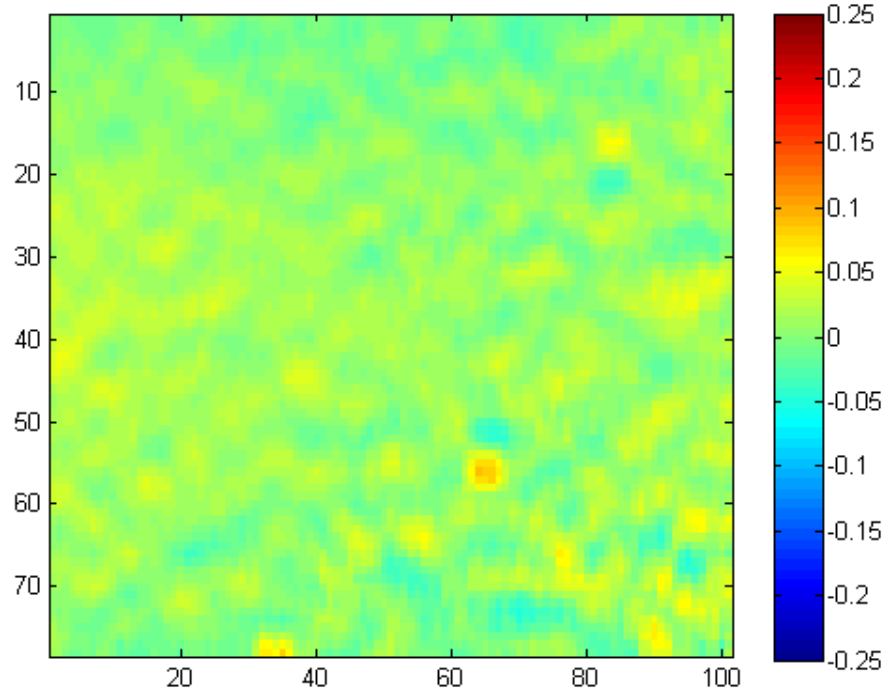

HDM: 15:1 Custom well, 20% uniaxial stretch, y-directional strain

Appendix J: Bill of Materials

Bill of Materials Table

Materials						
Date	**Company**	**Items**	**Quantity**	**Unit Cost**	**Shipping Cost**	**Notes**
11/28/2011	SSP Inc.	SSP-M823 Silicone Sheeting 0.004" x 12" x 12"	1	$30.00	$12.65	
1/18/2012	Scrap Yard	Aluminum Stock (1/8 in., 1/4 in., 5/8 in. plate)	1	$0	$0	Donated
1/18/2012	Scrap Yard	Stainless Steel (1/8 in., 1/2 in. plate and 3/16 in. angle)	1	$0	$0	Donated
1/20/2012	SparkFun	PRT-09684 Chameleon Face Plate Arduino	1	$4.95	$4.35	
1/20/2012	SparkFun	PRT-10746 Small Heastsink with Thermal Tape	4	$7.95	$4.35	
1/20/2012	SparkFun	ROB-10735 - Big Easy Drivers	4	$22.95	$4.35	
1/23/2012	Hammond Enclosures	Steel Enclosure (1458 Series)	1	$0	$0	Donated
1/25/2012	Haydon Kerk	35000 series size 14 stepper motor linear actuators with quadrature encoders	4	$0	$0	Donated
1/27/2012	Surplus Sales of Nebraska	CNES321AB 21 pin female connectors	4	$6.00	$12.25	
1/27/2012	Surplus Sales of Nebraska	CNEP321CCT-K 21 pin male connectors	4	$17.00	$12.25	
1/27/2012	12V Adapters	12V - 5Amp adapter	1	$32.98	$0	
2/3/2012	RobotShop	RB-Spa-616 Big Easy Driver Bipolar Motor	1	$22.95	$13.11	
2/6/2012	Electronics Salon	5 Amps Voltage Regulator Module	1	$19.80	$0	
3/15/2012	Ace Hardware	#6-32 1/4 in. Cap Screws	6	$0	$0	Donated
3/15/2012	Ace Hardware	#6-32 1/8 in. Cap Screws	26	$0	$0	Donated
3/15/2012	Ace Hardware	#4-40 1/2 in. Flathead Screws	16	$0.27	$0	
3/15/2012	Ace Hardware	#2-56 1/2 in. Flathead Screws	4	$0.27	$0	
3/15/2012	Ace Hardware	#2-56 1/2 in. Female Standoffs	4	$0	$0	Donated
3/15/2012	Ace Hardware	M3x.05 16mm Flathead Screws	16	$0.27	$0	
3/15/2012	Ace Hardware	#4-40 1/2 in. Female Standoffs	20	$0.27	$0	
4/2/2012	Digilent	ChipKit Max32	1	$49.50	$17.80	
Total				**$390.90**	**$81.11**	

Bill for Various Services Utilized in the Project

Services			
Date	**Company**	**Service**	**Cost**
2/9/2012	Vangy Tool	Baseplate Machining	$59.00
2/16/2012	Vangy Tool	Subplate and Hook Mount Machining	$90.00
3/12/2012	Vangy Tool	Hook, L Brackets, Blocks and Plate Modifications	$475.00
4/17/2012	H LA Rosee & Sons Inc.	Anodize Aluminum Components	$40.00
Total			**$664**

Total Cost of Materials and Services Including Shipping and Handling

Total Cost	
Unit	$390.9
Unit S&H	$81.11
Service	$664
Total	$1136.01